TECHNISCHE UNIVERSITÄT WIEN

Diploma Thesis

Investigation of δ-Functionalization of Aliphatic Amines through Photoredox Catalysis

Carried out for the purpose of obtaining the degree "Diplom-Ingenieur (Dipl.-Ing.)",
submitted at TU Wien, Faculty of Technical Chemistry, by

Katharina Schlögl

Mat.Nr.: 01425254

Untere Augartenstraße 14/2/2, 1020 Vienna

under the supervision of

Univ. Prof. Dipl.-Ing. Dr.techn. Marko Mihovilovic

Institute of Applied Synthetic Chemistry, E163

conducted under the supervision of

Prof. Tomislav Rovis

Columbia University in the City of New York

Vienna, 13.09.2019

Acknowledgements

I want to start by thanking Prof. Tomislav Rovis for the opportunity to perform the practical lab work that this thesis is based on in his lab and to work with him and his group at Columbia University for six months. It was a defining experience and an invaluable chance to expand my horizon not only in the world of science but also regarding everyday life. Besides introducing me to methodology research the group taught me new ways to think of problems and to approach solving them that will for sure be useful in my future.

Though mentioned second my gratitude towards Prof. Marko Mihovilovic for supervising this diploma thesis at the TU Wien is in no way less. I appreciate his advice throughout not only the conduction but also the writing process of the thesis. Furthermore, I want to emphasize his patience waiting for drafts, his swift corrections and that he put up with several time sensitive deadlines, not only on my end but therefore also on his.

Another person playing a big role in the successful and educative outcome of this diploma thesis was Melissa Ann Ashley, graduate student in Prof. Tomislav Rovis lab. Thanks to her close supervision I was able to develop a thorough understanding of photoredox chemistry, how to design optimizations and screens and how to best approach and design experiments to test new hypotheses and solve problems.

Furthermore, I want to thank the whole Rovis research group for having me, supporting me and making my time there not only productive and instructive but also a memorable and merry experience. I further want to express my special thanks towards Melissa Ann Ashley again as well as Dr. Corey Basch, Benjamin Ravetz, Martin Luff and Erik Phips for numerous fun lunch breaks, good talks and relaxing bar nights.

This whole diploma thesis grew around a stay in the group of Prof. Tomislav Rovis which would not have been possible without the support and scholarship of the Austrian Marshall Plan Foundation, towards whom I also want to express my gratitude. Their financial support enabled my stay abroad for the conduction of the practical work.

Last, I want to thank my whole family, my friends at home, my newly made friends in New York and especially my parents for supporting my decision to perform my diploma thesis abroad. It was their motivational speeches and confidence in me that pushed me through the elaborate preparations in Austria and the long and exhausting lab days in New York. Next to my parents Theresia and Bernhard Schlögl who always had an open ear for me, I want to thank Christoph Suster for bearing more arbitrary whining than any human being should be able to take.

Abstract

The purpose of this diploma thesis is to look into a new way to perform δ-functionalization at aliphatic amines *via* photoredox catalysis to further establish the incorporation of a cyano-group at this position as a swift and simple transformation. Such a modification could find applications in the late stage functionalization of drugs containing aliphatic amines, in the synthesis of compound libraries and the introduction of further functional groups at the δ-position as the cyano-group is an excellent functional handle. Known methods to perform such a transformation as they were developed by Leonori and Studer in 2018 require prefunctionalization of the aliphatic amine, which makes substrate syntheses more elaborate. The approach discussed in this diploma thesis as shown in Scheme 1 does not require such prefunctionalization.

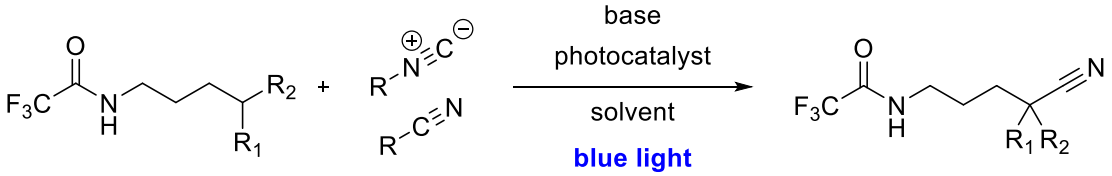

Scheme 1: General transformation and conditions of the attempted δ-cyanation explored within this thesis

The idea of this diploma thesis builds upon findings of the Rovis group, which was able to obtain a first initial hit for a δ-cyanation of a trifluoroacetamide prior to this work. Thereupon, they proposed a mechanism for this reaction featuring first a deprotonation step of the aliphatic amine, followed by a photocatalyzed oxidation, a *[1,5]*-H-atom transfer reaction, radical trapping and a reduction step to close the catalytic cycle.

The focus of this diploma thesis lies on optimizing the reaction conditions in order to improve the initial yield of 11% by NMR to about 80% to 90% on a tertiary substrate. Later, a scope of several trifluoroacetamides was planned to be explored to test the versatility of the reaction and to show its feasibility as an application in drug development on selected examples. Therefore, cyanide-sources, starting material and photocatalyst were synthesized. Moreover, elaborate screens of all the reaction components were conducted. Additional experiments and NMR studies were conducted to test several hypotheses that arose from obtained results.

Even though the δ-functionalization could not be pushed to the desired 90% NMR yield but only to 65% NMR yield, valuable insights in the reaction pathway, the role of its components and its kinetics were obtained. Furthermore, two secondary substrates were already successfully tested and δ-functionalized. One of those products was fully characterized.

Kurzfassung

Das Ziel dieser Diplomarbeit ist die Erforschung einer neuen Methode, um aliphatische Amine mittels Photoredoxchemie an der δ-Position zu funktionalisieren und somit die Einführung einer Cyanogruppe an dieser Position besser als schnelle und einfache Reaktion zu etablieren. Eine solche Transformation hat potenzielle Anwendungen in der Spätphasen-Funktionalisierung von Wirkstoffen mit aliphatischen Aminen und der Synthese von Substanzbibliotheken. Des Weiteren ist die Cyanogruppe an sich als geschütztes Amin zu betrachten und somit ein ausgezeichneter Ausgangspunkt für die Einführung weiterer funktioneller Gruppen. Literaturbekannte Methoden für solch eine δ-Cyan-Einführung von Leonori und Studer aus 2018 erfordern beide Präfunktionalisierung des aliphatischen Amins, wodurch die Substratsynthese aufwendiger wird. Die Reaktion, welche in dieser Diplomarbeit diskutiert wird, erfordert keine solche Präfunktionalisierung (Abbildung 1).

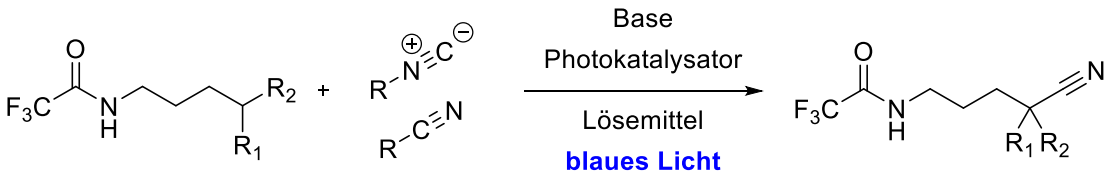

Abbildung 1: Überblick über die Reaktionsbedingungen und -komponenten der untersuchten δ-Cyanidierung

Die Idee für diese Diplomarbeit hat sich aus einer vorangegangenen Arbeit in der Rovis Gruppe entwickelt. Dabei erhielt die Rovis Gruppe eine erste Ausbeute für die Einführung einer Cyanidgruppe an der δ-Position von 11% nach NMR bei einem Trifluoroacetamid. Daraufhin postulierte die Gruppe einen Mechanismus für die Reaktion, in dem zuerst eine Deprotonierung des Substrates stattfindet, gefolgt von einer photokatalysierten Oxidation, einem *[1,5]*-H-Atom Transfer, dem Abfangen der Radikalspezies und einer Reduktion, um den katalytischen Zyklus zu schließen.

Während dieser Diplomarbeit lag der Fokus auf der Optimierung der Reaktionsbedingungen, um die erste Ausbeute von 11% per NMR auf 80% bis 90% für ein tertiäres Substrat zu erhöhen. Danach sollte ein Substratpool an Trifluoroacetamiden getestet werden, um die Vielfältigkeit der Reaktion zu überprüfen und ihre Anwendbarkeit in der medizinischen Chemie an ausgewählten Beispielen zu zeigen. Dafür wurden Cyanidquellen, Startmaterial und Photokatalysator synthetisiert. Anschließend wurden umfangreiche Screenings aller Reaktionskomponenten durchgeführt sowie zusätzliche Experimente und NMR Studien, um weitere während der Arbeit aufgekommene Hypothesen zu testen.

Obwohl die δ-Funktionalisierung nicht auf die gewünschte NMR Ausbeute von 90% gebracht werden konnte, sondern lediglich 65% Ausbeute nach NMR erzielt wurde, wurden wertvolle Informationen zum Reaktionsweg, den Rollen der einzelnen Komponenten und der Kinetik der Reaktion gewonnen. Außerdem wurden bereits zwei sekundäre Substrate erfolgreich getestet. Eines der dabei erhaltenen Produkte wurde weiter vollständig charakterisiert.

Abbreviations

2D-NMR	two-dimensional nuclear magnetic resonance spectroscopy
4CzIPN	2,4,5,6-Tetra(9H-carbazol-9-yl)isophthalonitrile
aq.	aqueous
bpm	bis(pyrazolyl)methane
cat.	catalyst
conj.	conjugated
COSY	H,H-correlated spectroscopy (NMR)
CV	cyclic voltammetry
d	doublet (NMR)
δ	chemical shift (NMR)
DCE	dichloroethane
DCM	dichloromethane
dd	doublet of doublet (NMR)
ddd	doublet of doublet of doublet (NMR)
degr.	degradation
DIPA	diisopropylamine
DMA	dimethylacetamide
DMF	*N,N*-dimethylformamide
DMSO	dimethyl sulfoxide
dtbbpy	4,4'-di-tert-butyl-2,2'-dipyridyl
equiv.	equivalent
EtOAc	ethylacetate
EWG	electron withdrawing group
HAT	hydrogen-atom transfer
HPLC	high performance liquid chromatography
HRMS	high resolution mass spectrometry
HSQC	hetero single quantum coherence (NMR)
***i*PrOH**	isopropanol
ISC	intersystem crossing
J	coupling constant (NMR)
LAH	lithium aluminium hydride
Lit.	literature
m	multiplet (NMR)
m.p.	melting point
m.w.	molecular weight
MeCN	acetonitrile
MeOH	methanol
MLCT	metal-to-ligand charge-transfer
MS	mass spectrometry
n.d.	not determined
NMR	nuclear magnetic resonance spectroscopy
opt.	optimized
phen	phenanthroline
PMA	phosphomolybdic acid
ppm	parts per million (NMR)
ppy	2-phenylpyridine
quant.	quantitative
rt	room temperature
s	singlet (NMR)
satd.	saturated
SET	single electron transfer
t	triplet (NMR)
THF	tetrahydrofuran
TLC	thin layer chromatography
TRIP-SH	triisopropylsilanethiol

Synthetic schemes

All compounds prepared or used as starting materials in this thesis are numbered in bold Arabic numerals. Compounds unknown to the literature are additionally underscored.

Synthesis of trifluoroacetamide starting material

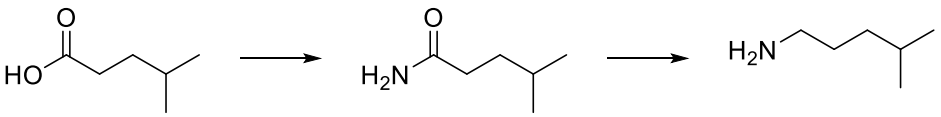

1 **2** **3**

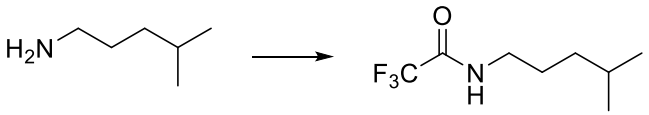

3 **4**

Syntheses of isocyanides

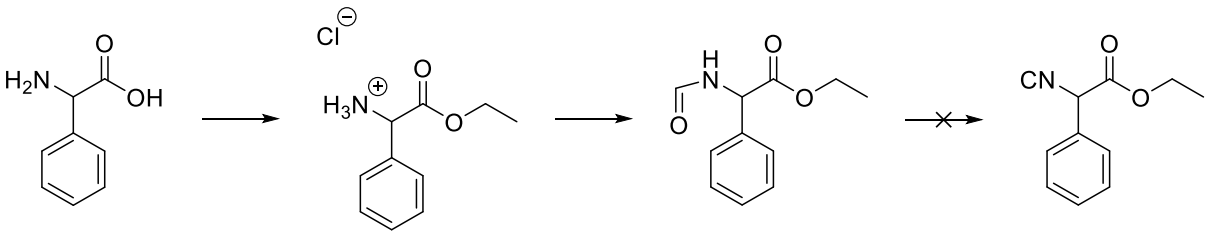

5 **6** **7** **8**

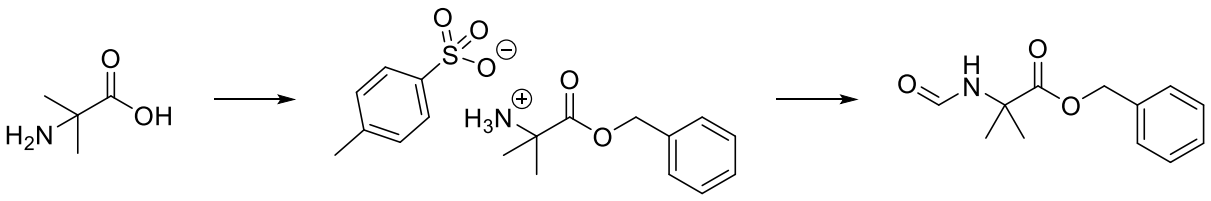

9 **10** **11**

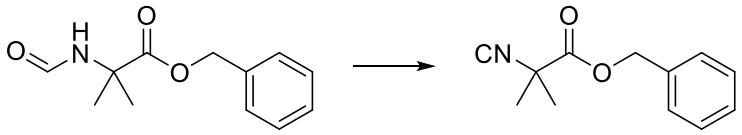

11 **12**

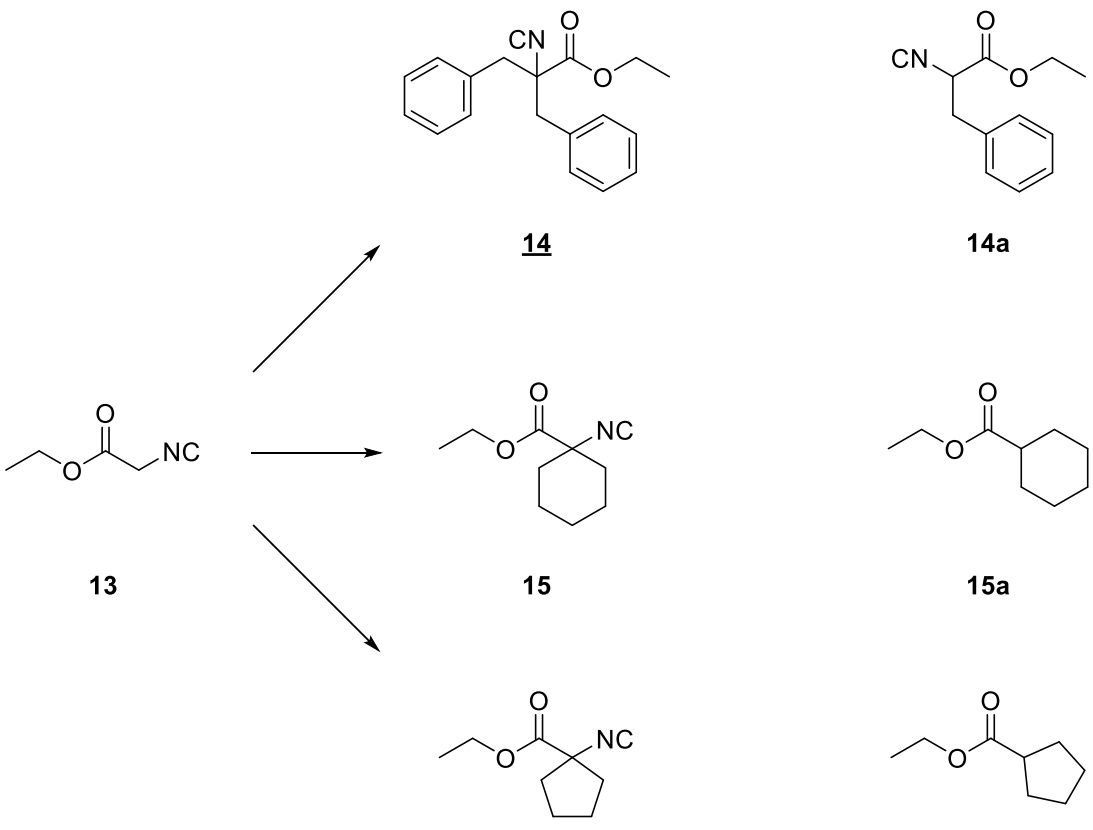

<u>14</u> **14a**

13 **15** **15a**

16 **16a**

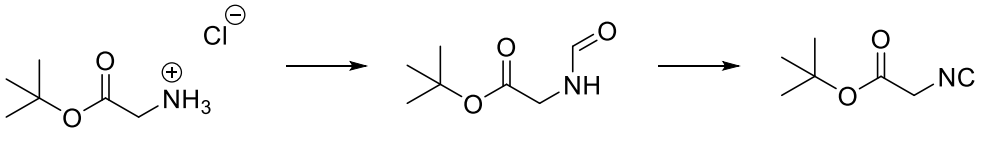

17 **18** **19**

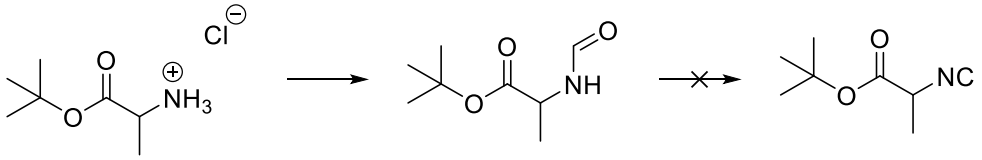

20 **21** **22**

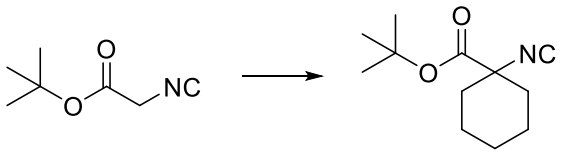

19 **<u>23</u>**

Synthesis of the Ir^{III}-photocatalyst

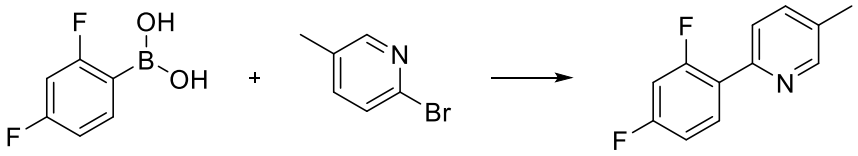

24 **25** **26**

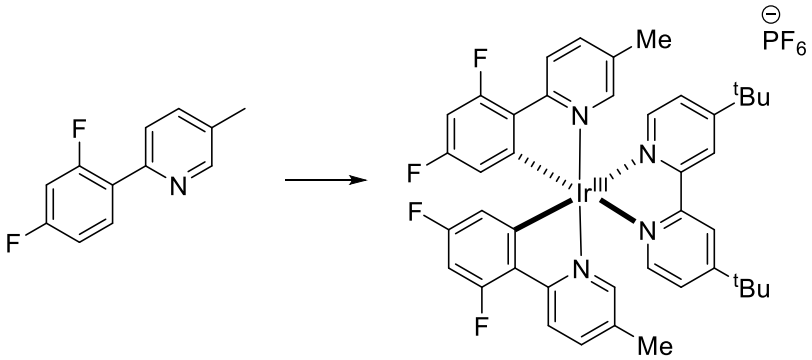

26 **27**

Photoredox catalyzed δ-functionalization of aliphatic amines

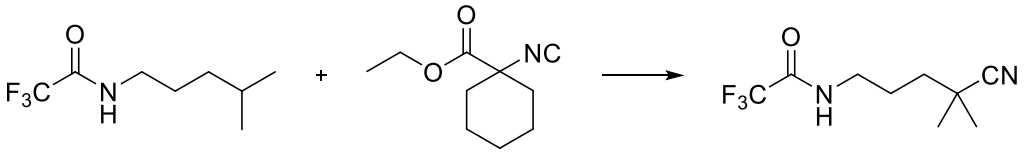

4 **15** **28**

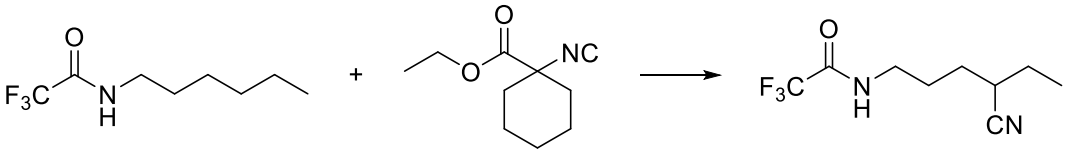

29 **15** **30**

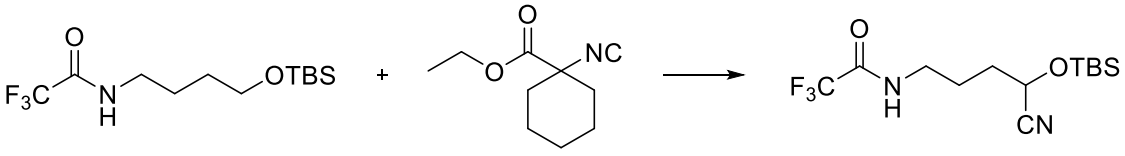

31 **15** **32**

Table of content

1. Introduction

1.1 Role and value of aliphatic amines and their derivatives in modern chemistry

The research during this diploma thesis was part of ongoing efforts in the Rovis group towards the selective δ-functionalization of aliphatic amine derivatives *via* photoredox catalysis. Previous work in the group had demonstrated the feasibility of using trifluoroacetamides to activate the δ-position of such substrates *via* a photoredox catalyzed *[1,5]*-hydrogen-atom transfer (HAT) reaction[1]. After initial studies limited to introducing electron-deficient olefin coupling partners at the δ-position, current aims in the Rovis group focus on expanding the scope of radical traps beyond olefins to implement for example a δ-cyanation transformation as it will be described within this thesis[1-2].

The main motivation for investigating such a transformation arises from the fact, that about 84% of the 1086 small-molecule drugs that were approved by the FDA through 2012 contained at least one nitrogen atom, which makes nitrogen the fourth most common element in pharmaceuticals after carbon, hydrogen and oxygen[3-4]. In addition to that, 146 (73%) of the top 200 pharmaceuticals products (by US retail sales) in 2012 are small-molecule-drugs, of which 67% further contain at least one aliphatic amine functionality[5]. Functionalization of aliphatic amines at the δ–position is therefore of special interest as it could simplify synthetic routes to many known drugs. Furthermore, such functionalizations would allow site-selective C(sp^3)-H bond activation at chemically indistinguishable aliphatic C(sp^3)-H bonds and thereby enable late stage functionalizations during tedious multi-stage syntheses. By the installation of a cyanide functional group through δ-cyanation a nitrogen containing moiety would be introduced in the molecular scaffold that also allows for further derivatization and reactivity.

1.2 Site-selective δ-functionalization of aliphatic amines; challenges and first examples

Looking at a typical aliphatic amine as depicted in Scheme 2, there are three different kinds of C(sp^3)-H bonds present in its carbon chain. The C(sp^3)-H bond next to the amine functional group is especially prone towards reactions, as it is the most electronically biased one. The C(sp^3)-H bond at the end of the carbon chain is the least sterically hindered and thereby offers possibilities for selective functionalization. However, in between those two types of C(sp^3)-H bonds several chemically indistinguishable C(sp^3)-H bonds are present, which are therefore hard to selectively functionalize. One way to functionalize the δ-position of such aliphatic amines selectively is *via* utilizing a Hofmann-Löffler-Freytag-reactivity[6] (Scheme 3) in an intramolecular *[1,5]*-H-atom transfer (HAT) event.

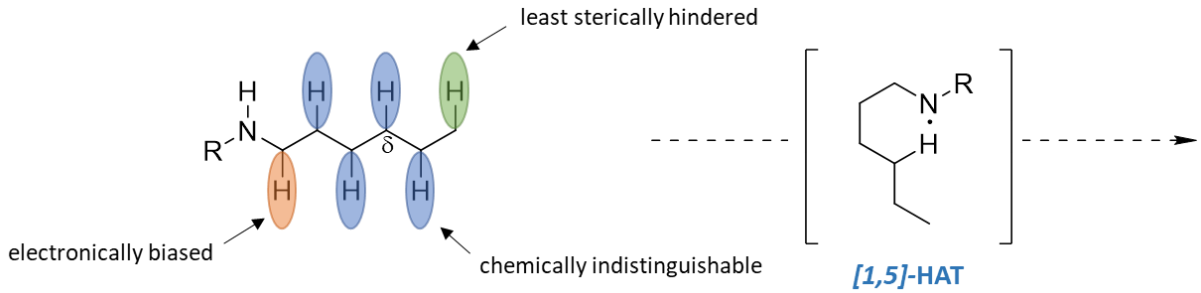

Scheme 2: Different kinds of C(sp³)-H bonds of an aliphatic amine and a way to selective δ-functionalize it

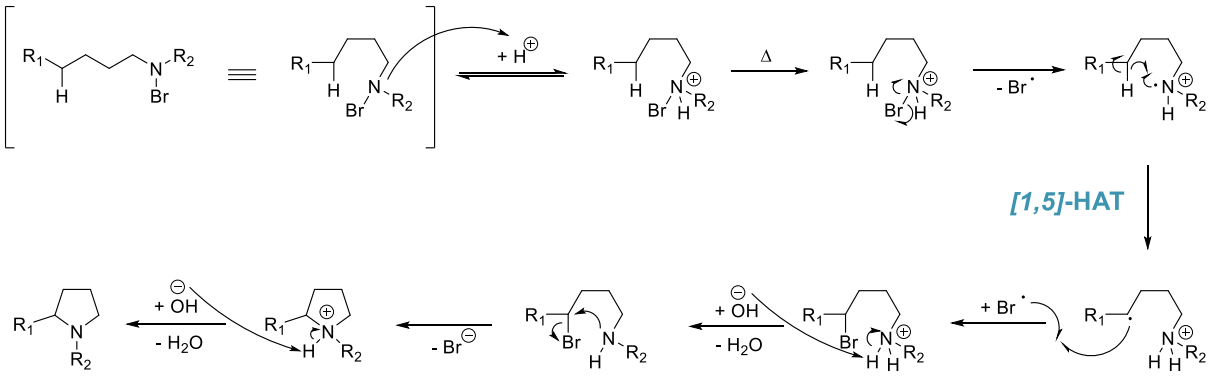

Scheme 3: Reaction mechanism of the Hofmann-Löffler-Freytag reaction[6] featuring an intramolecular [1,5]-HAT step

In 2016 Rovis[1] and Knowles[7] both showed the feasibility of such an approach towards the δ-functionalization of aliphatic amines by using electron-deficient olefins with electron withdrawing groups (EWG) as radical traps and coupling partners for partially protected amines in photoredox catalyzed reactions (Scheme 4). In 2018 Leonori[8] published a method expanding the scope of coupling partners from only electron-deficient olefins towards functional groups like for example halogens (F, Cl) or cyanide (Scheme 4). However, Leonori's approach requires prefunctionalization of the aliphatic amine which makes the amidyl radical formation step irreversible, thereby pushing the reaction towards the product. The necessity of this prefunctionalization makes the substrate synthesis for Leonori's approach more elaborate. Another approach towards δ-functionalization of likewise prefunctionalized aliphatic amines (N-allylsulfonyl substrates) was published by Studer[9] in 2018 (Scheme 4). Studer's group is also able to introduce several different functional groups at the δ-position though not by photoredox catalysis but radical initiation at a higher temperature.

- Rovis (2016)

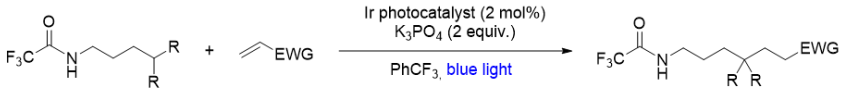

- Knowles (2016)

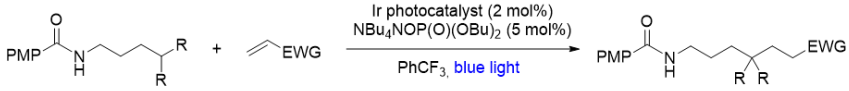

- Leonori (2018)

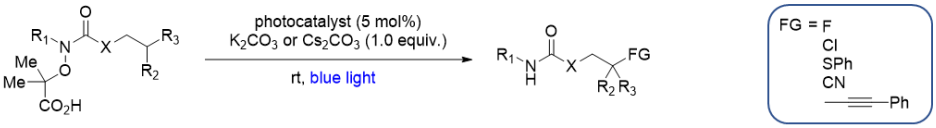

- Studer (2018)

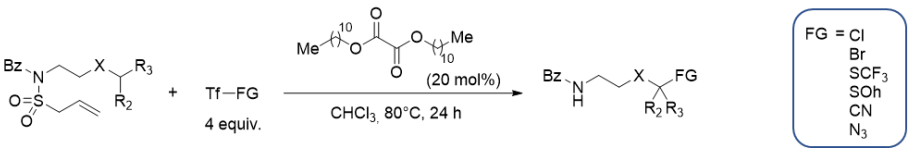

Scheme 4: Literature precedence for successful δ-funtionalization of aliphatic amines[1, 7-9]

The objective of this diploma thesis was to further work on the development of a mild method to introduce a cyanide group at the δ-position of a less prefunctionalized aliphatic amine like a trifluoroacetamide. Removing the necessity to prefunctionalize the substrate would simplify the synthesis of suitable substrates and thereby expand the scope of the transformation. Especially compared to Studer's approach, a photoredox catalyzed reaction would allow a lower reaction temperature, thereby further expanding the scope to more sensitive substrates.

1.3. Photoredox catalysis

Photoredox catalysis is a method that uses the energy of light to catalyze chemical reactions *via* single electron transfer (SET) events, which often provide broad new reactivity compared to more conventional methods. Typical characteristics of photoredox catalysis are the formation of excited state photocatalysts after excitation by light. Those excited state photocatalysts show especially good oxidizing and reducing abilities with high oxidation and reduction potentials. The excited states of the photocatalysts are outstandingly stable and long-lived (lifetimes longer than 1000 ns), which enables them to take part in bimolecular SET reactions. For shorter excited state lifetimes deactivation pathways are usually predominant. Although compounds behaving in such a manner like polypyridyl complexes of iridium and ruthenium have been known to act as catalysts since 1978, the true uprise of the field of photoredox catalysis only started in the early 2000s. Since then photoredox chemistry experienced rapid growth and expanded into many fields of application.[10-11]

The basics of photoredox catalysis are explained in Scheme 5. Looking at a typical photoredox catalyst like $[Ir(dF\text{-}CF_3\text{-}ppy)_2(dtbbpy)PF_6]$, an electron of the HOMO of the Ir^{III}-complex - a d-orbital of the Ir^{III}-metal center- can be promoted to a π^*-orbital of the dtbbpy-ligand, which is the LUMO of the complex, by irradiation with blue light. This excitation process is called metal-to-ligand charge-transfer (MLCT). During this MLCT intersystem crossing (ISC) takes place to form a long-lived triplet excited state of the photocatalyst. The excited state of the photocatalyst can then either act as a reductant with a reduction potential of $E_{1/2}^{IV/III*} = -0.89$ V and thereby loose its electron from the π^*-orbital or it can act as an oxidant with an oxidation potential of $E_{1/2}^{III*/II} = +1.21$ V while accepting a second electron in the single occupied d-orbital at the metal center. These described reduction and oxidation events are SET reactions. In order to participate in such a reduction or oxidation event the chosen substrate needs an oxidation or reduction potential within the photocatalyst's range of oxidation and reduction potentials. A photocatalyst can only oxidize substrates with oxidation potentials that are lower (less positive) than the photocatalyst's own. Accordingly, a substrate needs a lower (less negative) reduction potential than a photocatalyst in order to be reduced by it. In the case of photocatalysts, being a stronger reductant means having a higher reduction potential – the term higher therein refers to having an absolute higher value as reduction potential. That is due to the fact that reduction potentials are reported as negative values in volts.[10-11]

The duality of the reactivity of the triplet excited state of such photocatalysts makes them a valuable tool to use in many fine-tuned reactions. Additionally, photoredox catalysis allows for very mild reaction conditions. Photoredox catalyzed reactions usually take place at room temperature. The excitation wavelength of the Ir^{III}-photocatalyst shown in Scheme 5 is about 380 nm, though catalysis also works with slightly less energetic light with wavelengths of about 430 nm. The excitation wavelength for common Ru^{II} photocatalysts is about 450 nm, so even less energetic than the one for Ir^{III}-photocatalysts.[10-11]

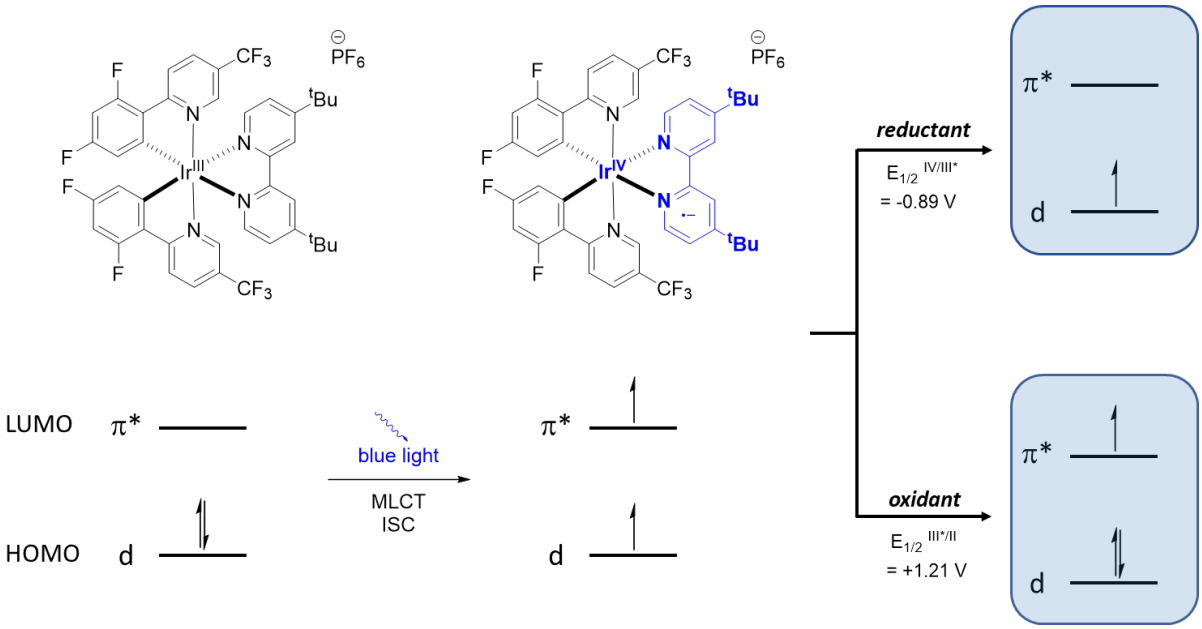

Scheme 5: Illustration of the basic concepts of photoredox catalysis[10-11]

1.4 Proposed mechanism

Previous efforts in the Rovis group have led to the postulation of a proposed reaction mechanism as shown in Scheme 6. The N-H bonds of trifluoroacetamides are sufficiently acidic to be deprotonated using bases like K_3PO_4 or even Cs_2CO_3 as the pK_a of the N-H bond is about 13.6. The nitrogen anion resulting from such deprotonation is oxidized by the excited state of the photocatalyst to give an electrophilic nitrogen radical. Subsequent *[1,5]*-HAT delivers a nucleophilic carbon-centered radical at the δ-position of the aliphatic amine. For the cyanation reaction, an attack of the nucleophilic carbon radical at the cyanide-source is proposed. Subsequent β-scission will yield the desired δ-cyanated product and a resulting radical species originating from the cyanide-source. This reaction step from the *[1,5]*-HAT product to the δ-cyanated product can also be called radical trapping of the nucleophilic carbon radical by a suitable radical trap or coupling partner. The thereby formed remaining radical species will then be reduced by the oxidized state of the photocatalyst to regenerate the ground state of the photocatalyst and thereby complete the catalytic cycle.

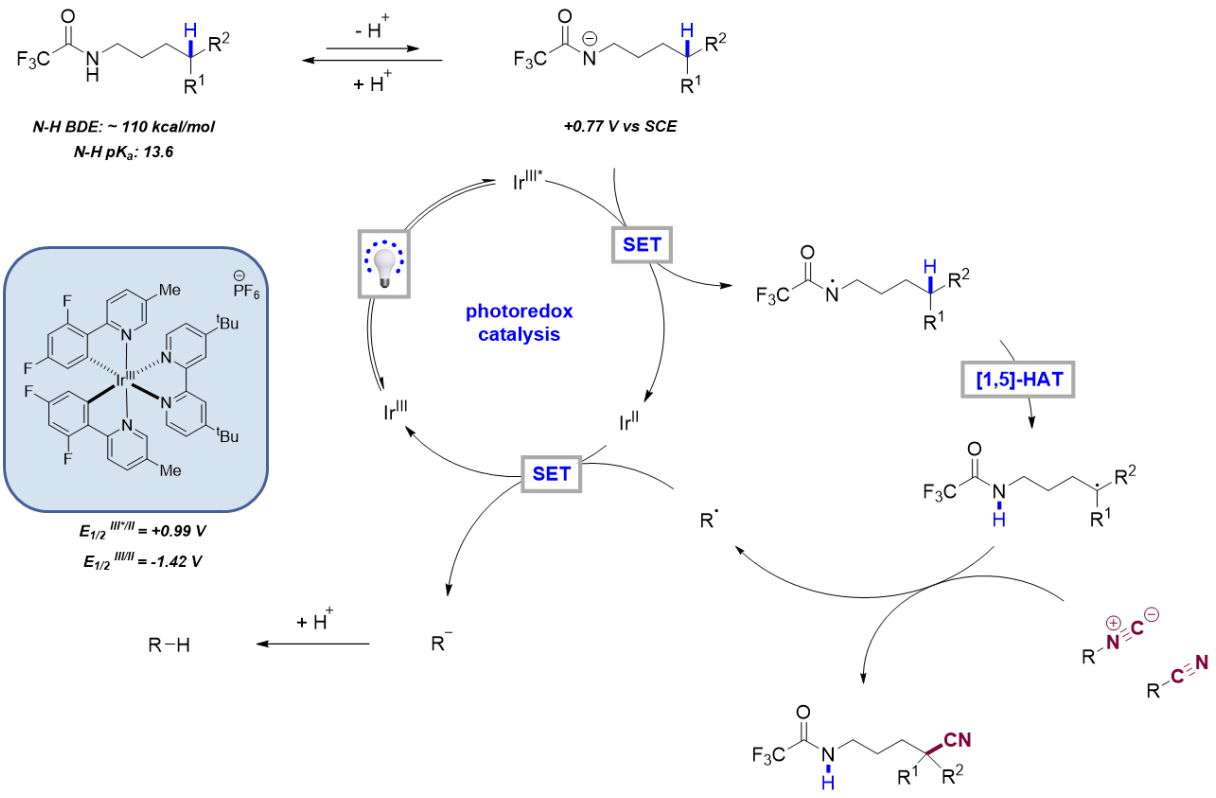

Scheme 6: Proposed reaction mechanism of the desired δ-cyanation at aliphatic amines

2. Results and discussion

2.1 Preparation of molecular probes

2.1.1 Preparation of the trifluoroacetamide starting material **4**

In order to perform optimization screens towards a sufficiently high yield of the attempted δ-cyanation reaction as shown in Scheme 6 in chapter *1.4 Proposed mechanism* first, a suitable trifluoroacetamide substrate had to be prepared. Compound **4** was chosen as that substrate, as it showed all required properties for a suitable test substrate (Scheme 7). Those requirements were being a protected amine with a free NH group and an oxidation potential within the range of the most common photoredox catalysts. Further, the aliphatic amine had to possess a C(sp^3)-H bond at the δ-position to participate in a *[1,5]*-HAT event. Preferably, this δ-position had to be a tertiary position, as radical stability trends and earlier work in the Rovis group[2] suggested, that tertiary substrates would give the best yields.

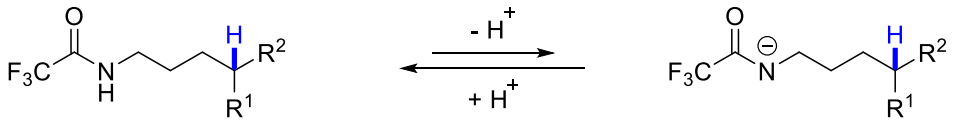

4

N-H BDE: ~ 110 kcal/mol
N-H pK_a: 13.6

+0.77 V vs SCE

*Scheme 7: Compound **4**, its deprotonation product and notable properties of them*

Therefore, compound **4** was synthesized following a three step literature procedure[1] (Scheme 8). After activation of the carboxylic acid **1** by acid chloride formation, crude amide **2** was obtained with a yield of 88% after nucleophilic substitution with aq. NH_3. Upon reduction of species **2** with LAH to compound **3** with a yield of 58%, the synthesis of substrate **4** was completed by introduction of the trifluoroacetamide protection group under basic conditions with a yield of 60%. Overall a yield of 30% was obtained after three steps, which is comparable to the literature[1] yield (32%, three steps).

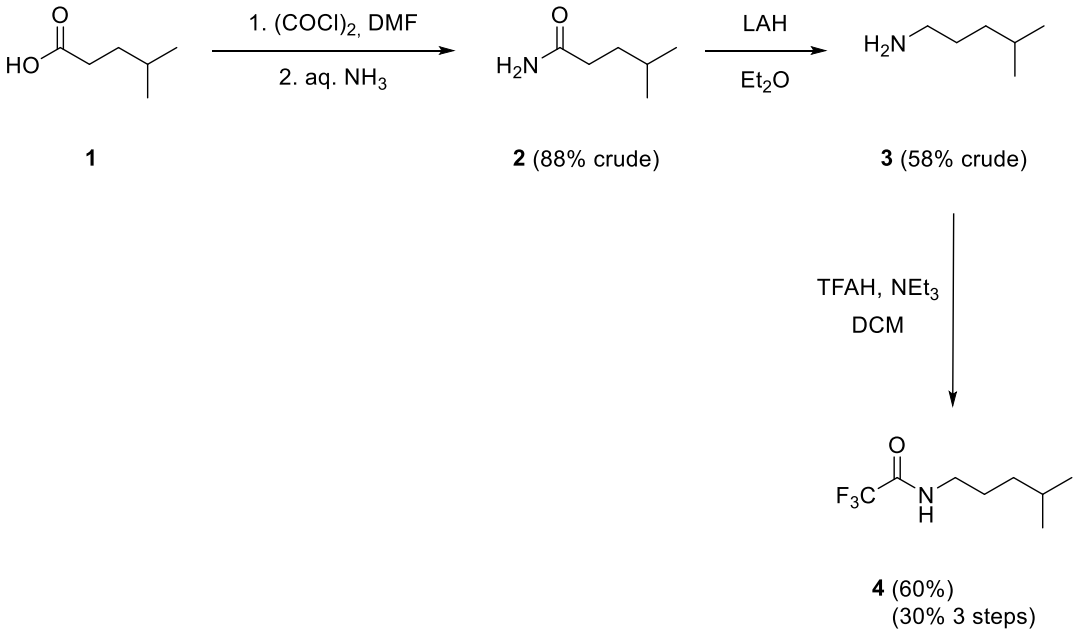

1

2 (88% crude)

3 (58% crude)

4 (60%)
(30% 3 steps)

*Scheme 8: Synthetic route towards trifluoroacetamide substrate **4***

2.1.2 Preparation of isocyanides

A library of several isocyanides was synthesized in order to test them as cyanide-sources. Different substitution patterns, substituents and overall scaffolds were planned to be synthesized in order to test trends regarding radical stability and kinetics of the radical trapping step of the mechanism.

Starting from the amino acid **5**, crude compound **6** was obtained in good yield after esterification and chloride formation following a literature procedure[12] (Scheme 9). Another literature procedure[13] resulting in high yield for esterification and tosyl-salt formation was used for the synthesis of compound **10** starting from compound **9** (Scheme 10).

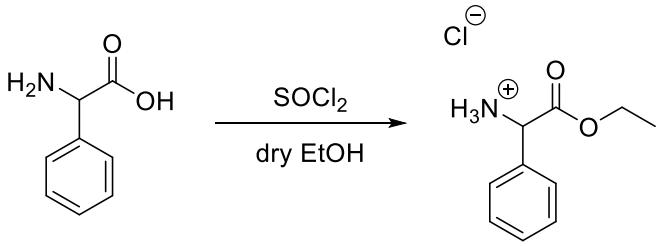

5 **6** (94% crude)

*Scheme 9: Synthesis of compound **6***

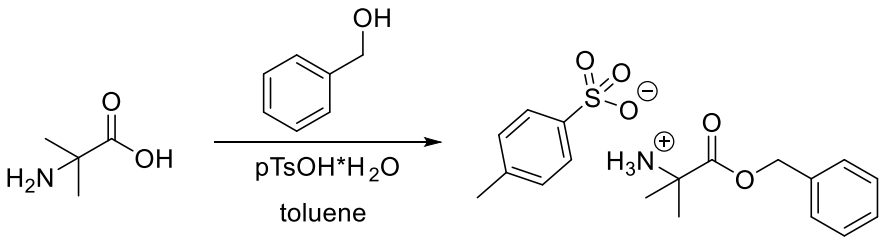

9 **10** (86% crude)

*Scheme 10: Synthesis of compound **10***

With the salts **6** and **10** and the commercially available compounds **17** and **20** in hand, the next step was the formation of the free amines followed by formylation of those intermediates towards **7**, **11**, **18** and **21**. For all of these compounds the same literature procedure[12] to liberate the amine and another literature procedure[14] to form the formamide were used successfully with satisfying yields (Scheme 11). Both steps were quantitative in the literature[12, 14], the lower yields for compounds **18** and **21** are due to material loss during the extractions of the liberated amines.

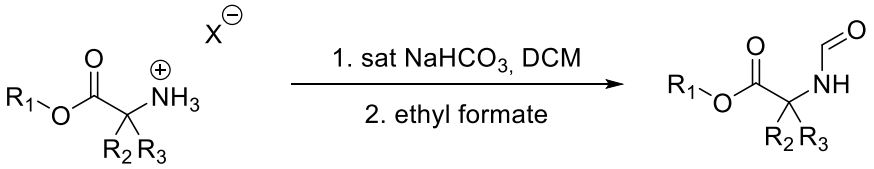

6 R_1 = Et R_2 = Ph R_3 = H X^- = Cl^-
10 R_1 = Bn R_2 = Me R_3 = Me X^- = Tos^-
17 R_1 = Et R_2 = Ph R_3 = H X^- = Cl^-
20 R_1 = t-Bu R_2 = Me R_3 = H X^- = Cl^-

7 R_1 = Et R_2 = Ph R_3 = H (quant.)
11 R_1 = Bn R_2 = Me R_3 = Me (98%)
18 R_1 = Et R_2 = Ph R_3 = H (63%)
21 R_1 = t-Bu R_2 = Me R_3 = H (76%)

*Scheme 11: Towards the formamide compounds **7, 11, 18** and **21** via formation of the free amines of **6, 10, 17** and **20** and the formylation of those*

Next, isocyanide formation by dehydration of the formamides **7**, **11**, **18** and **21** in the presence of an amine base was attempted using a protocol from the same literature source[14] as used for the prior step. However, slight modifications to the literature procedure were necessary as the base DIPA was not available during first attempts of the isocyanide formation. Therefore, DIPA was substituted by Et_3N in most of the reactions. $POCl_3$ was used as dehydrating agent (Scheme 12).

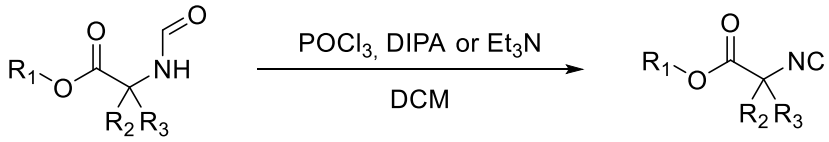

7 R_1 = Et R_2 = Ph R_3 = H
11 R_1 = Bn R_2 = Me R_3 = Me
18 R_1 = t-Bu R_2 = H R_3 = H
21 R_1 = t-Bu R_2 = Me R_3 = H

8 R_1 = Et R_2 = Ph R_3 = H (0%)
12 R_1 = Bn R_2 = Me R_3 = Me (44%)
19 R_1 = t-Bu R_2 = H R_3 = H (66%)
22 R_1 = t-Bu R_2 = Me R_3 = H (0%)

*Scheme 12: Isocyanide formation via dehydration of compounds **7, 11, 18** and **21***

The synthesis of compounds **12** and **19** could be completed without complications albeit only with moderate yields. Literature[14] yields for that reaction step are 76% and 87%. Compound **12** was obtained using Et_3N as base, while DIPA was used for the synthesis of compound **19**. This suggests, that the choice of the base does not influence the outcome of the reaction as long as an amine base is used.

However, the desired products **8** and **22** could not be obtained, neither using DIPA nor Et_3N as base. As both of those compounds are mono-substituted at the α-position to the formamide, the hypothesis that this substitution pattern might shut down the reaction mechanism was postulated. Compounds **8** and **22** would have been desirable test reagents for the δ-cyanation as they would have formed secondary radicals upon radical trapping, which would have shown moderate stability. However, as other cyanide-sources had already shown promising results at the time of these syntheses, no attempts to synthesize compounds **8** and **22** through other routes were conducted.

Following up the dissatisfying results regarding the syntheses of compounds **8** and **22**, synthesizing different secondary isocyanides through another approach was considered. Therefore, nucleophilic substitution employing compound **13** was attempted in order to provide benzylated compound **14a**

similar to a literature procedure[15]. However, the product obtained was not the mono-substituted compound **14a** but the disubstituted compound **14** (Scheme 13). Even though substrate **14** was not the expected product, it could still be utilized in later screens.

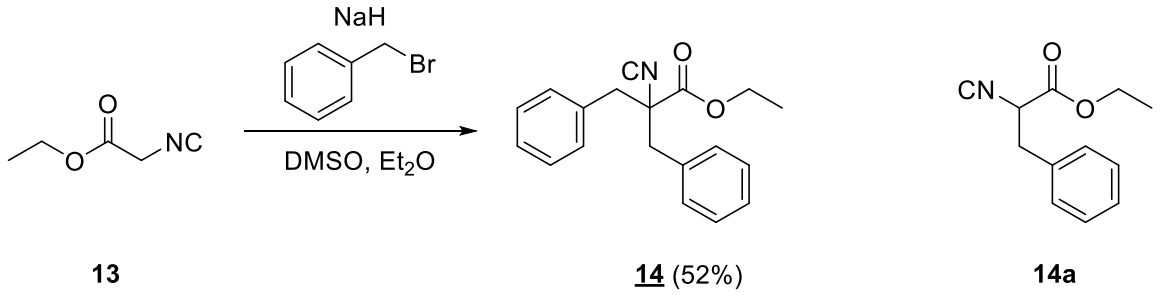

*Scheme 13: Synthesis of disubstituted compound **14** instead of mono-substituted compound **14a***

In order to synthesize further tertiary isocyanides, as those seemed to be the best cyanide-sources, the introduction of a cyclohexylring *via* a double nucleophilic substitution at compound **13** towards compound **15** was conducted. The procedure as found in the literature[15] yielded compound **15** in satisfying amounts. Following the same literature procedure[15], compound **16** was synthesized and compound **23** could be obtained successfully after the synthesis of compound **19** as starting material (Scheme 14). The literature[15] yields for compounds **15** and **16** were 56% and 54%.

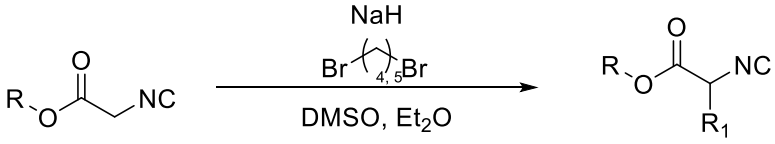

13 R = Et
19 R = t-Bu

15 R = Et R_1 = cyclohexyl (52%)
16 R = Et R_1 = cyclopentyl (68%)
23 R = t-Bu R_1 = cyclohexyl (70%)

*Scheme 14: Syntheses of compounds **15**, **16** and **19** via a double nucleophilic substitution*

2.1.3 Preparation of the Ir^{III}-photocatalyst

Photocatalyst **27** was prepared following a literature procedure[16] for all required steps. First, ligand **26** was synthesized. Through a Suzuki cross-coupling of the adequate boronic acid **24** and the halogenated aromatic compound **25**, ligand **26** was obtained as colorless crystals after elaborate purification due to incomplete conversion (Scheme 15). In addition, a slightly impure fraction of 1.008 g (28%, crude) was collected for later purification.

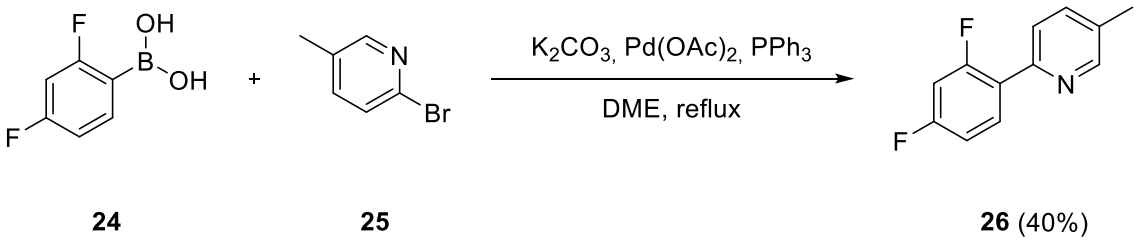

24 **25** **26** (40%)

*Scheme 15: Suzuki cross-coupling of substrates **24** and **25** towards ligand **26***

With ligand **26** in hand, the first step of the synthesis towards photocatalyst **27** was the formation of a chloro-bridged dimeric species of the Ir^{III}-photocatalyst. This was achieved by refluxing ligand **26** with $Ir^{III}Cl_3$ hydrate overnight in a solvent mixture of 2-methoxyethanol and water. The obtained dimer was then treated with dtbbpy in order to give compound **27** by ligand exchange (Scheme 16). The literature[16] yields for the ligand preparation and the photocatalyst synthesis through dimerization and ligand exchange were both typically between 60% and 80%.

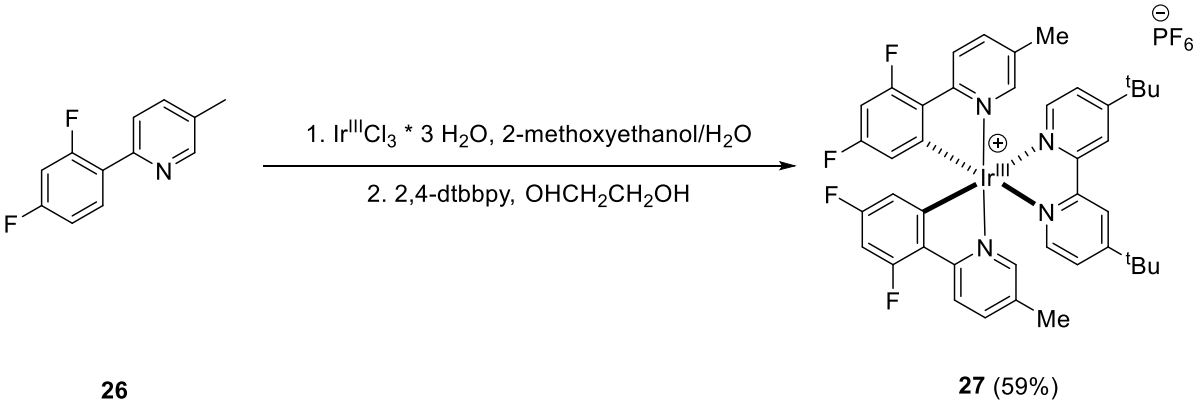

26 **27** (59%)

*Scheme 16: Two-step synthesis of photocatalyst **27** by dimerization and ligand exchange*

2.2 Optimization of the initial reaction conditions

An initial hit for the attempted δ-cyanation reaction had already been obtained in the Rovis group prior to the work described in this thesis. Thereby substrate **4** was exposed to reaction conditions as shown in Scheme 17 resulting in an NMR yield of 11% of the desired compound **28**. With this initial reaction conditions to work with several screens were performed testing different cyanide-sources, photocatalysts, solvents, bases and concentrations. Additionally, screens testing different reaction times, reaction temperatures and further hypotheses were conducted. All these screens will be described in this following chapters.

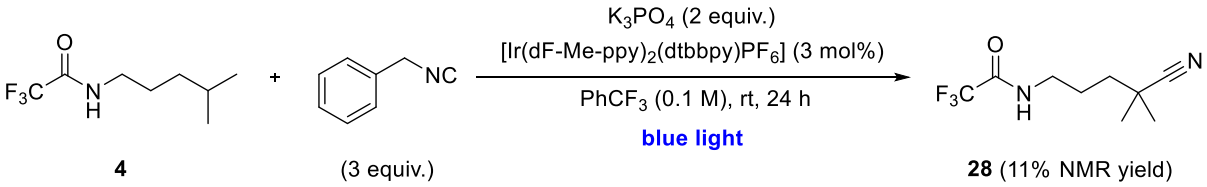

*Scheme 17: Reaction conditions with which the initial hit for the δ-cyanation of an aliphatic amine **4** was obtained*

2.2.1 Optimization of the cyanide-source

According to the mechanism shown in Scheme 6 in *1.4 Proposed mechanism*, isocyanides as well as cyanides were considered to be proper cyanide-sources for the photoredox catalyzed δ-cyanation of aliphatic amines like substrate **4**. This is further illustrated in Scheme 18. Using the same reaction conditions as the ones that gave the initial hit for compound **28,** several isocyanide and cyanide screens were conducted using blue light with a wavelength of 450 nm.

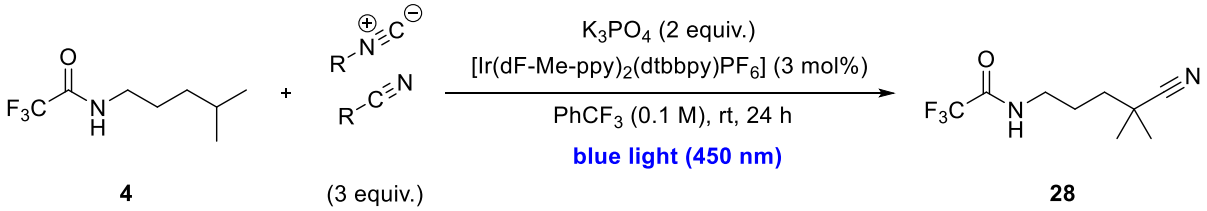

Scheme 18: Reaction conditions used screening for the best cyanide-source - either an isocyanide or cyanide

Designing those screens, a couple of aspects had to be considered thinking of a reasonable scope of isocyanides and cyanides to be tested. The proposed mechanism with β-scission after the radical trapping of the nucleophilic carbon radical by the cyanide-source suggested that the structure of the organic residue R* had to fit several criteria illustrated in Scheme 19. First, the formed radical R* had to be stable enough to be favorably formed competing with the nucleophilic carbon radical obtained after *[1,5]*-HAT. Further, the radical R* formed by β-scission had to be reduceable by the used photocatalyst in order to close the photocatalytic cycle.

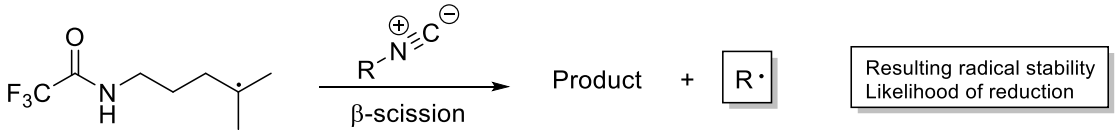

Scheme 19: Proposed mechanism of β-scission towards a R radical species and its crucial properties*

A recent publication of the Rovis group[2] had shown that compounds similar to those depicted in Scheme 20 should be able to be reduced by photocatalyst **27** which was used for the initial screens. Therefore, an ester scaffold was used as basis scaffold for the design of most of the isocyanides synthesized during this thesis and ordered for screens.

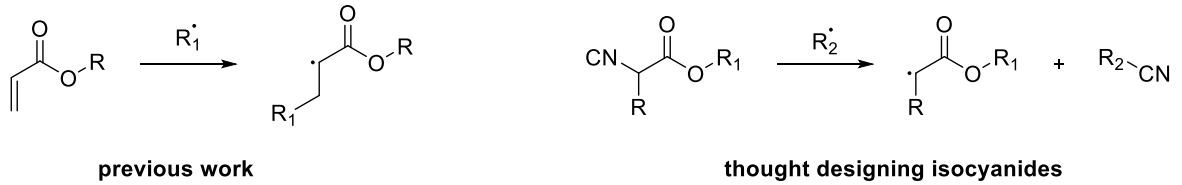

Scheme 20: The substrate used in a paper from the Rovis group[2] and the thereof evolved idea for the isocyanide design for this work

The isocyanides and cyanide tested during the first screens are shown in Scheme 21. Isocyanides **12**, **14** and **15** were synthesized prior to the test reactions as described in chapter *2.1.2 Preparation of isocyanides*, all other substrates were purchased. Trimethylsilyl cyanide was screened as one of the first substrates and no product formation could be observed. As this substance is known[17] to be a working radical trap, it was reasoned that its poor radical trap behavior in the δ-cyanation reaction might be due to the weaker charge distribution of the cyanide group compared to the isocyanide group. This weaker charge distribution would make an attack of the cyanide by the nucleophilic carbon radical as proposed in chapter *1.4 Proposed mechanism* less likely and slower than a similar attack of the radical species at an isocyanide. Furthermore, the carbon of the cyanide group is more sterically hindered to participate in a reaction than the carbon of the isocyanide group. Therefore, no further cyanides were screened as cyanide-sources.

Further screens showed that tertiary isocyanides gave the highest NMR yields as long as their organic residues were not too bulky, which can be easily seen by comparison of the reaction yields of compounds **12**, **14** and **15** (Scheme 21). Going alongside the highest observed NMR yield throughout the screen, compound **15** was chosen as cyanide-source for subsequent screens.

Even though they were not the highest yielding substrates, the results with α-methylbenzylisocyanide and 1,1,3,3-tetramethylbutylisocyanide should be noted too. α- Methylbenzylisocyanide gave a pretty good NMR yield of 30% as a commercially available secondary substrate (Scheme 21). The tertiary carbon radical formed by 1,1,3,3-tetramethylbutylisocyanide after radical trapping should not be able to be reduced by the photocatalyst at all but somehow 20% yield were observed by NMR, anyway. Therefore, both of those cyanide-sources were revisited at a later point in the optimization process (*vide infra, 2.3.4 Revisiting isocyanides*).

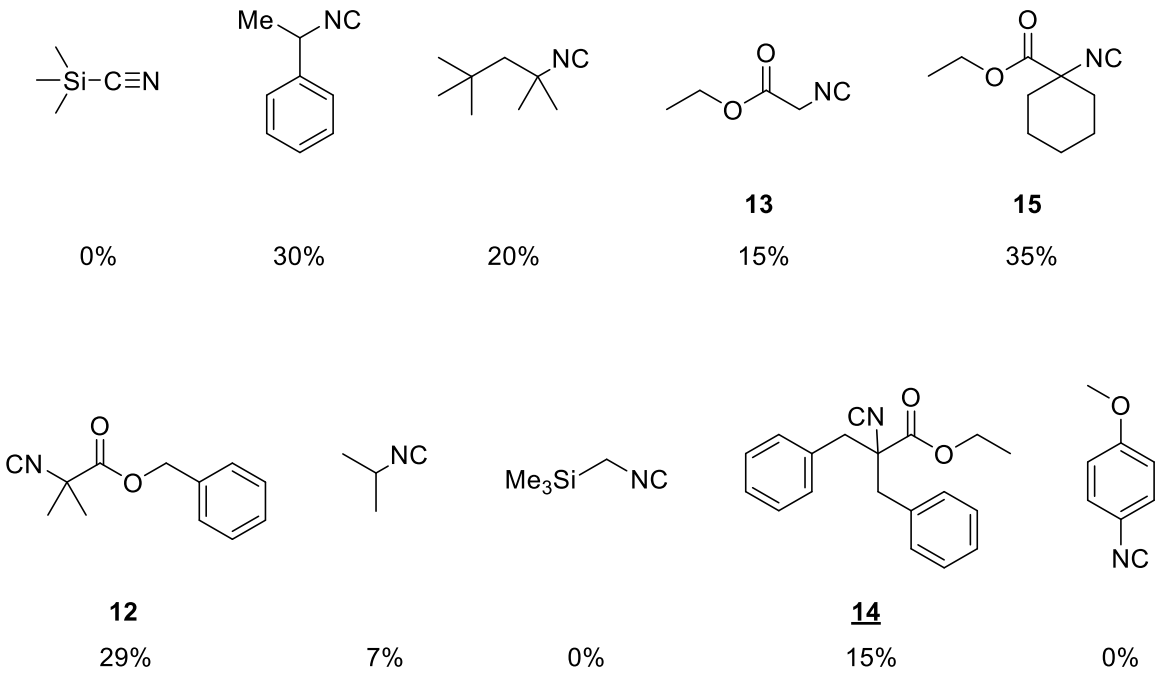

Scheme 21: NMR yields for the isocyanides and cyanide screened in a first cyanide-source screen

2.2.2 Optimization of the photocatalyst

After compound **15** was chosen as cyanide-source, screens testing different photocatalysts were conducted. The reaction conditions for those screens are shown in Scheme 22, blue light with a wavelength of 450 nm was used. Overall eight different photocatalysts were tested including several Ir^{III}-photocatalysts, one Ru^{II}-photocatalyst, one acrdinium salt (structure see Scheme 23) and 4CzIPN as organic catalyst. The obtained NMR yields as well as the exact formulas of the photocatalysts are listed in Table 1. For the tested Ir^{III}-photocatalysts degradation could be monitored *via* ^{19}F-NMR analysis. Photocatalysts 1 to 4 showed two to three different sets of signals in the ^{19}F-NMR corresponding to the signals of the PF_6^--counterion, the two fluorine substituents at the ppy ligands and the CF_3-group at the ppy ligand. Through comparison of the signals of the two fluorine substituents at the ppy ligands from the pure photocatalysts to the signals of the two fluorine substituents at the ppy ligands from the photocatalysts after the reactions, photocatalyst degradation could be studied. The signals for the fluorine substituents at the ppy ligands showed a chemical shift of about -105 ppm to -110 ppm. That chemical shift region is typical for sp^2 signals in fluorine NMR spectroscopy. Therefore, photocatalyst degradation was monitored by observing changes in the signal patterns of the sp^2 region in the ^{19}F-NMRs.

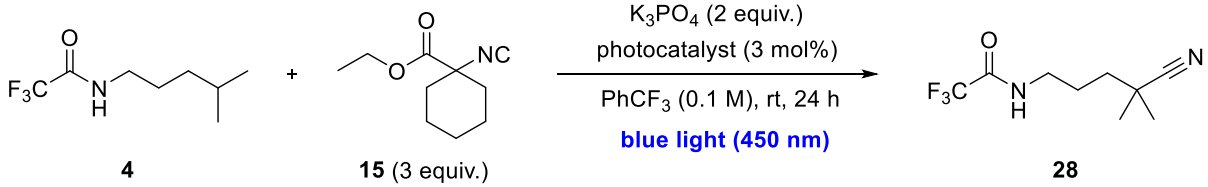

Scheme 22: Reaction conditions used to screen several photocatalysts

Table 1: Overview of the screened photocatalysts and the obtained results

entry	photocatalyst	cat. degr. sp^2 region	yield NMR
1	$[Ir(dF\text{-}CF_3\text{-}ppy)_2(dtbbpy)PF_6]$	yes	36%
2	$[Ir(dF\text{-}Me\text{-}ppy)_2(dtbbpy)PF_6]$	yes	36%
3	$[Ir(dF\text{-}OMe\text{-}ppy)_2(dtbbpy)PF_6]$	yes	34%
4	$[Ir(dF\text{-}CF_3\text{-}ppy)_2(phen)PF_6]$	yes	26%
5	4CzIPN	/	16%
6	$Ru(bpm)_3Cl_2$	/	0%
7	acridinium salt	/	12%
8	$Ir(ppy)_3$	/	4%

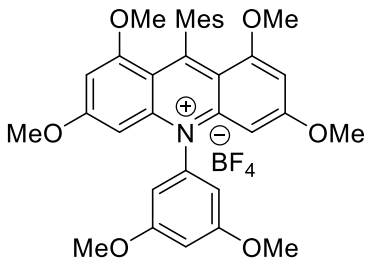

Scheme 23: Structure of the acridinium salt used for photocatalyst screen number 7

As it can be seen in Table 1, photocatalysts 1 and 2 gave about the same NMR yield. As it was known from earlier work in the Rovis group[18], photocatalyst 2 tends to show slightly higher yields in similar reactions to the δ-cyanation. Furthermore, the oxidation and reduction potential of photocatalyst 2 seemed to be preferential for the desired reaction compared to the ones of photocatalyst 1, as will be emphasized further in later test reactions (*vide infra*, *2.3.1 Mass balance and ethylcyclohexanecarboxylate **15a** formation*). Photocatalysts 1 and 2 and their oxidation and reduction potentials that are relevant for the reaction mechanism are depicted in Scheme 24.

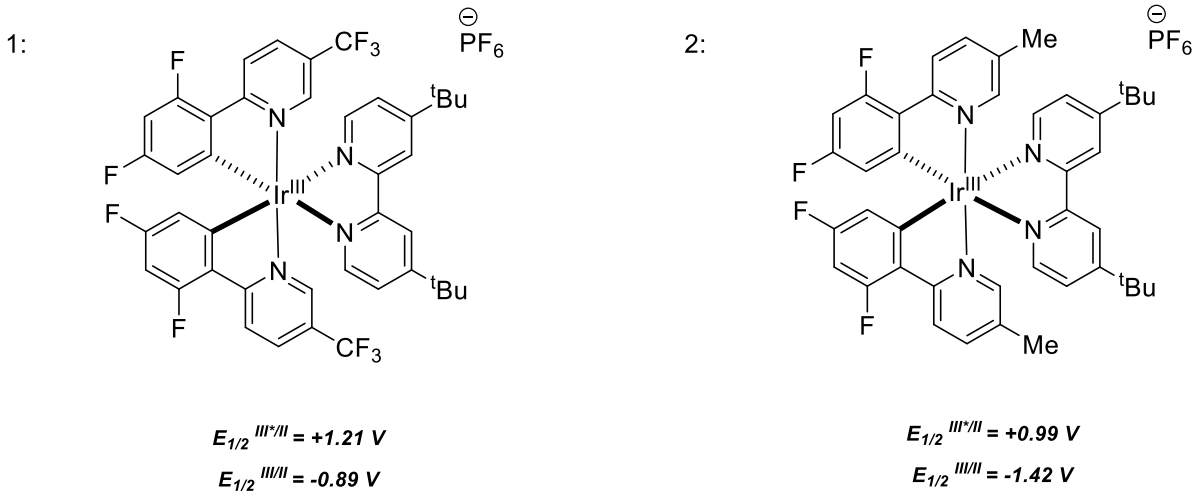

Scheme 24: Photocatalysts 1 ([Ir(dF-CF_3-ppy)$_2$(dtbbpy)PF_6]) and 2 ([r(dF-Me-ppy)$_2$(dtbbpy)PF_6]) and their oxidation and reduction potentials relevant for the reaction mechanism

2.2.3 Optimization of the solvent

Following the cyanide-source and the photocatalyst screens, elaborate solvent screens were conducted (Scheme 25). As solvent effects tend to play an important and often unpredictable role in photochemical reactions, a first elaborate screen with isocyanide **13** was conducted. Since isocyanide **13**, unlike the highest yielding isocyanide **15**, was commercially available and therefore not as valuable a reagent, it could be used in elaborate screens more easily than compound **15**.

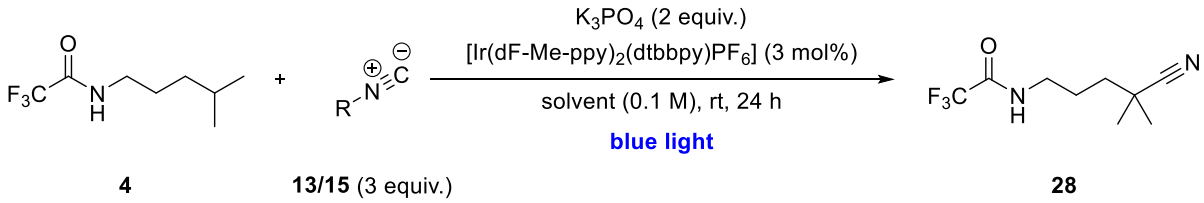

Scheme 25: Reaction conditions used for the conducted solvent screens

The solvent screen conducted with isocyanide **13** included 18 solvents overall. The results for all 18 solvents are shown in Table 24 in the appendix ordered by decreasing yield, the results for the eight most interesting solvents are shown in Table 2. As it can be seen, quite a lot of solvents gave higher yields than trifluorotoluene as it was used in screens up to then. The one solvent that deserves special attention is mesitylene. The obtained result of 35% NMR yield was not expected but was reasoned to be due to H-atom donor effects of the solvent. However, as mesitylene has an inconveniently high boiling point, which leads to elaborate workups, *p*-xylene was tested as substitute solvent for mesitylene. With toluene as solvent a high yield was observed as well. The yields obtained for mesitylene and *p*-xylene were about the same using isocyanide **13** as cyanide-source.

*Table 2: Obtained yields and cat. degr. for the eight most interesting solvents of the solvent screen with isocyanide **13***

entry	solvent	cat. degr. sp^2 region	yield NMR
1	mesitylene	yes	35%
2	*p*-xylene	yes	34%
3	toluene	yes	29%
4	acetonitrile	no	24%
5	cyclohexane	no	20%
6	dioxane	yes	20%
7	hexane	no	16%
8	$PhCF_3$	no	12%

Moving on to solvent screens with compound **15**, the eight best solvents from the screens with isocyanide **13** shown in Table 2 were used. Additionally, mesitylene with some water was tested as solvent system in order to see if increased base solubility through water addition would improve the obtained yield. The results for those screens are listed in Table 3, again with decreasing NMR yield. The first five entries shall be discussed further.

Mesitylene showed a far higher NMR yield than the other solvents. An isolated yield of compound **28** of 60% was obtained for mesitylene as solvent in addition to the observed NMR yield of 70%. In contrast to the solvent screen with compound **13**, the NMR yield with *p*-xylene was way lower this time than the yield with mesitylene. This meant that *p*-xylene was no longer an appropriate substitute for mesitylene as solvent. Furthermore, the solvent system mesitylene/water showed a drastically decreased yield compared to sole mesitylene as solvent. This suggested that water shuts down the reaction. As *p*-xylene and toluene showed about the same yield, they were both used in later base and concentration screens so no differences in their behavior might be missed. Last, cyclohexane as solvent should be pointed out. Even though the observed yield by NMR was lower than with mesitylene, *p*-xylene and toluene the photocatalyst degradation seemed to be less in cyclohexane compared to those three solvents. As less photocatalyst degradation should overall be beneficial for the reaction, cyclohexane was also included in subsequent base and concentration screens as discussed in chapter *2.2.4 Optimization of the used base and the reaction concentration*.

*Table 3: Obtained yields and catalyst degradation for the solvent screens conducted with isocyanide **15***

entry	solvent	cat. degr. sp^2 region	yield NMR
1	mesitylene	yes	70% (60% isolated)
2	toluene	yes	54%
3	*p*-xylene	yes	51%
4	cyclohexane	no	48%
5	mesitylene + 40 µL H_2O	yes	46%

6	$PhCF_3$	yes	34%
7	dioxane	yes	29%
8	acetonitrile	yes	18%
9	benzonitrile	no	16%

To sum up, elaborate solvent screens with isocyanides **13** and **15** were conducted. Mesitylene, *p*-xylene, toluene and cyclohexane were found to be the most beneficial solvents for the desired δ-cyanation reaction. No side reactions and side products could be observed in any of the solvents at this point. The improved yield in mesitylene was explained by its H-atom donor properties. Mesitylene was not chosen as reaction solvent due to its high boiling point.

2.2.4 Optimization of the used base and the reaction concentration

The base screens were tightly coupled to the results of the solvent screen and the conduct of the concentration screens. This led to the base and concentration screens being performed in parallel. Initial base screens were conducted using K_3PO_4, K_2CO_3, Na_2CO_3, Cs_2CO_3 and quinuclidine as bases in cyclohexane and toluene as solvents. The reaction conditions used are depicted in Scheme 26, the results are listed in Table 4.

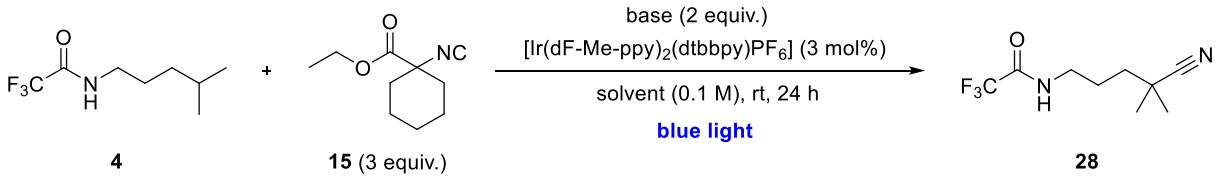

Scheme 26: Reaction conditions used for the conducted base screens in different solvents

Table 4: Results for the initial base screens in toluene and cyclohexane

entry	base	solvent	cat. degr. sp^2 region	yield NMR
1	K_3PO_4	toluene	yes	54%
2	K_2CO_3	toluene	yes	26%
3	Na_2CO_3	toluene	no	0%
4	Cs_2CO_3	toluene	yes	43%
5	quinuclidine	toluene	n.d.	0%
6	K_3PO_4	cyclohexane	no	48%
7	K_2CO_3	cyclohexane	no	31%
8	Na_2CO_3	cyclohexane	no	0%
9	Cs_2CO_3	cyclohexane	no	54%
10	quinuclidine	cyclohexane	n.d.	0%

These initial base screens revealed that different bases gave the highest yields in toluene and cyclohexane (Table 4). In toluene K_3PO_4 gave the highest NMR yield with 54% whereas Cs_2CO_3 yielded only 43% in toluene. In cyclohexane Cs_2CO_3 gave the highest NMR yield with 54% and K_3PO_4 yielded only 48%. According to those results the subsequent concentration screens were conducted with several different base-solvent systems. Overall four base-solvent systems were screened using four different concentrations during the concentration screens. The full results for those screens can be found in Table 25 in the appendix, the results for the system Cs_2CO_3 in cyclohexane are shown in Table 5.

Table 5: Results for the concentration screen conducted with Cs_2CO_3 in cyclohexane as solvent

entry	conditions	concentration	cat. degr. sp^2 region	yield NMR
1	cyclohexane, Cs_2CO_3	0.05 M	no	65%
2	cyclohexane, Cs_2CO_3	0.1 M	no	54%
3	cyclohexane, Cs_2CO_3	0.2 M	no	53%
4	cyclohexane, Cs_2CO_3	0.4 M	no	46%

Looking at the results in Table 25 it can be seen that K_3PO_4 did not impact the observed yields at all. In comparison to that, a lower concentration seemed to be beneficial for reactions conducted with Cs_2CO_3 in cyclohexane as the results in Table 5 show, even though no trend could be observed for the system Cs_2CO_3 and *p*-xylene (Table 25).

Considering all results obtained during those screens and the pK_a values of the bases used, two trends following the solubility of the counterion and the pK_a value of the base could be observed as depicted in Scheme 27. The δ-cyanation reaction is a heterogeneous reaction as neither the photocatalyst nor the base fully dissolve. Therefore, higher solubility of the base increases the reaction yield as results from the initial base screen confirm (Table 4). Solubility of bases goes alongside the size of their counterions – bigger counterions can be solubilized more easily. Therefore, Caesium was concluded to be the most beneficial counterion.

counterion
Na^+
K^+
Cs^+

increasing solubility

conj. base	pK_a
SO_4^{2-}	6.91
CO_3^{2-}	10.25
PO_4^{3-}	12.5
OH^-	15.7

increasing basicity

Scheme 27: Basicity and solubility trends observed for different conjugated bases and their counterions

Next, pK_a values of some common conjugated bases were compared to the pK_a value of the trifluoroacetamide substrate **4,** which is 13.6 (see Scheme 7). In order to obtain fully deprotonated trifluoroacetamide, a base with a pK_a value higher than substrate **4**'s one would be needed. As actually neither PO_4^{3-} nor CO_3^{2-} have a higher pK_a value than substrate **4**, it was concluded that the reaction could take place with only a small amount of deprotonated trifluoroacetamide in the reaction mixture.

Moreover, it was observed that the solubility of the base seemed to impact the reaction kinetics more than the base's actual pK_a value. This was reasoned as Cs_2CO_3 gave a far higher yield in cyclohexane though its lower pK_a value than K_3PO_4 did. The argument, that a better base solubility as achieved by larger counterions improves the yield, goes alongside the fact, that higher yields are observed for lower reaction concentrations in systems with Cs_2CO_3 but not for systems with K_3PO_4. K_3PO_4 seems to have too low of a solubility in the tested solvents to show a trend with concentration, whereas Cs_2CO_3 seems to have a sufficiently high solubility to show a beneficial concentration effect.

Considering the trends depicted in Scheme 27 a couple of more bases were decided to be tested. It was concluded that Cs_3PO_4 might be a good base for the desired δ-cyanation reaction, but unfortunately that base was not commercially available. Another base that seemed reasonable to test was CsOH as the pK_a of OH^- with -15.7 is lower than the pK_a of substrate **4** and Cs^+ as counterion should assure good solubility. Furthermore, Cs_2SO_4 was tested too because of its assumed good solubility albeit low basicity and its availability. KOH was tested due to its high basicity. The results of those second base screens are shown in Table 6. Those screens were conducted using photocatalyst [Ir(dF-Me-ppy)$_2$(dtbbpy)PF_6], three equivalents of isocyanide **15** and 0.05 M cyclohexane for 24 h at rt with blue light (427 nm) as reaction conditions.

Table 6: Results of the second base screen with Cs_2SO_4, KOH and CsOH

entry	base	pK_a	cat. degr. sp^2 region	yield NMR
1	Cs_2SO_4	6.91	no	0%
2	KOH	15.7	yes	7%
3	CsOH (50%wt in H_2O)	15.7	yes	15%

Unfortunately, those three bases did not show any improved reaction yields. To the contrary, the OH^- bases mainly decomposed the starting material giving a low yield for the desired product. Cs_2SO_4 on the other hand seemed to be too weak a base to give any reactivity at all.

Considering all the results obtained during these elaborate base and concentration screens the base-solvent system Cs_2CO_3 in cyclohexane was chosen for further optimizations and test reactions as the observed yield of 65% by NMR was only outperformed by the yield achieved in mesitylene with K_3PO_4.

2.2.5 Testing different reaction times, temperatures, base equivalents and isocyanide equivalents

With the improved reaction conditions as shown in Scheme 28, further screens testing factors like reaction time, reaction temperature, base equivalents and isocyanide equivalents were conducted. As catalyst degradation did not seem to be as severe in cyclohexane as solvent compared to toluene or *p*-xylene, an improved yield was expected for longer reaction times. Regarding the reaction temperature a higher temperature was reasoned to increase the reaction rate and maybe increase the solubility of the heterogenous reaction compounds. Base equivalents were varied to gain a better understanding of the kinetics and the role of the base in the reaction. In addition, varying the

isocyanide equivalents was expected to display if an excess of isocyanide was necessary to accelerate the reaction or if stochiometric amounts would give the same yield.

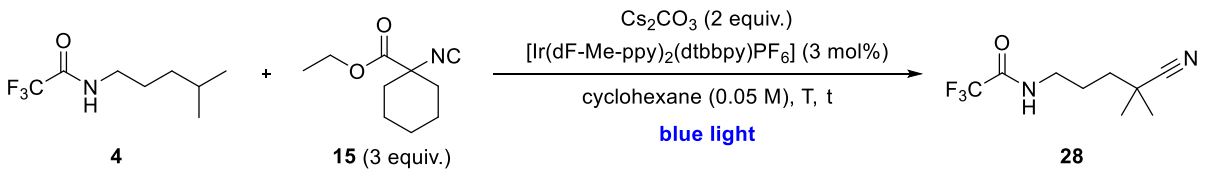

Scheme 28: Optimized reaction conditions for the δ-cyanation after cyanide-source, photocatalyst, solvent, base and concentration screens

The results and exact conditions of the conducted screens are shown in Table 7 to Table 10. A longer reaction time unfortunately did not increase the yield, neither did a higher reaction temperature nor varying the base equivalents. A stochiometric amount of isocyanide together with a stochiometric amount of base did show nearly the same yield as the former optimized reaction conditions with three equivalents of isocyanide **15** and two equivalents of base. As stochiometric amounts of reagents are preferable to excess reagents, these results were valuable for later substrate scope reactions. However, further screens were still conducted with three equivalents of isocyanide **15** and two equivalents of base for better comparability of the results. Once the reaction will yield about 80-90%, revisiting those stochiometric amounts of reagents will be interesting to see if the yield will still stay the same. If so, the substrate scope can be conducted with stochiometric conditions instead of excess reagents.

Table 7: Results for several reaction conditions after 45/48 hours reaction time

entry	conditions	t	cat. degr. sp^2 region	yield NMR
1	cyclohexane, K_3PO_4, 0.1 M	48 h	no	51%
2	cyclohexane, Cs_2CO_3, 0.1 M	48 h	no	49%
3	cyclohexane, Cs_2CO_3, 0.05 M	45 h	no	60%

Table 8: Results for several reaction temperatures using otherwise optimized reaction conditions as shown in Scheme 28

entry	conditions	T	cat. degr. sp^2 region	yield NMR
1	optimized	40°C	some	42%
2	optimized	rt	no	65%
3	optimized	22°C	no	57%

Table 9: Results for screens varying base equivalents and reaction time using otherwise optimized reaction conditions as shown in Scheme 28

entry	conditions	base + time	cat. degr. sp^2 region	yield NMR
1	optimized	1 equiv, 24 h	no	62%
2	optimized	2 equiv, 24 h	no	65%
3	optimized	3 equiv, 24 h	some	62%
4	optimized	1 equiv, 48 h	some	62%
5	optimized	2 equiv, 48 h	some	60%
6	optimized	3 equiv, 48 h	some	61%

*Table 10: Results using stochiometric amounts of isocyanide **15** and varying base equiv., otherwise optimized reaction conditions as shown in Scheme 28*

entry	conditions	isocyanide 15 and base equiv.	cat. degr. sp^2 region	yield NMR
1	optimized	1 and 2	some	62%
2	optimized	1 and 1	some	63%

Categorizing longer reaction times, a higher reaction temperature and more base equivalents as harsher reaction conditions, it can be said that such harsher reaction conditions generally lead to more photocatalyst degradation as well as more starting material decomposition but not to a higher yield. In case of an increased reaction temperature the yield dropped. Overall, these screens showed that the desired reaction seemed to be sensitive to harsh reaction conditions. This emphasizes the beneficial use of photoredox catalysis for the δ-cyanation further, as photoredox catalysis generally allows milder reaction conditions than common approaches[10-11].

2.3 Problem solving

2.3.1 Mass balance and ethylcyclohexanecarboxylate **15a** formation

Conducting the desired δ-cyanation reaction under optimized reaction conditions yielding 65% by NMR as shown in Scheme 29, an according mass balance of 0.65 equivalents of ethylcyclohexanecarboxylate **15a** and 2.35 equivalents of isocyanide **15** were expected. However, ^{1}H-NMR analysis showed that actually 0.95 equivalents of the byproduct ethylcyclohexanecarboxylate **15a** were formed and only 1.93 equivalents of isocyanide **15** remained. That meant that the subjected isocyanide **15** participated in an unknown side reaction. Performing cyclic voltammetry (CV) on isocyanide **15**, its reduction potential was found to be -0.79 V vs Ag/AgCl electrodes. The voltammogram can be found in the appendix (Figure 4). That observed reduction potential of –0.79 V meant that the reduction potential of **15** was within the range of the photocatalyst's **27** reduction potential. Therefore, an unwanted reduction of the isocyanide **15** to ethylcyclohexanecarboxylate **15a** could potentially close the catalytic cycle competing with the desired δ-cyanation, leaving the nucleophilic carbon-radical species to react in some other manner. A proposed mechanism for this alternative reaction pathway is shown in Scheme 30.

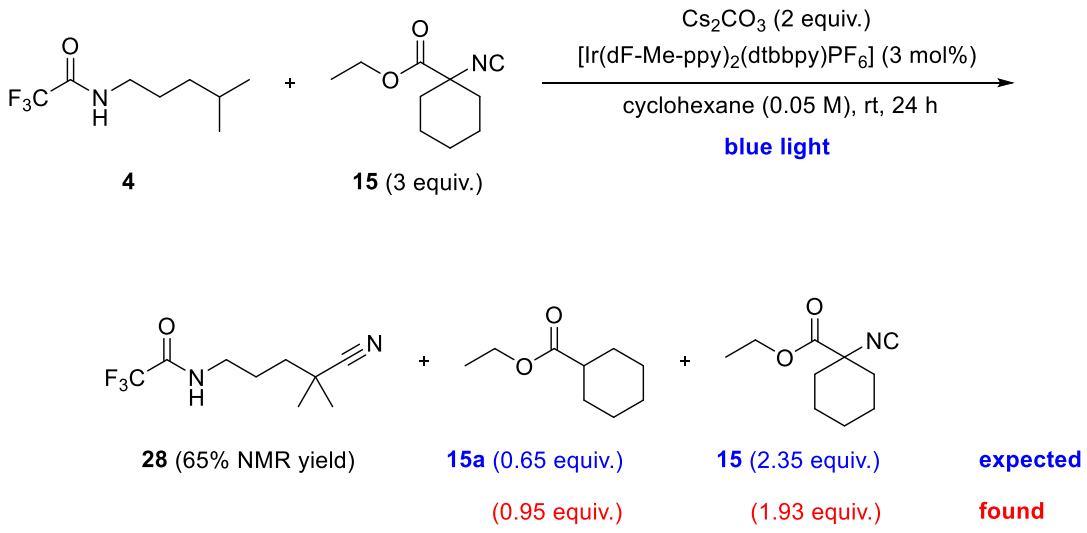

*Scheme 29: δ-cyanation under optimized reaction conditions yielding excess byproduct **15a***

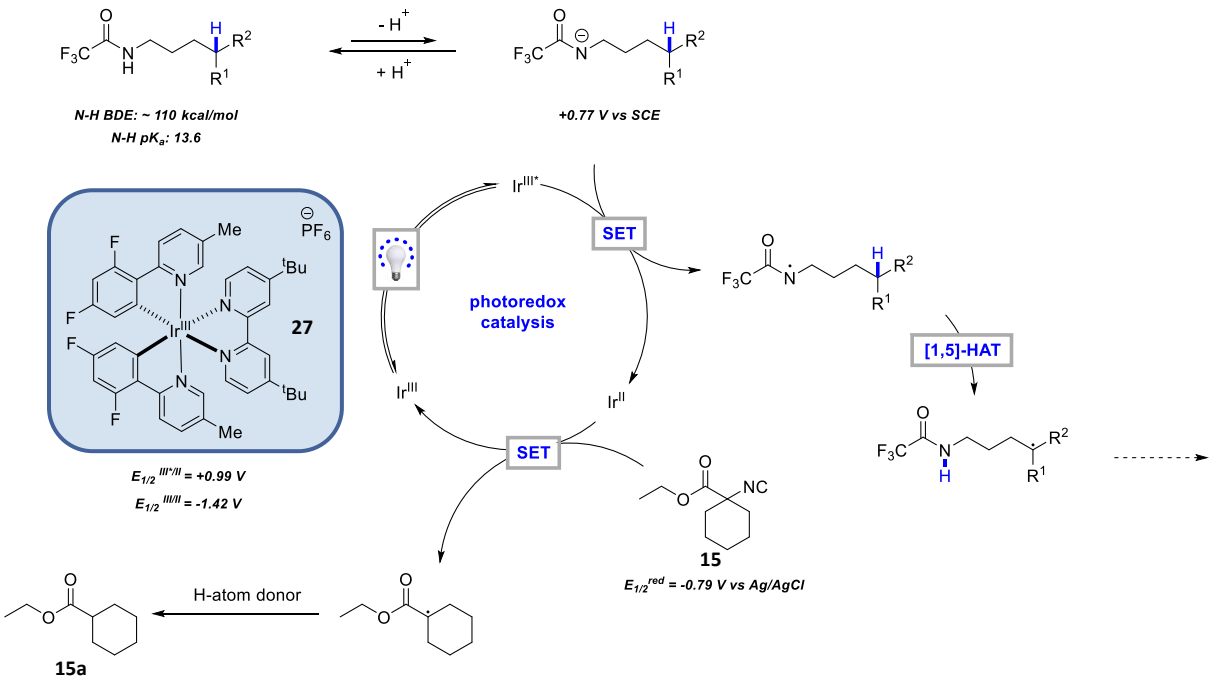

*Scheme 30: Proposed mechanism for an alternative reduction step yielding byproduct **15a***

In order to test this hypothesis, experiments using triethylamine (E_{ox} = + 0.96 V)[19] as sacrificial substrate to be oxidized by the photocatalyst **27** were conducted in toluene and cyclohexane. The exact reaction conditions and results can be seen in Scheme 31 and Table 11. It was observed that cyclohexane as well as an excess of Cs_2CO_3 as external base seem to favor the excess formation of ethylcyclohexanecarboxylate **15a**. The term external base is used for Cs_2CO_3. Triethylamine can facilitate its own deprotonation yielding 10% of the byproduct. Without a sacrificial substrate like triethylamine no reaction can take place. However, this experiment seemed not to be conclusive as triethylamine could form the α-substituted cyanide product. In that case the formed species **15a** would just be an expected byproduct, not the product of an alternative reduction step in the catalytic cycle. Therefore, the experiment was repeated with aniline (E_{ox} = + 0.98 V)[19] as sacrificial substrate as anilin did not provide an α-position to be readily functionalized. The reaction was conducted in cyclohexane with and without Cs_2CO_3 as sacrificial base (Scheme 32, Table 12). This time no reaction could be observed. This suggested that a side reaction *via* a mechanism as proposed in Scheme 30 is not taking place.

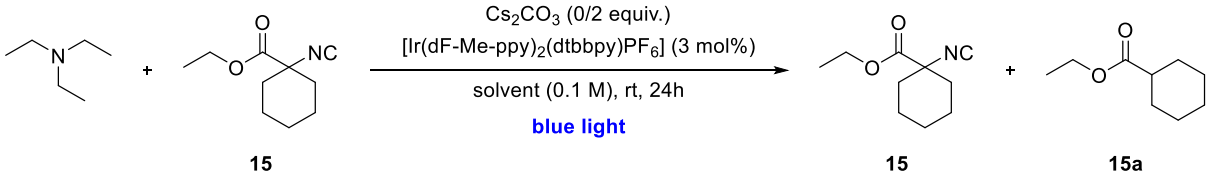

*Scheme 31: Reaction conditions using triethylamine to test direct reduction of isocyanide **15** by the photocatalyst **27***

*Table 11: Results of first reactions testing direct isocyanide **15** reduction by the photocatalyst **27** using triethylamine as substrate*

entry	solvent	control	15a yield by NMR
1	toluene	2 equiv. Cs_2CO_3	9%
2	toluene	0 equiv. Cs_2CO_3	4%
3	toluene	no Et_3N	0%
4	cyclohexane	2 equiv. Cs_2CO_3	17%
5	cyclohexane	0 equiv. Cs_2CO_3	10%
6	cyclohexane	no Et_3N	0%

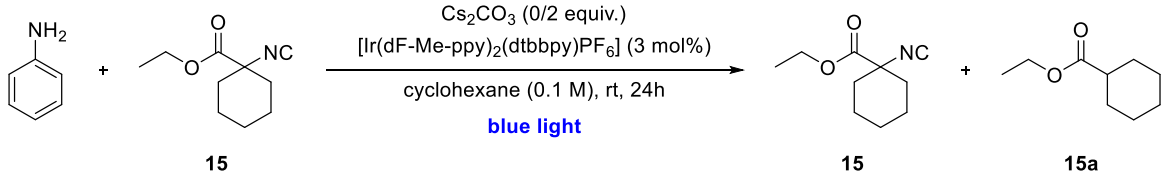

*Scheme 32: Reaction conditions using aniline to test direct reduction of isocyanide **15** by the photocatalyst **27***

*Table 12: Results testing direct isocyanide **15** reduction by the photocatalyst **27** using aniline as substrate*

entry	solvent	control	15a yield by NMR
1	cyclohexane	2 equiv. Cs_2CO_3	0%
2	cyclohexane	0 equiv. Cs_2CO_3	0%

Another possibility to suppress the undesired reduction of isocyanide **15** by the photocatalyst was seen in using a less reducing photocatalyst. Therefore, instead of photocatalyst **27** [Ir(dF-Me-ppy)$_2$(dtbbpy)PF$_6$], [Ir(dF-CF$_3$-ppy)$_2$(dtbbpy)PF$_6$] was used as photocatalyst in two test reactions (Figure 1, Table 13). Optimized conditions were used except the changes noted in Table 13. Unfortunately, using this less reducing photocatalyst resulted in lower yields, unchanged excess formation of byproduct and more severe photocatalyst degradation.

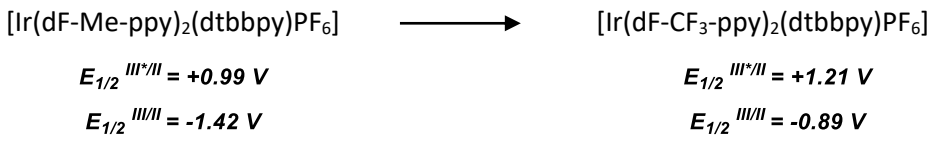

*Figure 1: Redox potentials for the two photocatalysts used in screens to suppress excess byproduct **15a** formation*

Table 13: Results using a less reductive photocatalyst [Ir(dF-CF_3-ppy)$_2$(dtbbpy)PF_6] in toluene and cyclohexane

entry	solvent	base	byproduct	cat. degr. sp^2 region	yield NMR
1	toluene, 0.05 M	K_3PO_4	0.21 equiv.	yes	26%
2	cyclohexane, 0.05 M	Cs_2CO_3	0.48 equiv.	yes	35%

2.3.2 Solvent effects

2.3.2.1 Cyclohexanecarbonitrile formation

Considering the fact that mesitylene gave the highest NMR yield in prior screens the hypothesis was made that this might be due to its H-atom donor qualities. If so, mesitylene might accelerate the δ-cyanation reaction by reduction of the tertiary carbon radical obtained after radical trapping and simultaneous generation of a very labile primary carbon radical.

Next to this reaction accelerating effect of such a H-atom donation it was also considered that such a primary carbon radical could then interfere with the radical trapping of the tertiary nucleophilic carbon radical intermediate after *[1,5]*-HAT by participating in a competing reaction with isocyanide **15** itself (Scheme 33). If that were the case, the reaction product (3,5-dimethylphenyl)acetonitrile would be formed and should be visible by analytical methods. However, (3,5-dimethylphenyl)acetonitrile could not be found by neither NMR, GC-MS nor UHPLC.

Continuing this thought process, analytical data for reactions in other solvents like toluene, *p*-xylene and cyclohexane was checked for the according reaction products as depicted in Scheme 33. Even though no cyanated toluene or *p*-xylene species could be found, minor amounts of cyclohexanecarbonitrile were detected by GC-MS. This was surprising as cyclohexane was the only solvent not expected to participate in a reaction pathway as depicted in Scheme 33, as its C(sp^3)-H bonds are quite strong and therefore hard to break and cyclohexane is not considered to be a H-atom donating solvent.

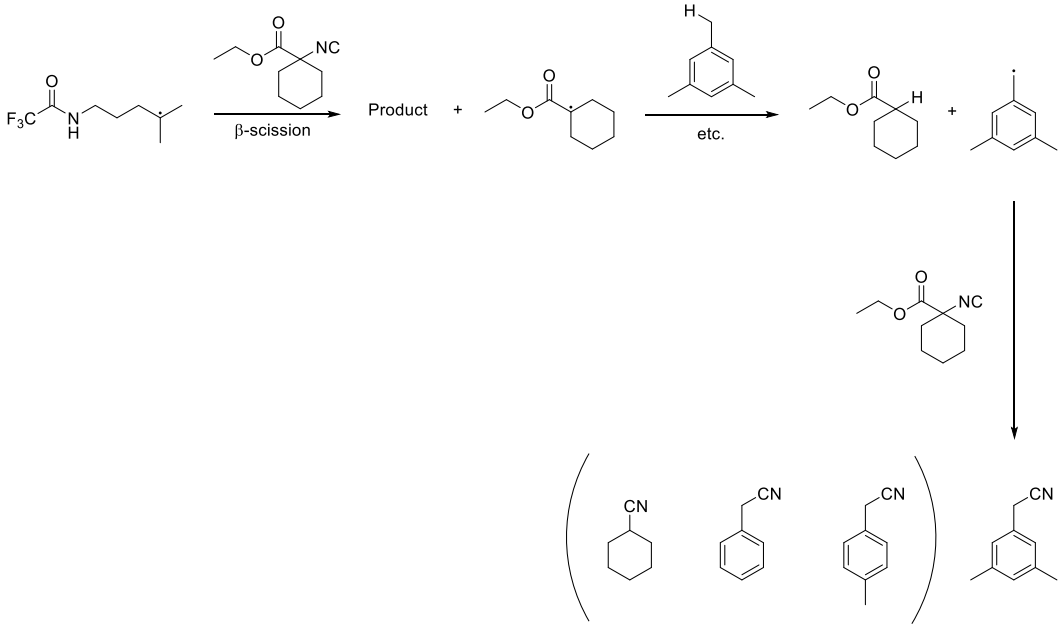

Scheme 33: Proposed altered reaction pathway considering H-atom donation by the solvent

One hypothesis how the cyclohexanecarbonitrile might be formed was deesterification of the isocyanide **15** followed by isomerization from the isocyanide to the cyanide functionality. To test this hypothesis isocyanide **16** with a five-membered ring at the α-position to the isocyanide group instead of a six-membered ring was synthesized. Then, isocyanide **16** was subjected to the optimized reaction conditions to test if cyclohexanecarbonitrile would still be formed (Scheme 34). The observed cyclohexanecarbonitrile formation with isocyanide **16** meant that the cyclohexanecarbonitrile was formed by the solvent, not the isocyanide. The fact that cyclohexanecarbonitrile is not observed in any other solvents supports this hypothesis. GC-MS analysis confirmed that the found compound was indeed cyclohexanecarbonitrile and not cyclohexylcarboisonitrile. GC-MS further eliminated the possibility of the cyclohexanecarbonitrile being a fragment of the isocyanide **15** on the GC-MS. It is still unclear how the cyclohexanecarbonitrile species is formed exactly.

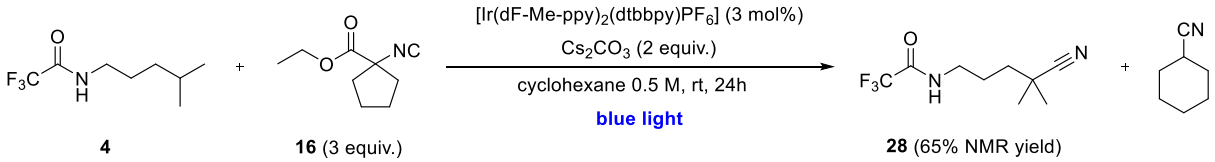

*Scheme 34: Reaction conditions used to investigate cyclohexanecarbonitrile formation with isocyanide **16***

2.3.2.2 Mesitylene as a reagent

As mesitylene was not a suitable solvent for the reaction due to reasons mentioned earlier it was tested as a reagent instead, hoping that its favorable effects on the reaction would still appear. Therefore, the reaction was conducted under optimized conditions with additional mesitylene as reagent in equivalents ranging from one to three. Unfortunately, the yield did not increase. All observed yields were lower than the highest yield without mesitylene. Even though a trend of a slight increase from one to two equivalents of mesitylene could be observed, adding even more mesitylene heavily decreased the yield. Moreover, catalyst degradation was worsened by mesitylene addition. The results of the conducted experiments are shown in Table 14, the exact reaction conditions in Scheme 35.

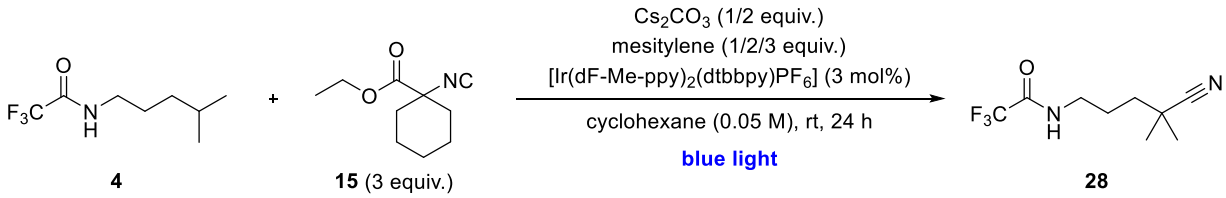

Scheme 35: Reaction conditions used to test mesitylene as a reagent

Table 14: Results using mesitylene as a reagent in cyclohexane as solvent

entry	base	mesitylene	byproduct	cat. degr. sp^2 region	yield NMR
1	1 equiv.	1 equiv.	0.85 equiv.	yes	58%
2	2 equiv.	1 equiv.	0.84 equiv.	yes	56%
3	2 equiv.	2 equiv.	0.92 equiv.	yes	61%
4	2 equiv.	3 equiv.	0.94 equiv.	yes	43%

2.3.3 Testing H-atom donors as reagents

As the main reason for the better reactivity in mesitylene was believed to be its H-atom donor properties, other H-atom donors were decided to be tested as reagents. A similar approach had shown success in an earlier project in the Rovis group[20]. Including additional H-atom donors like thiols or disulfides in the catalytic cycle changed the proposed mechanism of the reaction from the one illustrated in Scheme 6 to the one shown in Scheme 36.

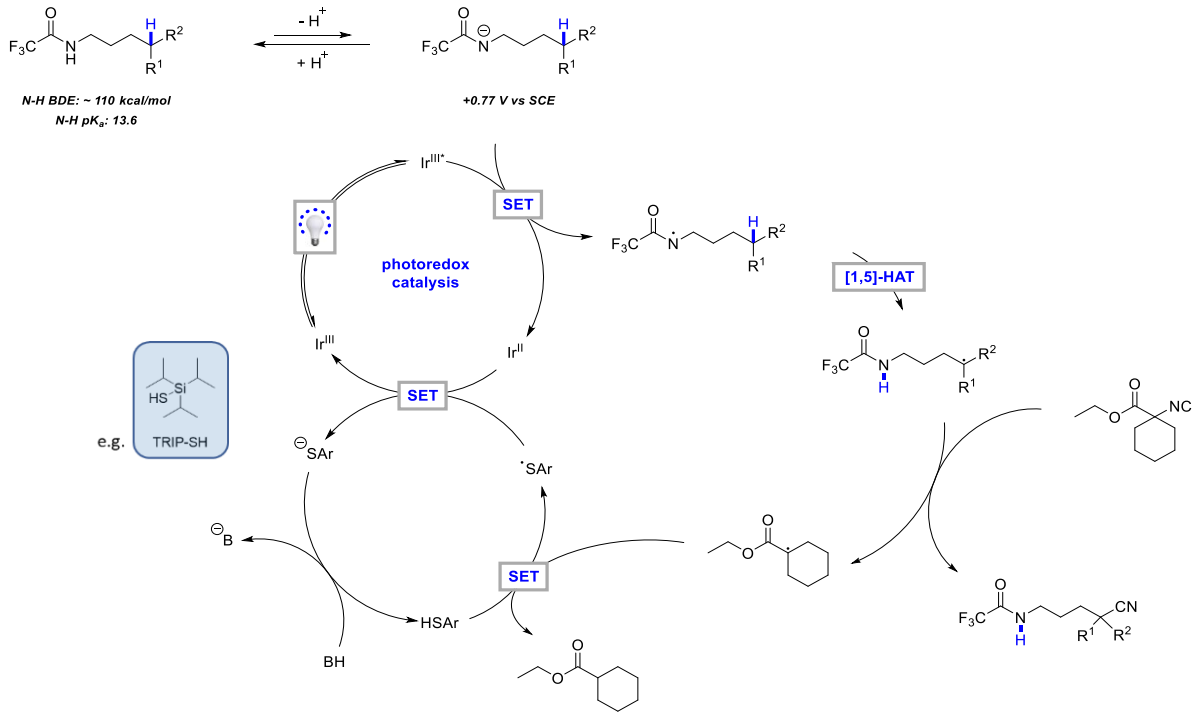

Scheme 36: Proposed mechanism of the δ-cyanation including a H-atom donor in the catalytic cycle

The tertiary carbon radical formed after radical trapping of the *[1,5]*-HAT product by the cyanide-source would not be the species reduced by the photocatalyst anymore. Instead the H-atom donor would reduce the *[1,5]*-HAT product, thereby forming a sulfur-radical species. Such sulfur-radical species are known to be able to be reduced by photocatalyst **27**[20]. Such a reduction would result in an anionic sulfur species after SET. This anionic sulfur compound would then be reprotonated by an external base to close the catalytic cycle. With this approach an unexpectedly hard reduction step of the formed tertiary radical after radical trapping by the photocatalyst could be circumvented. Even though the reduction of the tertiary radical should not be an issue due to the choice of the isocyanide (see chapter *2.2.1 Optimization of the cyanide-source*) H-atom donors were still tested as reagents to see if there would still be a beneficial effect.

Several different H-atom donors were tested under varying reaction conditions as shown in Scheme 37 and Table 15. Thiophenol was the only H-atom donor that was soluble in the reaction solvent cyclohexane. Therefore, mixtures of cyclohexane and toluene as solvent were used in experiments 6 and 7 whereas experiment 8 was conducted in pure toluene. Unfortunately, none of the conducted experiments in Table 15 resulted in an increased yield. To sum up, most of the tested reaction conditions and H-atom donors led to a drop in yield and more severe photocatalyst degradation compared to the optimized conditions (Table 5).

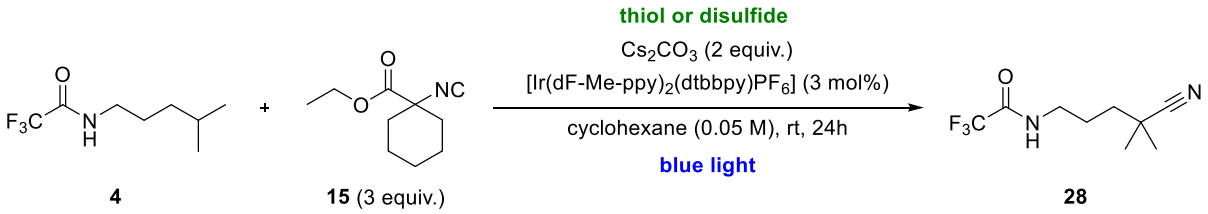

Scheme 37: Reaction conditions used to test the effects of H-atom donors as reagents

Table 15: Exact conditions and results of the experiments conducted to test the influence of H-atom donors on the desired δ-cyanation

entry	conditions	cat. degr. sp^2 region	yield NMR
1	TRIP-SH (0.2 equiv.)	yes	57%
2	triphenylsilanethiol (0.2 equiv.)	yes	57%
3	diphenyl disulfide (0.2 equiv.)	some	44%
4	bis(4-methoxyphenyl)disulfide (0.1 equiv.)	yes	43%
5	thiophenol (0.2 equiv.)	no	45%
6	diphenyl disulfide (0.1 equiv.), 1 mL cyclohexane + 1 mL toluene	yes	40%
7	diphenyl disulfide (0.1 equiv.), 2 mL cyclohexane + 3 drops toluene	some	47%
8	diphenyl disulfide (0.1 equiv.), 1 mL toluene, K_3PO_4	yes	19%

2.3.4 Revisiting isocyanides

At this point of the project some newly synthesized and ordered isocyanides were tested to see if different organic residues next to the isocyanide group or at the ester would influence the reaction in a way improving the yield. Moreover, two already tested isocyanides that were discussed in *2.2.1 Optimization of the cyanide-source* were revisited and subjected to the by then improved reaction conditions. Additionally, more isocyanides were tested as cyanide-sources in the presence of H-atom donor reagents.

2.3.4.1 Newly synthesized isocyanides

Isocyanide **16** had been synthesized to test if the cyclohexanecarbonitrile formation was due to deesterification of isocyanide **15** or if the cyclohexanecarbonitrile was formed by the solvent as discussed in chapter *2.3.2.1 Cyclohexanecarbonitrile formation*. Therefore, an initial result for compound **16** as cyanide-source had already been obtained and showed that the yield under optimized reaction conditions was similar to the yield with compound **15**. In further consequence compound **16** was subjected to a variety of different reaction conditions to test if different reaction concentrations would have a beneficial impact on the yield. Moreover, it was investigated if the five-membered ring next to the isocyanide group showed better reactivity than the six-membered ring in compound **15**

(Scheme 38). Unfortunately, even though the obtained yields with isocyanide **16** were good they were no improvement to subsequent obtained results (Table 16).

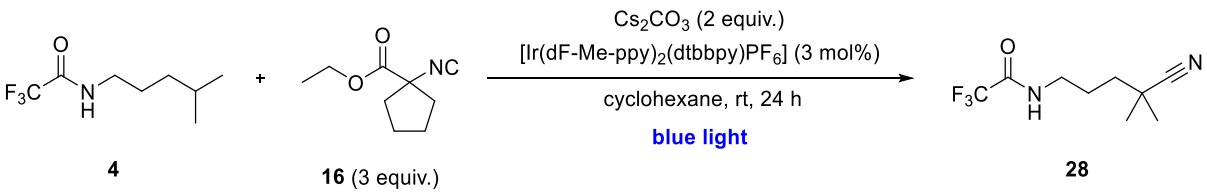

*Scheme 38: Reaction conditions used to test isocyanide **16** as cyanide-source*

*Table 16: Results for a concentration screen in cyclohexane with isocyanide **16***

entry	conditions	cat. degr. sp^2 region	yield NMR
1	cyclohexane 0.2 M	no	55%
2	cyclohexane 0.1 M	no	59%
3	cyclohexane 0.05 M	yes	61%
4	cyclohexane 0.033 M	some	54%

In addition, isocyanide **19** and isocyanide **23** were synthesized, whereby isocyanide **19** was the precursor for compound **23**. Their syntheses were started while deesterification of the isocyanide still seemed a possibility for the cyclohexanecarbonitrile formation. It was intended to test if another residue at the ester of the isocyanide would suppress deesterification. Even though by the time the syntheses were finished it had already been shown that cyclohexanecarbonitrile was formed by another pathway, it was decided to still test isocyanides **19** and **23** as cyanide-sources. Both isocyanides were subjected to the optimized reaction conditions as shown in Scheme 39. For compound **19** a surprisingly high yield of 39% by NMR was obtained in comparison to isocyanide **13** (Table 17). The reason for this behavior will be discussed in the following chapter *2.3.4.2 Newly commercially obtained* isocyanide alongside results presented there. The NMR yield for isocyanide **23** was comparable to the NMR yield with isocyanide **15** (Table 17).

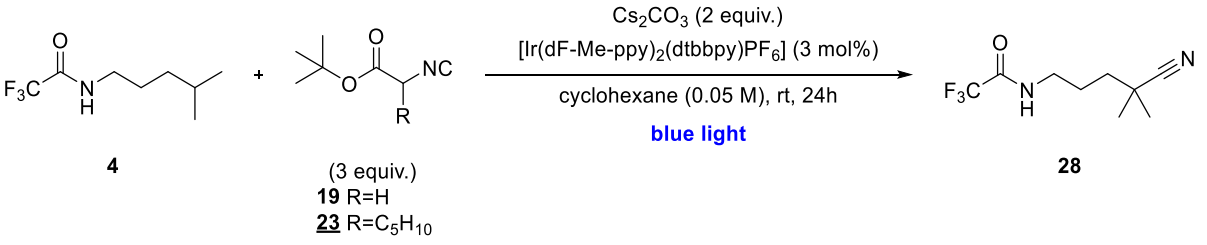

*Scheme 39: Isocyanides **19** and **23** subjected to the optimized reaction conditions for the δ-cyanation*

*Table 17: Results for δ-cyanation in cyclohexane with isocyanide **19** and **23***

entry	cyanide-source	cat. degr. sp^2 region	yield NMR
1	isocyanide **19**	yes	38%
2	isocyanide **23**	yes	59%

2.3.4.2 Newly commercially obtained isocyanides

In addition to the syntheses of compounds **19** and **23**, two more isocyanides as shown in Scheme 40 were commercially obtained. Those were considered interesting as methyl isocyanoacetate had yet another organic residue at the ester functionality and 1-adamantyl isocyanide was expected to result in a stable tertiary carbon radical after radical trapping of the *[1,5]*-HAT product. The reduction of that stable tertiary radical by the photocatalyst was considered to be difficult but subjection of additional H-atom donors was expected to circumvent this issue according to the thought process discussed in *2.3.3 Testing H-atom donors as reagents*.

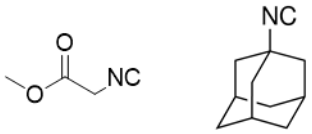

Scheme 40: Newly commercially obtained isocyanides methyl isocyanoacetate (left) and 1-adamantyl isocyanide (right)

These isocyanides were subjected to the optimized reaction conditions as shown in Scheme 29, changes are documented in Table 18 and Scheme 41. As shown in Table 18, results with 1-adamantyl isocyanide did not lead to any product formation at all; neither in trifluorotoluene nor in any other solvent with or without H-atom donors. Trifluorotoluene was the solvent used for the initial cyanide-source screens and was therefore tested again in this case as reference point to maintain comparability of the results. Methyl isocyanoacetate on the other hand showed an interesting trend compared to results obtained with isocyanides **13** and **19** (Scheme 41). Within this series of isocyanides, where the main difference was their decreasing polarity with the size of the bulk as their organic residue at the ester functionality, a trend of the obtained yield alongside the solubility of the isocyanide in cyclohexane could be observed. Methyl isocyanoacetate with its methyl residue and therefore predominant effect of the hydrophilic ester functionality did not show any reactivity towards δ-cyanation at all. The ethyl residue of compound **13** seemed to improve the lipophilicity of the isocyanide enough to allow some reactivity towards δ-cyanation, whereas the even bulkier tert-butyl group led to a jump in yield up to 39% by NMR.

Table 18: Results for the screens with 1-adamantyl isocyanide as cyanide-source

entry	conditions	cat. degr. sp^2 region	yield NMR
1	$PhCF_3$ 0.1 M, K_3PO_4	no	0%
2	optimized	yes	0%
3	optimized + thiophenol	yes	0%

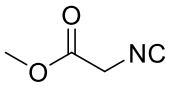
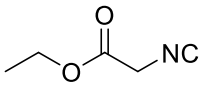
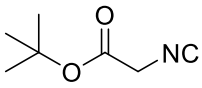

13 **19**

0% NMR yield $PhCF_3$ 0.1 M, K_3PO_4
0% NMR yield optimized

20% NMR yield
cyclohexane 0.1 M, K_3PO_4

39% NMR yield

*Scheme 41: Comparison of the results for δ-cyanation with methyl isoycanoacetate, compound **13** and compound **19***

Expanding this thought process to other isocyanides used during the thesis like compounds **15**, **16** or **19** not only the residues at the ester functionalities but especially the introduced five- and six-membered rings next to the isocyanide functional groups seem to benefit reactivity by increasing the lipophilicity of the isocyanides. Therefore, it can be said that even though the ester functionality seems to be beneficial for the reducibility of the formed radicals after radical trapping by the photocatalyst (see Scheme 20), they can cause problems in the reaction solvent cyclohexane regarding reactivity.

2.3.4.3 Revisiting isocyanides with additional H-atom donor subjection

Thinking about the isocyanides already tested in *2.2.1 Optimization of the cyanide-source*, there were two isocyanides that occurred especially interesting. α-Methylbenzylisocyanide showed a pretty high yield even though it formed a mediocre stable secondary radical intermediate after radical trapping. On the other hand, this secondary radical should be more readily reduced by the photocatalyst **27** than a tertiary radical intermediate. Therefore, α-methylbenzylisocyanide was subjected to the optimized reaction conditions. The result is shown in Table 19. Even though the obtained yield of 40% by NMR was not bad, it was also not an improvement to the already achieved 65% NMR yield under optimized conditions.

Table 19: Result for α-methylbenzylisocyanide subjected to the optimized δ-cyanation conditions

entry	conditions	cat. degr. sp^2 region	yield NMR
1	optimized	yes	40%

Moreover, 1,1,3,3-tetramethylbutylisocyanide showed a surprisingly high yield of 20% in the initial screens (Scheme 21) even though the formed tertiary radical should not be able to be reduced by the photocatalyst **27** at all. Therefore, 1,1,3,3-tetramethylbutylisocyanide was tested under several reaction conditions including using H-atom donor solvents and providing H-atom donor reagents like thiophenol. An easier reduction pathway enabled by H-atom donors could be especially beneficial for this isocyanide scaffold. Unfortunately, none of the tested reaction conditions as shown in Table 20 showed good reactivity for the desired δ-cyanation. H-atom donor addition seemed to totally suppress the desired δ-cyanation.

Table 20: Results obtained for 1,1,3,3,-tetramethylbutylisocyanide under several reaction conditions

entry	alterations from opt. conditions	cat. degr. sp^2 region	yield NMR
1	toluene 0.1 M, K_3PO_4	yes	14%
2	*p*-xylene 0.1 M, K_3PO_4	yes	15%
3	$PhCF_3$ 0.1 M, K_3PO_4, thiophenol	no	0%
4	cyclohexane 0.05 M, Cs_2CO_3, thiophenol	no	0%

2.3.5 NMR time studies

In order to gain better insight into the kinetics of the reaction NMR time studies were conducted. The first set of NMR time studies was conducted in the glove box using a 427 nm blue Kessil LED covered by tinfoil without a fan which led to a reaction temperature of approximately 40°C. Two NMR studies were conducted in parallel, one using isocyanide **15** the other one using isocyanide **16**. Both NMR studies were conducted under optimized conditions except for the elevated reaction temperature.

The NMR time studies were performed taking several aliquots of 50 µL of the two reaction mixtures over the course of 24 hours. See Table 26, Table 27, Figure 5 and Figure 6 in the appendix for the exact time points of the measurements and the obtained results. The taken aliquots were added to a stock solution of 0.1 M mesitylene as internal standard in $CDCl_3$. ^{1}H-NMRs were measured to track the reaction progress. Those ^{1}H-NMRs were used to quantify the amount of product **28**, starting material **4**, isocyanide **15** and isocyanide byproduct **15a** at any observed time point considering the decreasing reaction volume with every sample taken. During the analysis of the obtained data it became obvious, that the product showed only limited miscibility with the reaction solvent cyclohexane. Moreover, the concentration of the 0.1 M internal standard proved to be too high, as the signals of the internal standard were so big in the ^{1}H-NMR that quantification of the reaction components was difficult to achieve and showed a large error. Therefore, the obtained results as shown in *5.5 Full results of the three NMR time studies* in the appendix did not show a conclusive correlation.

To circumvent the miscibility issue of the product **28** a third NMR time study with isocyanide **15** under optimized conditions was conducted setting up eight reaction vials in parallel. This was necessary to enable a full workup for every investigated timepoint. However, it must be noted that such a setup is not ideal for NMR time studies as reaction conditions in different vials are never exactly the same and therefore not perfectly comparable. For this third NMR time study an internal standard of 0.033 M trimethoxybenzene in MeCN was used. The signals of starting material **4**, isocyanide **15**, product **28** and isocyanide-byproduct **15a** were clearly visible and quantifiable by ^{1}H-NMR analysis. Working up the whole reaction every time enabled monitoring of the catalyst degradation more closely.

The results obtained during this third NMR time study are shown in Figure 2. Table 28 showing the full obtained data can be found in the appendix together with Figure 7, a copy of Figure 2. Decreasing amounts of starting material **4** and isocyanide **15** are visible, same as an increase of product **28** and isocyanide-byproduct **15a**. The graph shows two irregularities, one at the data point of 4 hours for isocyanide **15** and one at the datapoint of 12 hours for byproduct **15a**. Those irregularities are most likely measuring errors or due to the ratios of the different reagents in each reaction vial.

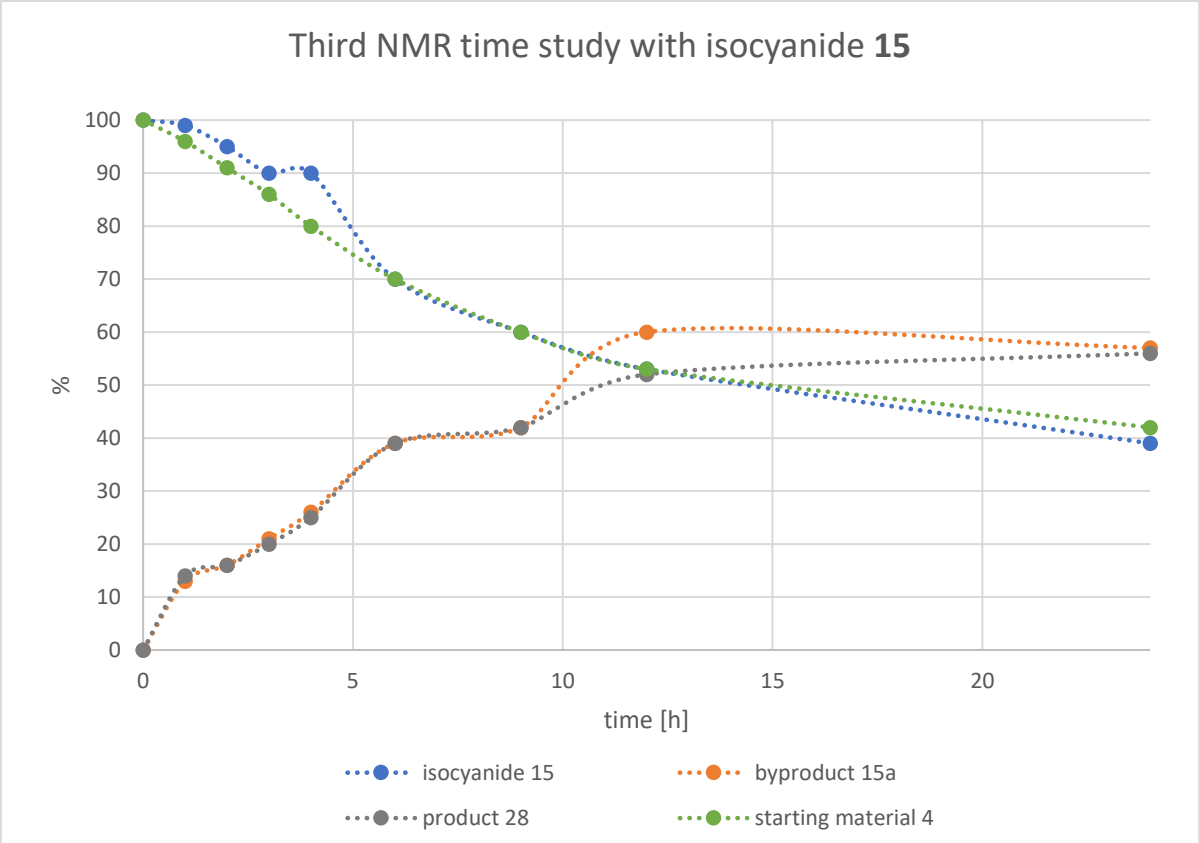

*Figure 2: Results for the third NMR time study conducted with isocyanide **15** under optimized reaction conditions*

As mentioned above, it was possible to monitor catalyst degradation during the third NMR time study. This was the first time during this thesis that it was possible to clearly distinguish between signals from intact photocatalyst and degraded photocatalyst. Thereby it became obvious that the photocatalyst had been degrading in most of the reactions conducted up to that point even when the ^{19}F-NMR had looked like it did not. That is because the signals of intact and degraded photocatalyst in the ^{19}F-NMR are close together and the small amount of 3 mol% photocatalyst made it hard to track it appropriately. The photocatalyst degradation over time as observed *via* ^{19}F-NMR during the third NMR time study is depicted in Figure 3. The formation of new fluorine peaks at -102.56 ppm, -104.61 ppm, -105.90 ppm, -108.16 ppm and -108.54 ppm could be observed. Those peaks are next to the initial photocatalyst sp^2-fluorine signals at -105.27 ppm and -108.23 ppm. This suggests photocatalyst degradation *via* aryl-fluorine migration or exchange, possibly through a nucleophilic aromatic substitution pathway. Such a loss of the aryl-fluorines at the ligands of the photocatalyst would lead to higher electron densities at the ligands and therefore at the Ir^{III}-metal center itself. This would lead to a lower oxidation potential of the photocatalyst in further consequence which could suppress the productive oxidation of the deprotonated starting material **4** thereby shutting down the δ-cyanation reaction pathway. Moreover, a new fluorine peak at -125.39 ppm could be observed, which is still in the sp^2 region of fluorine signals but quite distant from the original photocatalyst fluorine signals.

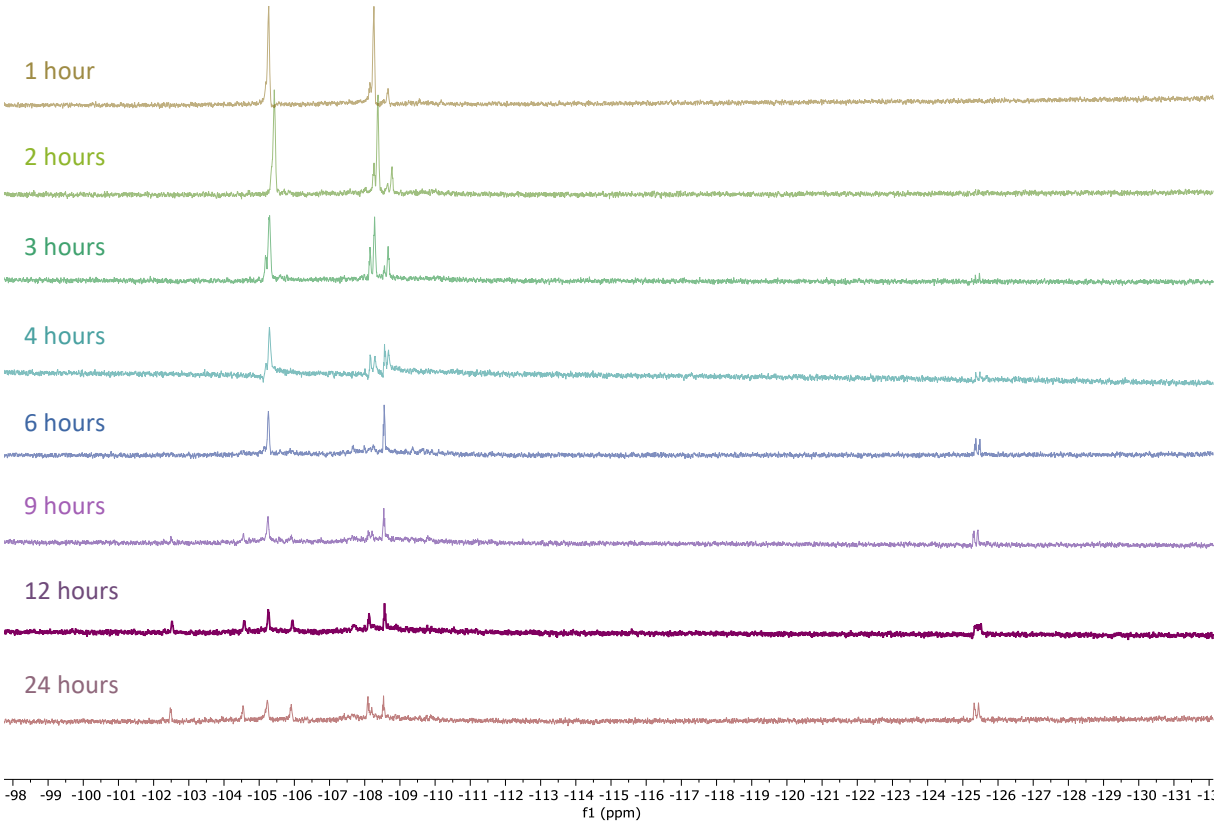

*Figure 3: ^{19}F-NMRs showing photocatalyst **27** degradation as observed during the third NMR time study with isocyanide **15***

One of the next steps in the project should be the investigation of ways to either suppress this observed photocatalyst degradation or to find a more stable photocatalyst with suitable oxidation and reduction potentials.

2.3.6 Product subjection

As the NMR time studies showed a stagnation of product formation and photocatalyst degradation, product inhibition was considered another possible reason for slowing down the reaction. In order to test that hypothesis and whether the product could react back to form starting material again, two test reactions were set up. In those test reactions the product was subjected to two different sets of reaction conditions. First, a reaction as shown in Scheme 42 was set up using the optimized reaction conditions except addition of product **28** instead of starting material **4**. This reaction was conducted to test if the product was stable under the reaction conditions. Due to the bad miscibility of the product in cyclohexane the transfer of product **28** to the reaction mixture was only partial (about 40% according to ^{1}H-NMR analysis after 24 hours). Therefore, no quantitative conclusions can be drawn from the observed results of this reaction. However, qualitative information could be obtained. It was observed that no starting material **4** was formed during the reaction time of 24 hours. Moreover, isocyanide **15** slightly degraded under the used reaction conditions as 0.23 equiv. of byproduct **15a** were observed after 24 hours. As quantitative conclusions were not possible it is unclear if product **28** played a role in the reaction mechanism leading to the formation of byproduct **15a**.

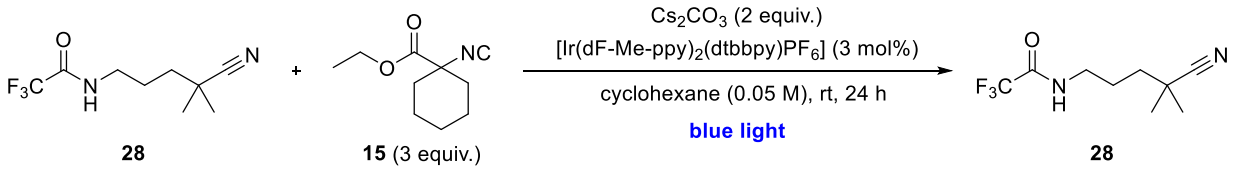

*Scheme 42: Experiment conducted to test if product **28** was stable under the depicted reaction conditions*

The second experiment with product subjection was designed to test if product **28** could act as a cyanide-source itself. This was considered a possibility to limit the amount of obtainable product as it would be consumed again as cyanide-source over the course of the reaction. Therefore, a reaction as shown in Scheme 43 was set up and stopped after 24 hours. This experiment again gave only qualitative information due to incomplete transfer of the product **28** to the reaction vial because of miscibility issues with the solvent (about 45% according to ^{1}H-NMR analysis after 24 hours). Nevertheless, no reactivity was observed and product **28** did not act as cyanide source for a δ-cyanation of the subjected substrate. However, the photocatalyst seemed to be fully degraded after 24 hours.

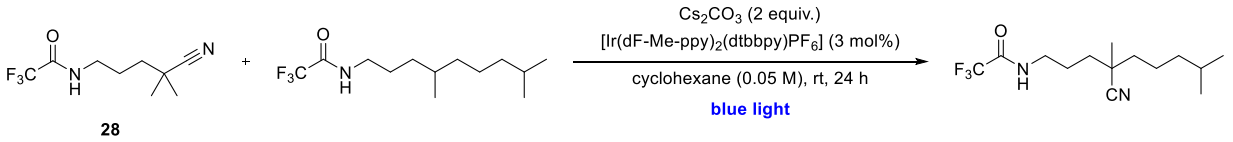

*Scheme 43: Experiment conducted to test if product **28** could act as cyanide-source in a δ-cyanation reaction itself*

2.3.7 Additional experiments conducted

In addition to the test reactions discussed so far, a couple of more reactions were conducted testing smaller hypotheses and thoughts.

First, different amounts of photocatalysts **27** were used to test if improving the catalyst loading would increase the yield as common for homogeneous catalysis. Therefore, photocatalyst loadings of 1 mol% as well as 6 mol% were tested. In addition, sequential addition of 3 mol% photocatalyst was performed whereby 1.5 mol% of photocatalyst were added at the beginning of the experiment and the other 1.5 mol% of photocatalyst were added after 4 hours reaction time. Therefore, the reaction vial was transferred into the glove box. Optimized reaction conditions as shown earlier in Scheme 29 were used for those reactions. The results are listed in Table 21 which also includes the optimized result with 3 mol% photocatalyst for better comparability. Due to the bad solubility of the photocatalyst an improved catalyst loading did not result in a higher yield. On the contrary, the excess photocatalyst seemed prone to degradation as severe photocatalyst degradation was observed in experiment 4 with 6 mol% photocatalyst. The sequential addition of photocatalyst did not improve the yield either. This is most likely because the reaction mixture is already saturated with photocatalyst after addition of 1.5 mol%. The additionally added 1.5 mol% of undegraded photocatalyst cannot dissolve in the reaction mixture to take part in the reaction.

*Table 21: Results for test reactions performed under optimized reaction conditions varying photocatalyst **27** loadings*

entry	photocatalyst loading	cat. degr. sp^2 region	yield NMR
1	1 mol%	some	61%
2	1.5 mol% + 1.5 mol% after 4 h	some	61%
3	3 mol%	some	65%
4	6 mol%	yes	54%

In an attempt to suppress photocatalyst degradation, a reaction with additional 3 mol% dtbbpy was conducted under otherwise optimized conditions. Providing additional ligand dtbbpy was supposed to suppress ligand loss and exchange. However, with a yield of 63% by NMR no improvement in the reaction outcome was observed and photocatalyst degradation was still an issue as seen in ^{19}F-NMR.

To confirm the proposed mechanism discussed in chapter *1.4 Proposed mechanism* controls under the optimized reaction conditions were conducted. For those controls three reactions were set up in parallel; one without light penetration wrapped in tinfoil, one without photocatalyst and one without base. All three control experiments did not show any product formation (Table 22), thereby supporting a mechanism through photoredox catalysis as proposed in Scheme 6.

Table 22: Results for control reactions to support the proposed mechanism of δ-cyanation via *photoredox catalysis*

entry	conditions	control	yield NMR
1	optimized	no light	0%
2	optimized	no photocatalyst	0%
3	optimized	no base	0%

2.4 Summary and outlook

The target reaction of a photoredox catalyzed δ-cyanation of trifluoroacetamides was improved from an initial hit with 11% NMR yield towards a yield of 65% by NMR. Even though the full optimization of the reaction up to 80-90% NMR yield was not achieved, with the obtained 65% yield by NMR good progress towards the final goal was made. During the optimization process about 200 test reactions were conducted optimizing reaction conditions such as the employed cyanide-source, base, photocatalyst, solvent, time, temperature and concentration. In order to provide substrates for those optimization screens 18 different compounds were synthesized. Two of these compounds were not known to the literature.

With these substrates and the optimized reaction conditions yielding 65% product by NMR in hand two secondary substrates were tested in the desired δ-cyanation reaction yielding the desired products. One of these products could be sufficiently purified to fully characterize it, the second product was only obtained as crude material during this thesis. Its purification and full characterization will be one of the next steps in the project.

NMR time studies and product subjection experiments were conducted giving rise to valuable information about the reaction kinetics and the stability of the product **28** and photocatalyst **27** under the reaction conditions.

As the goal of an optimization up to 80-90% NMR yield has not been achieved yet, this will stay the next challenge within the project. Once optimized, the limitations of the transformation will be explored by subjecting an array of aliphatic amine derivatives to the reaction conditions. More tertiary, secondary and primary trifluoroacetamide substrates will be tested and characterized. In order to achieve the boost in yield towards 80-90% a possible next step could be working on suppressing the observed photocatalyst degradation or trying another suitable, more stable photocatalyst. One of the main issues causing a low reaction yield so far is the heterogeneity of the reaction as the used base, as well as the photocatalyst and the formed product show bad solubility and miscibility with the solvent. However, this might be a difficult issue to solve as more polar solvents showed lower yields and even more severe photocatalyst degradation.

3. Experimental part

3.1. General methods

3.1.1 Light boxes

All photoredox reactions were conducted in inhouse-built light boxes lined with tinfoil, equipped with stir plates, fans for cooling and two Kessil PR160 LED photoredox lights set to an intensity of 100. Lights with a wavelength of 427 nm were used unless noted otherwise. The average distance between the reaction vials and the Kessil LEDs was about 10 cm.

3.1.2 Melting points (m.p.)

Melting points were determined using a SRS DigiMelt MPA 160 using a heating ramp of 2°C/min.

3.1.3 Nuclear magnetic resonance spectra (NMR):

NMR spectra were recorded from $CDCl_3$ or toluene-d_8 solutions at 27°C. For 400 MHz ^{1}H-NMR, 101 MHz ^{13}C-NMR and 476 MHz ^{19}F-NMR Brucker Avance III 400 spectrometers were used, for 500 MHz ^{1}H-NMR, 126 MHz ^{13}C-NMR and 471 MHz ^{19}F-NMR a Brucker Avance III 500 spectrometer was used. For ^{1}H-NMR tetramethylsilane was used as internal standard, whenever possible spectra were calibrated to the solvent residual peak as tabulated in the literature[21]. The chemical shifts (δ) are reported in ppm, coupling constants (J) in Hz. Assignments were based on COSY and HSQC experiments. Unclear assignments in NMR codes are marked by "*".

3.1.4 HRMS

All HRMS samples were dissolved in methanol with a concentration of about 10 µg/mL. The analyses were obtained from Columbia University Mass Spectrometry Facility on a JOEL JMSHX110HF mass spectrometer using ASAP^{+} ionization.

3.1.5 UPLCMS

All LCMS samples were dissolved in methanol with a concentration of about 1 mg/mL. The analyses were performed on an ACQUITY UPLC H-Class instrument equipped with an ACQUITY PDA detector and an ACQUITY QDa detector. The mobile phases water containing formic acid (0.1%) and acetonitrile with a gradient from 0% to 100% of acetonitrile were used.

3.1.6 GC-MS

All GC-MS samples were dissolved in methanol with a concentration of about 1 mg/mL. The analyses were performed on an Agilent Technologies 7890B GC system coupled with an Agilent Technologies 5977B MSD instrument with an EI ionization method.

3.1.7 TLC

TLCs were performed for reaction monitoring and analytical data collection whenever possible. Therefore, silica gel SiliCycle® 250 µm, 60 Å plates were used with either EtOAc/hexane or DCM/hexane as solvents. The spots were visualized by either using UV light (254 nm) or staining the plates with one of the three stains shown in Table 23. TLC plates stained with $KMnO_4$ or PMA stain were heated after staining, plates stained with cerium stain were air dried in order to longer visualize the obtained spots.

Table 23: Recipes for the TLC stains used during the thesis

Cerium TLC stain	**$KMnO_4$ TLC stain**	**PMA TLC stain**
4 g cerium sulfate	3 g $KMnO_4$	20 g phosphomolybdic acid
10 g phosphomolybdic acid	10 g K_2CO_3	200 mL abs. ethanol
24 mL conc. H_2SO_4	300 mL deion. water	
376 mL water		

3.1.8 Column chromatography

All column chromatographies were manual columns run with silica gel SiliCycle®SilicaFlash® P60, 40-63 µm, 60 Å purchased from Sigma Aldrich. As eluent gradients of EtOAc and distilled hexane or DCM and distilled hexane were used. For the final purification of product **32** pentane and chloroform was used.

3.2 Reagents and solvents

All chemicals were used directly from commercial sources and used without further purification, unless noted otherwise. Solvents for reactions were used without further purification, water-free solvents were available at the institute, no distilling was necessary. Hexane for column chromatography was distilled prior to use, for UPLC, GC-MS and HRMS measurements solvents with a suitable grade were used.

3.3 Synthetic procedures and analytical data

All procedures were conducted under argon atmosphere in dry glassware unless stated otherwise.

3.3.1 4-Methylpentanamide (**2**)

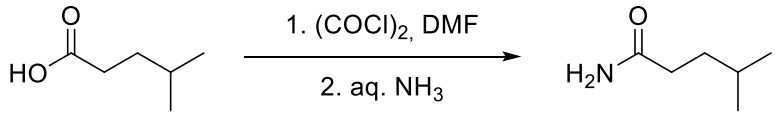

1 **2**

Procedure: Amide formation [1]

Dry DCM (150 mL, 0.3 M) was charged into a flask under argon atmosphere and cooled to 0°C. The starting material **1** (5.4 mL, 43.04 mmol, 1.00 equiv.) was added, then oxalyl chloride (4.1 mL, 47.35 mmol, 1.10 equiv.) was added slowly at 0°C. DMF (5 drops) was added to start the reaction which was indicated by gas formation. The reaction was warmed to rt. After 140 min gas formation stopped whereupon the solvent was evaporated to give the acid chloride as yellowish liquid with some solid material. The material was dissolved in THF (86 mL, 2 mL per mmol acid chloride). The solution was added slowly to cooled (0°C) aq. NH_3 (14.8 M, 30%) (86 mL, 2 mL per mmol acid chloride). The reaction mixture was warmed to rt and stirred overnight. After 19 h reaction monitoring *via* TLC showed full conversion (EtOAc/hexane 1:4, cerium stain). The reaction mixture was diluted with EtOAc (50 mL) and the aqueous and organic layer were separated. The aqueous layer was extracted with EtOAc (3 x 100 mL). The combined organic layer was washed with brine (75 mL) followed by drying over Na_2SO_4 and filtration. The solvent was evaporated under reduced pressure to give 4.343 g crude material as colorless powder. ^{1}H-NMR showed sufficiently pure product **2** to be used without further purification for the next step.

Yield: 4.343 g (88%) crude pure according to ^{1}H-NMR

Physical properties:

Sum formula, m.w.: $C_6H_{13}NO$, 115.18

m.p.: 114.4-116.3°C (EtOAc) (Lit.[22] 120.5-121.0°C (benzene/hexane))

R_f: 0.17 in EtOAc/hexane 1:1

^{1}H NMR (400 MHz, $CDCl_3$) δ 5.53 (s, 2H, NH_2), 2.30 – 2.17 (m, 2H, C***H*₂**(NH_2)), 1.67 – 1.49 (m, 3H, CH + CH_2), 0.91 (d, *J* = 6.4 Hz, 6H, 2x CH_3) ppm.

3.3.2 4-Methylpentan-1-amine (**3**)

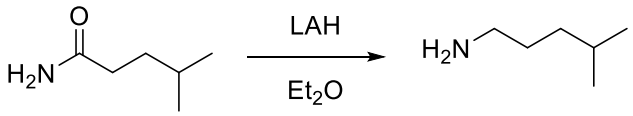

2 **3**

Procedure: Amide reduction to amine [1]

Dry Et_2O (125 mL, 0.3 M) was charged into a flask under argon atmosphere and cooled to 0°C. The starting material **2** (4.343 g, 37.71 mmol, 1.00 equiv.) was added which resulted in a heterogenous reaction mixture, then LAH (3.571 g, 94.27 mmol, 2.50 equiv.) was added in portions over the course of 30 min at 0°C. The reaction was warmed to rt and stirred overnight. After 27 h reaction control *via* TLC (EtOAc/hexane 1:1, $KMnO_4$ stain) showed nearly full conversion, the reaction mixture was cooled to 0°C. Water (3,6 mL, 1 mL per 1 g of LAH) was added slowly. Next, freshly prepared 15% NaOH (3.6 mL, 1 mL per 1 g of LAH) and water (11.2 mL, 3 mL per 1 g LAH) were added. The reaction was warmed to rt. After 20 min the reaction mixture was filtered through a pad of Celite, which was washed with Et_2O (100 mL). The organic layer was dried over Na_2SO_4, filtered and the solvent was cautiously evaporated at rt to give 2.232 g crude product **3** as yellowish oil. ^{1}H-NMR was measured that showed about 80% conversion of the starting material **2** to the desired product **3**.

Yield: 2.232 g (58%) crude with 20% starting material according to ^{1}H-NMR

Physical properties:

Sum formula, m.w.: $C_6H_{15}NO$, 101.19

R_f: 0.80 in EtOAc/hexane 9:1

NMR data: product 3 and starting material 2 were obtained in a ratio of 80% (product) to 20% (starting material), only product peaks are reported here

^{1}H NMR (400 MHz, $CDCl_3$) δ 2.66 (t, J = 7.1 Hz, 2H, CH_2), 1.54 (m, J = 13.3, 7.2, 4.7 Hz, 1H, CH), 1.50 – 1.37 (m, 4H, NH_2 + CH_2), 1.22 – 1.14 (m, 2H, CH_2), 0.88 (d, J = 6.6 Hz, 6H, 2x CH_3) ppm.

Spectral data are in accordance with the literature[23].

3.3.3 2,2,2-Trifluoro-*N*-(4-methylpentyl)acetamide (**4**)

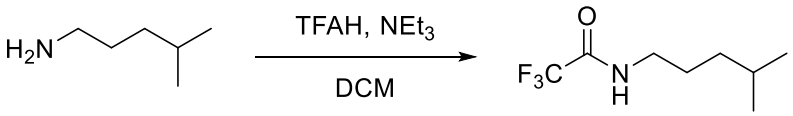

3 **4**

Procedure: Trifluoroacetamide formation [1]

Dry DCM (90 mL, 0.25 M) was charged into a flame-dried flask under argon atmosphere. The starting material **3** (2.232 g, 22.06 mmol, 1.00 equiv.) and triethylamine (6.2 mL, 44.12 mmol, 2.00 equiv.) were added. The reaction mixture was cooled to 0°C, then trifluoroacetic anhydride (3.0 mL, 20.96 mmol, 0.95 equiv.) was slowly added at 0°C. The reaction was warmed to rt and stirred overnight. After reaction monitoring *via* TLC (EtOAc/hexane 1:9, cerium stain) which showed full conversion the reaction was quenched with satd. aq. NH_4Cl (30 mL) after 17 h. The aqueous and organic layer were separated and the aqueous phase was diluted with water (30 mL). The aqueous phase was extracted with DCM (3 x 50 mL). The combined organic layer was dried over Na_2SO_4, filtered and the solvent was evaporated to give 5.973 g of a yellow liquid with a colorless residue as crude material **4**. The crude material was purified by column chromatography (100 g silica column, 0-10% EtOAc in hexane) to give 3.771 g of still slightly impure yellow material **4**. The material was purified by column chromatography again (100 g silica column, 0-15% EtOAc in hexane) to give 2.608 g pure product **4** as colorless oil according to ^{1}H-NMR analysis.

Yield: 2.608 g (60%), 30% over three steps

Physical properties:

Sum formula, m.w.: $C_8H_{14}F_3NO$, 197.20

R_f: 0.45 in EtOAc/hexane 1:9

^{1}H NMR (400 MHz, $CDCl_3$) δ 6.26 (s, 1H, NH), 3.35 (q, *J* = 6.8 Hz, 2H, C***H*₂**(NH)), 1.64 – 1.50 (m, 3H, CH_2 + CH), 1.27 – 1.16 (m, 2H, CH_2), 0.90 (d, *J* = 6.6 Hz, 6H, 2x CH_3) ppm.

^{13}C NMR (101 MHz, CDCl3) δ 157.4 (q, $^2J_{CF}$ = 36.7 Hz(CON)), 116.0 (q, $^1J_{CF}$ = 287.8 Hz(CF_3)), 40.4 (CH_2 (NH)), 35.9 (CH_2), 27.8 (CH)*, 27.0 (CH_2)*, 22.5 (2x CH_3) ppm.

^{19}F NMR (376 MHz, $CDCl_3$) δ -75.98 (CF_3) ppm.

Spectral data are in accordance with the literature[1].

3.3.4 L-(+)-α-Phenylglycine ethyl ester hydrochloride (**6**)

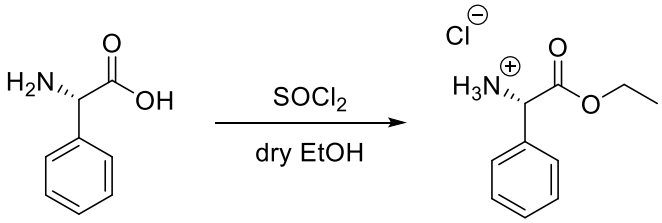

5 **6**

Procedure: Esterification[12]

The starting material **5** (5,000 g, 33.08 mmol, 1.00 equiv.) was dissolved in dry EtOH (50 mL) in a flame dried flask. The reaction mixture was cooled to 0°C, then $SOCl_2$ (6.00 mL, 82.69 mmol, 2.50 equiv.) was slowly added at 0°C. The reaction mixture was refluxed at 95°C for 10 min to dissolve the starting material. The reaction mixture was cooled to rt and stirred vigorously for 22 h. The solvent was evaporated to give a slightly yellow powder which was washed with Et_2O (400 mL), filtered and dried under reduced pressure to give crude material **6** as colorless platelets. ^{1}H-NMR showed sufficiently pure product **6** to be used it for the next step without further purification.

Yield: 6.735 g (94%) crude >90% purity according to ^{1}H-NMR

Physical properties:

Sum formula, m.w.: $C_{10}H_{14}ClNO_2$, 215.68

m.p.: 185.2-186.8°C (Et_2O) (Lit.[24] 182-183°C (Et_2O))

^{1}H NMR: (500 MHz, $CDCl_3$) δ 9.15 (s, 3H, NH_3), 7.66 – 7.45 (m, 2H, 2x H Ph), 7.37 – 7.33 (m, 3H, 3x H Ph), 5.13 (s, 1H, CH), 4.22 – 4.02 (m, 2H, CH_2), 1.14 (t, J = 7.1 Hz, 3H, CH_3) ppm.

Spectral data are in accordance with the literature[25].

3.3.5 Ethyl (S)-2-(formyl-amino)-2-phenylacetate (**7**)

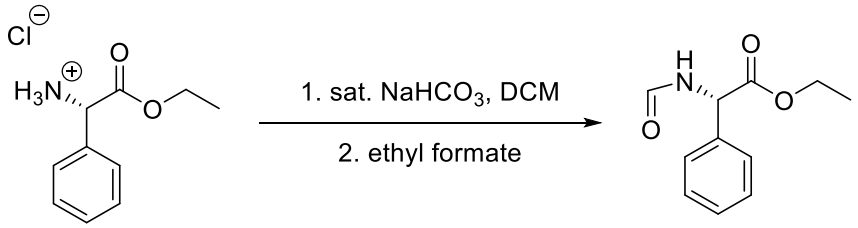

6 **7**

Procedure: Formation of the free amine[12] followed by formamide formation (similar to[14])

Starting material **6** (3.593 g, 16.74 mmol, 1.00 equiv.) was dissolved in aq. satd. $NaHCO_3$ (100 mL) and the aqueous phase was extracted with DCM (3 x 100 mL). The organic layer was dried over Na_2SO_4, filtered and the solvent was evaporated under reduced pressure to give 2.840 g of crude free base amine. The free base amine (2.505 g, 13.98 mmol, 0.84 equiv.) was transferred into a flame dried flask under argon atmosphere. Ethyl formate (42 mL) was added and the reaction mixture was heated to reflux overnight at an oil bath temperature of 68°C. Reaction monitoring *via* TLC (EtOAc/hexane 1:10, PMA stain) showed complete conversion after 15 h and the reaction mixture was concentrated under reduced pressure to give crude material **7** as yellow oil.

Yield: 2.923 g (quant.) crude >85% purity according to ^{1}H-NMR

Physical properties:

Sum formula, m.w.: $C_{11}H_{13}NO_3$, 207.23

R_f: 0.56 in EtOAc/hexane 2:1

^{1}H-NMR Free Amine: (400 MHz, $CDCl_3$) δ 7.41 – 7.27 (m, 5H, 5xH Ph), 4.61 (s, 1H, CH), 4.25 – 4.04 (m, 2H, CH_2), 2.20 (s, 2H, NH_2), 1.21 (t, J = 7.1 Hz, 3H, CH_3) ppm.

^{1}H NMR Formamide: (400 MHz, $CDCl_3$) δ 8.25 (t, J = 1.2 Hz, 1H, H(C=O)), 7.41 – 7.30 (m, 5H, 5xH Ph), 6.66 (s, 1H, NH), 5.65 (dd, J = 7.4, 1.0 Hz, 1H, CH), 4.34 – 4.11 (m, 2H, CH_2), 1.22 (t, J = 7.1 Hz, 3H, CH_3) ppm.

Spectral data are in accordance with the literature[25].

3.3.6 α-Aminoisobutyric acid benzyl ester *p*-toluenesulfonate (10)

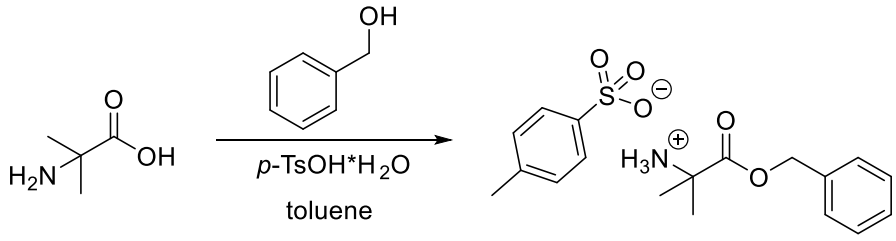

9 **10**

Procedure: Esterification[13]

The starting material **9** (4,999 g, 48.49 mmol, 1.00 equiv.) and *p*-TsOH*H_2O (9.228 g, 48.49 mmol 1.00 equiv.) were dissolved in toluene (50 mL). Benzylic alcohol (20 mL, 193.95 mmol, 4.00 equiv.) was added. The water condenser was filled up with toluene (12 mL) and the reaction was heated to reflux. After 17 h the reaction mixture was cooled to rt and the colorless precipitate was filtered and washed with Et_2O (200 mL). The material was dried under reduced pressure to give product **10** as colorless powder.

Yield: 15.121 g (86%) crude pure according to ^{1}H-NMR

Physical properties:

Sum formula, m.w.: $C_{18}H_{23}NO_5S$, 365.44

m.p.: 145.4-148.3°C (Et_2O) (Lit.[26] 150-152°C (MeOH/Et_2O))

^{1}H NMR (400 MHz, $CDCl_3$) δ 8.32 (s, 3H, NH_3), 7.73 (d, *J* = 8.2 Hz, 2H, 2x H Ph(Tos)), 7.29 – 7.28 (m, 5H, 5x H Ph(Bn)), 7.10 (d, *J* = 7.7 Hz, 2H, 2x H Ph(Tos)), 5.11 (s, 2H, CH_2), 2.32 (s, 3H, CH_3(Tos)), 1.54 (s, 6H, 2x CH_3) ppm.

Spectral data are in accordance with the literature[27].

3.3.7 Benzyl 2-formamido-2-methylpropanoate (11)

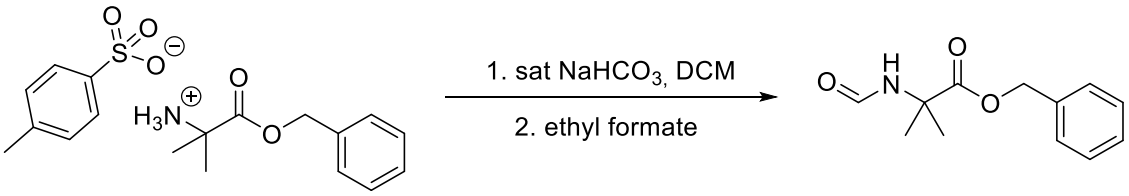

10 **11**

Procedure: Formation of the free amine (similar to[12]) followed by formamide formation (similar to[14])

Starting material **10** (5.684 g, 15.55 mmol, 1.00 equiv.) was dissolved in aq. satd. $NaHCO_3$ (100 mL) and the aqueous phase was extracted with DCM (3 x 100 mL). The organic layer was dried over Na_2SO_4, filtered and the solvent was evaporated under reduced pressure to give 1.601 g of crude free amine. The free amine (1.416 g, 7.33 mmol, 0.47 equiv.) was transferred into a flame dried flask under argon atmosphere. Ethyl formate (22 mL) was added and the reaction mixture was heated to reflux overnight at an oil bath temperature of 68°C. Reaction monitoring *via* TLC (EtOAc/hexane 1:3, PMA stain) showed complete consumption of the starting material after 15 h and the reaction mixture was concentrated under reduced pressure to give crude material **11**[28] as colorless powder.

Yield: 1.588 g (98%) crude >80% purity according to ^{1}H-NMR

Physical properties:

Sum formula, m.w.: $C_{12}H_{15}NO_3$, 221.26

R_f: 0.54 in EtOAc:hexane 2:1

m.p.: 67.4-69.3°C (ethyl formate)

^{1}H NMR Free Amine: (400 MHz, $CDCl_3$) δ 7.39 – 7.31 (m, 5H, 5x H Ph), 5.15 (s, 2H, CH_2), 2.25 (s, 2H, NH_2), 1.39 (s, 6H, 2x CH_3) ppm.

^{1}H NMR Formamide: (400 MHz, $CDCl_3$) δ 8.12 (d, J = 1.7 Hz, 1H, H(C=O)), 7.36 (td, J = 5.4, 3.4 Hz, 5H, 5x H Ph), 6.24 (s, 1H, NH), 5.19 (s, 2H, CH_2), 1.64 (s, 6H, 2x CH_3) ppm.

3.3.8 Benzyl 2-isocyano-2-methylpropanoate (12)

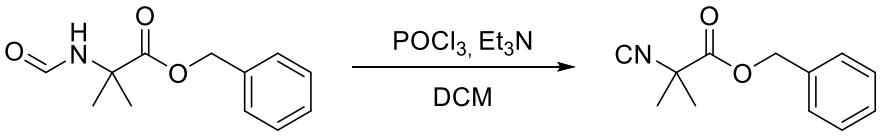

11 **12**

Procedure: Isocyanide formation (similar to[14])

The starting material **11** (1.025 g, 4.63 mmol, 1.00 equiv.) was dissolved in dry DCM (14 mL) and cooled to 0°C. Et_3N (2.4 mL, 17.14 mmol, 3.70 equiv.) was added followed by slow $POCl_3$ (520 µL, 5.56 mmol, 1.20 equiv.) addition at 0°C. The reaction mixture was stirred at 0°C for 28 h. Reaction monitoring *via* TLC (EtOAc/hexane 1:10, cerium stain) showed a new and more apolar product spot. The reaction was worked up by addition of aq. satd. Na_2CO_3 (15 mL) and extraction of the aqueous layer with DCM (2 x 25 mL). The combined organic layer was washed with brine (2 x 25 mL) and 1M HCl (2 x 25 mL) followed by drying over Na_sSO_4, filtered and the solvent was evaporated under reduced pressure to give a red oil as crude material **12**. The crude material was purified by column chromatography (45 g silica column, 0-20% EtOac in hexane) to give a clear oil as pure product **12** confirmed by ^{1}H-NMR analysis.

Yield: 416 mg (44%)

Physical properties:

Sum formula, m.w.: $C_{12}H_{13}NO_2$, 203.24

Rf: 0.35 in EtOAc/hexane 1:10

^{1}H NMR (400 MHz, $CDCl_3$) δ 7.38 (s, 5H, 5x H Ph), 5.24 (s, 2H, CH_2), 1.68 (s, 6H, 2x CH_3) ppm.

^{13}C NMR (101 MHz, $CDCl_3$) δ 169.5 (COOR), 158.2 (NC), 135.0 (1x C Ph), 128.9 (2x C Ph), 128.8 (1x C Ph), 128.2 (2x C Ph), 68.3 (CH_2), 59.8 (C q.), 27.6 (2x C CH_3) ppm.

Spectral data are in accordance with the literature[29].

3.3.9 Ethyl 2-benzyl-2-isocyano-3-phenylpropanoate (**14**)

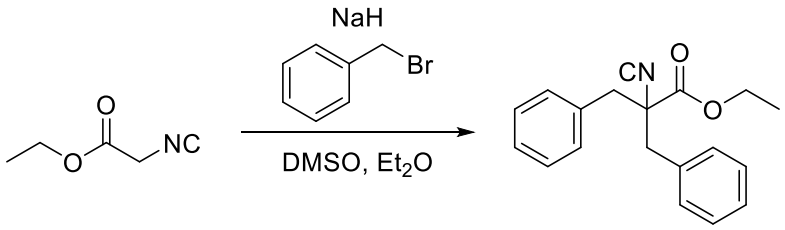

13 **14**

Procedure: Alkylation (similar to[15])

Starting material **13** (0.97 mL, 8.84 mmol, 1.00 equiv.) and benzylbromide (1.05 mL, 8.84 mmol, 1.00 equiv.) were added to a mixture of dry DMSO (8.4 mL) and dry Et_2O (35 mL). The reaction mixture was cooled to 0°C. NaH 60% in mineral oil (713 mg, 17.68 mmol, 2.00 equiv.) was added in small portions over the course of 30 min at 0°C. Afterwards the reaction mixture was warmed to rt, then it was refluxed at 47°C oil bath temperature overnight. Reaction monitoring *via* TLC (EtOAc/hexane 1:10, cerium stain) showed full consumption of the benzylbromide after 15 h. The reaction mixture was diluted with water (25 mL) and extracted with Et_2O (5 x 30 mL). The combined organic layer was washed with water (3 x 25 mL), dried over Na_2SO_4, filtered and the solvent was evaporated to give a yellow oil as crude material. The crude material was purified by column chromatography (45 g silica column, 0-10% EtOAc in hexane) to give a yellow oil as pure product **14** according to NMR analysis.

Yield: **670 mg (52%)**

Physical properties:

Sum formula, m.w.: $C_{19}H_{19}NO_2$, 293.37

R_f: 0.37 in EtOAc/hexane 1:9

Mass Data: HRMS (ASAP+) m/z: calc. for $C_{19}H_{19}NO_2$ $[M+H]^+$: 294.1494, found: m/z = 294.1509

^{1}H NMR (400 MHz, $CDCl_3$) δ 7.36 – 7.26 (m, 10H, 2x 5H Ph), 4.05 (q, J = 7.2 Hz, 2H, C***H*₂**(CH_3)), 3.36 (d, J = 13.6 Hz, 2H, CH_2 Bn), 3.07 (d, J = 13.5 Hz, 2H, CH_2 Bn), 1.05 (t, J = 7.2 Hz, 3H, CH_3) ppm.

^{13}C NMR (101 MHz, $CDCl_3$) δ 168.1 (COOR), 161.4 (NC), 133.7 (2x C Ph), 130.4 (2x 2C Ph), 128.6 (2x 2C Ph), 128.0 (2x C Ph), 70.3 (C(q)), 62.7 (CH_2), 45.0 (2xC CH_2 Bn), 13.9 (CH_3) ppm.

3.3.10 Ethyl 1-isocyanocyclohexane-1-carboxylate (**15**)

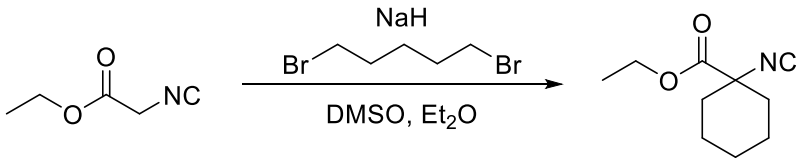

13 **15**

Procedure: Alkylation[15]

Starting material **13** (2.90 mL, 26.52 mmol, 1.00 equiv.) and 1,5-dibromopentane (3.60 mL, 26.52 mmol, 1.00 equiv.) were added to a mixture of dry DMSO (25 mL) and dry Et_2O (100 mL). The reaction mixture was cooled to 0°C. NaH 60% in mineral oil (2.120 g, 53.04 mmol, 2.00 equiv.) was added in small portions over the course of 60 min at 0°C. Afterwards the reaction mixture was warmed to rt, then it was refluxed at 50°C oil bath temperature overnight. Reaction monitoring *via* TLC (EtOAc/hexane 1:10, cerium stain) showed nearly full conversion of the starting material and a new product spot after 26.5 h. The reaction mixture was diluted with water (50 mL) and extracted with Et_2O (4 x 75 mL). The combined organic layer was washed with water (3 x 75 mL), dried over Na_2SO_4, filtered and the solvent was evaporated to give a yellow oil as crude material. The crude material was purified by column chromatography (45 g silica column, 0-5% EtOAc in hexane) to give a slightly yellow oil that still showed impurities by ^{1}H-NMR. Therefore, the material was purified by column chromatography again (100 g silica column, 0-5% EtOAc in hexane) to give the desired product **15** as clear oil pure according to NMR analysis.

Yield: 2.497 g (52%)

Physical properties:

Sum formula, m.w.: $C_{10}H_{15}NO_2$, 181.24

R_f: 0.48 in EtOAc/hexane 1:10

^{1}H NMR: (400 MHz, $CDCl_3$) δ 4.25 (q, J = 7.2, 1.8 Hz, 2H, CH_2), 1.99 (d, J = 13.3 Hz, 2H, $CH_2(C_6H_{10})$), 1.88 – 1.76 (t, 2H, $CH_2(C_6H_{10})$), 1.76 – 1.63 (m, 5H, 5x $H(C_6H_{10})$), 1.32 (t, J = 7.0, 1.6 Hz, 3H, CH_3), 1.29 – 1.22 (m, 1H, 1x $H(C_6H_{10})$) ppm.

^{13}C NMR: (101 MHz, $CDCl_3$) δ 169.7 (COOR), 158.8 (NC), 64.5 (d, J = 6.6 Hz(C(q))), 62.6 (CH_2), 34.4 (2x $C(C_6H_{10})$), 24.6 ($C(C_6H_{10})$), 21.1 (2x $C(C_6H_{10})$), 14.1 (CH_3) ppm.

Spectral data are in general in accordance with the literature[30]. However, HSQC shows that the literature[30] misassigned one proton signal as they are missing the proton at 1.29-1.22 ppm but assigned it instead to the multiplet at 1.76-1.63 ppm to fit the proton count.

3.3.11 Ethyl 1-isocyanocyclopentane-1-carboxylate (16)

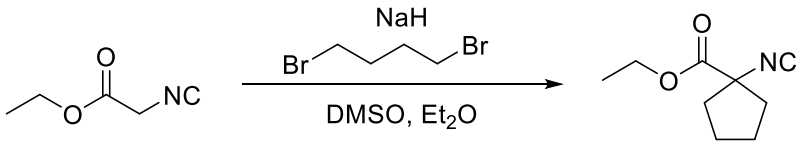

13 **16**

Procedure: Alkylation[15]

Starting material **13** (2.90 mL, 26.52 mmol, 1.00 equiv.) and 1,4-dibromopentane (3.17 mL, 26.52 mmol, 1.00 equiv.) were added to a mixture of dry DMSO (25 mL) and dry Et_2O (100 mL). The reaction mixture was cooled to 0°C. NaH 60% in mineral oil (2.120 g, 53.04 mmol, 2.00 equiv.) was added in small portions over the course of 20 min at 0°C. Afterwards the reaction mixture was warmed to rt, then it was refluxed at 53°C oil bath temperature overnight. Reaction monitoring *via* TLC (EtOAc/hexane 1:10, cerium stain) showed full conversion of the starting material and a new product spot after 19 h. The reaction mixture was diluted with water (75 mL) and extracted with Et_2O (3 x 75 mL). The combined organic layer was washed with water (3 x 75 mL), dried over Na_2SO_4, filtered and the solvent was evaporated to give a yellow oil as crude material. The crude material was purified by column chromatography (100 g silica column, 0-7.5% EtOAc in hexane) to give the desired product **16** as clear oil pure according to NMR analysis.

Yield: 2.991 g (68%)

Physical properties:

Sum formula, m.w.: $C_9H_{13}NO_2$, 167.21

R_f: 0.47 in EtOAc/hexane 1:10

^{1}H NMR: (500 MHz, $CDCl_3$) δ 4.26 (q, J = 7.1 Hz, 2H, CH_2), 2.27 – 2.16 (m, 4H, 2x $CH_2(C_5H_8)$), 2.05 – 1.80 (m, 4H, 2x $CH_2(C_5H_8)$), 1.32 (t, J = 7.1 Hz, 3H, CH_3) ppm.

^{13}C NMR: (126 MHz, $CDCl_3$) δ 169.7 (COOR), 158.5 (t, J = 4.3 Hz(NC)), 69.0 – 68.9 (t(C(q))), 62.8 (***C***$H_2(CH_3)$), 40.2 (2x $C(C_5H_8)$), 24.2 (2x $C(C_5H_8)$), 14.1 (CH_3) ppm.

Spectral data are in accordance with the literature[30].

3.3.12 *N*-Formyl-tert-butyl glycinate (**18**)

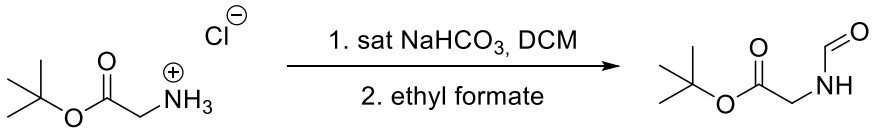

17 **18**

Procedure: Formation of the free amine (similar to[12]) followed by formamide formation (similar to[14])

Starting material **17** (7.370 g, 43.96 mmol, 1.00 equiv.) was dissolved in aq. satd. $NaHCO_3$ (100 mL) and the aqueous phase was extracted with DCM (3 x 75 mL). The organic layer was dried over Na_2SO_4, filtered and the solvent was evaporated under reduced pressure to give crude free amine as yellow oil. The free amine (3.187 g, 24.29 mmol, 0.55 equiv.) was transferred into a flame dried flask under argon atmosphere. Ethyl formate (60 mL) was added and the reaction mixture was heated to reflux overnight at an oil bath temperature of 68°C. Reaction monitoring *via* TLC (EtOAc/hexane 2:1, $KMnO_4$ stain) showed complete conversion after 24 h and the reaction mixture was concentrated under reduced pressure to give crude material **18** as slightly yellow oil.

Yield: 4.420 g (63%) crude >85% purity according to ^{1}H-NMR

Physical properties:

Sum formula, m.w.: $C_7H_{13}NO_3$, 159.19

R_f: 0.47 in EtOAc/hexane 2:1

^{1}H NMR (400 MHz, $CDCl_3$) δ 8.25 – 8.21 (s, 1H, CH(C=O)), 6.18 (s, 1H, NH), 3.98 (dd, J = 5.1, 0.9 Hz, 2H, CH_2), 1.48 (s, 9H, 3x CH_3) ppm.

Spectral data are in accordance with the literature[31].

3.3.13 tert-Butyl isocyanoacetate (19)

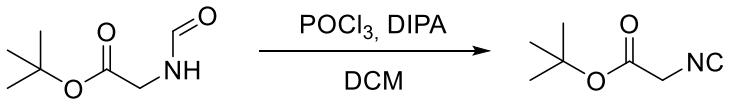

18 **19**

Procedure: Isocyanide formation (similar to[14])

The starting material **18** (3.998 g, 25.13 mmol, 1.00 equiv.) was dissolved in dry DCM (76 mL) and cooled to 0°C. Et_3N (12.96 mL, 92.97 mmol, 3.70 equiv.) was added followed by slow $POCl_3$ (2.8 mL, 30.15 mmol, 1.20 equiv.) addition at 0°C. The reaction mixture was stirred at 0°C for 3 h. Reaction monitoring *via* TLC (EtOAc/hexane 1:10, cerium stain) showed a new and more apolar product spot. The reaction was worked up by addition of aq. satd. Na_2CO_3 (15 mL) and the aqueous layer was diluted with water (30 mL). The aqueous layer was extracted with DCM (4 x 75 mL). The combined organic layer was washed with brine (2 x 100 mL) and 1M HCl (2 x 100 mL) followed by drying over Na_sSO_4, filtered and the solvent was evaporated under reduced pressure to give a red oil as crude material **19**. The crude material was purified by column chromatography (100 g silica column, 0-10% EtOAc in hexane) to give a yellow oil as pure product **19** confirmed by ^{1}H-NMR analysis.

Yield: 2.418 mg (66%)

Physical properties:

Sum formula, m.w.: $C_7H_{11}NO_2$, 141.17

Rf: 0.34 in EtOAc/hexane 1:9

^{1}H NMR (500 MHz, $CDCl^3$) δ 4.11 (s, 2H, CH_2), 1.49 (s, 9H, 3x CH_3) ppm.

^{13}C NMR (126 MHz, $CDCl_3$) δ 162.9 (COOR), 160.7 (NC), 84.2 (***C***$(CH_3)_3$)), 44.4 (t, *J* = 8.5 Hz(CH_2)), 28.0 (3x CH_3) ppm.

Spectral data are in accordance with the literature[31].

3.3.14 *N*-Formyl-L-alanine tert-butyl ester (**21**)

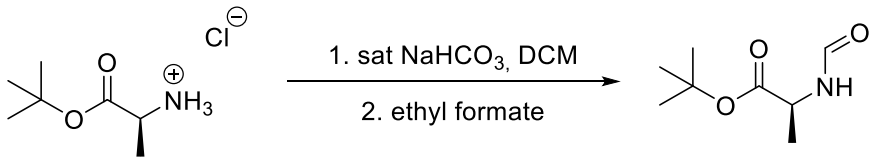

20 **21**

Procedure: Formation of the free amine (similar to[12]) followed by formamide formation (similar to[14])

Starting material **20** (226.6 mg, 1.25 mmol, 1.00 equiv.) was dissolved in aq. satd. $NaHCO_3$ (20 mL) and the aqueous phase was extracted with DCM (5 x 50 mL, 3 x 30 mL). The organic layer was dried over Na_2SO_4, filtered and the solvent was evaporated under reduced pressure to give crude free amine as yellow oil. The free amine (128.7 mg, 0.89 mmol, 0.71 equiv.) was transferred into a 15 mL high pressure tube under argon atmosphere. Ethyl formate (2 mL) was added and the reaction mixture was heated to reflux overnight at an oil bath temperature of 70°C. Reaction monitoring *via* TLC (EtOAc/hexane 2:1, $KMnO_4$ stain) showed complete conversion after 24 h and the reaction mixture was concentrated under reduced pressure to give crude material **21** as slightly yellow oil.

Yield: 163 mg (76%) crude >80% purity according to ^{1}H-NMR

Physical properties:

Sum formula, m.w.: $C_8H_{15}NO_3$, 173.21

R_f: 0.48 in EtOAc/hexane 2:1

^{1}H NMR (400 MHz, $CDCl_3$) δ 8.17 (s, 1H, CH(C=O)), 6.19 (s, 1H, NH), 4.55 (pd, J = 7.1, 1.0 Hz, 1H, CH), 1.48 (s, 9H, 3x CH_3 tBu), 1.41 (d, J = 7.1 Hz, 3H, CH_3(CH)) ppm.

Spectral data are in accordance with the literature[32].

3.3.15 tert-Butyl 1-isocyanocyclohexane-1-carboxylate (23)

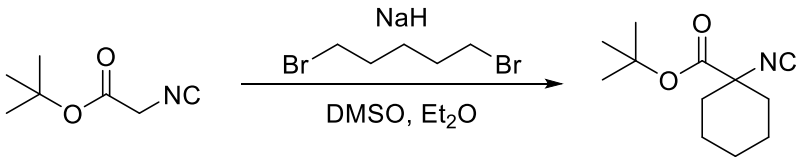

19 **23**

Procedure: Alkylation (similar to[15])

Starting material **19** (813 mg, 5.75 mmol, 1.00 equiv.) and 1,5-dibromopentane (782 µL, 5.75 mmol, 1.00 equiv.) were added to a mixture of dry DMSO (6 mL) and dry Et_2O (24 mL). The reaction mixture was cooled to 0°C. NaH 60% in mineral oil (472 mg, 11.81 mmol, 2.05 equiv.) was added in small portions over the course of 20 min at 0°C. Afterwards the reaction mixture was warmed to rt, then it was refluxed at 54°C oil bath temperature overnight. Reaction monitoring *via* TLC (EtOAc/hexane 1:10, cerium stain) showed full conversion of the starting material and a new product spot after 19 h. The reaction mixture was diluted with water (30 mL) and extracted with Et_2O (3 x 30 mL). The combined organic layer was washed with water (3 x 30 mL), dried over Na_2SO_4, filtered and the solvent was evaporated to give a yellow solid as crude material. The crude material was purified by column chromatography (100 g silica column, 0-10% EtOAc in hexane) to give the desired product **23** as colorless powder pure according to NMR analysis.

Yield: 842 mg (70%)

Physical properties:

Sum formula, m.w.: $C_{12}H_{19}NO_2$, 209.29

R_f: 0.67 in EtOAc/hexane 1:9

m.p.: 56.1-58.2 (EtOAc/hexane)

Mass Data: HRMS (ASAP+) m/z: calc. for $C_{12}H_{19}NO_2$ $[M+H]^+$: 210.1494, found: m/z = 210.1484

^{1}H NMR: (500 MHz, $CDCl_3$) δ 1.96 (d, *J* = 13.4 Hz, 2H, $CH_2(C_6H_{10})$), 1.78 (td, *J* = 13.4, 12.8, 5.7 Hz, 2H, $CH_2(C_6H_{10})$), 1.74 – 1.61 (m, 5H, 5x $H(C_6H_{10})$), 1.49 (s, 9H, 3x CH_3), 1.30 – 1.18 (m, 1H, 1x $H(C_6H_{10})$) ppm.

^{13}C NMR: (126 MHz, $CDCl_3$) δ 168.6 (COOR), 158.0 (NC), 83.2 ($C(CH_3)_3$)), 65.1 (C(NC)), 34.3 (2x $C(C_6H_{10})$), 27.9 (3x CH_3), 24.6 ($C(C_6H_{10})$), 21.2 (2x $C(C_6H_{10})$) ppm.

3.3.16 5-Methyl-2-[(2,4-difluorophenyl)-2-oxoethyl]pyridine (26)

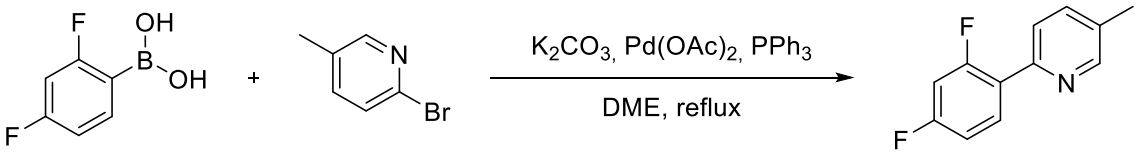

24 **25** **26**

Procedure: Suzuki cross-coupling (similar to[16])

A 2-necked roundbottom flask was equipped with (2,4-difluorophenyl)-boronic acid **24** (3.308 g, 20.95 mmol, 1.20 equiv.), 2-bromo-5-methylpyridine **25** (3.009 g, 17.49 mmol, 1.00 equiv.), PPh_3 (452 mg, 1.72 mmol, 0.10 equiv.) and K_2CO_3 (6.059 g, 47.10 mmol, 2.70 equiv.). DME (20 mL) was added and the mixture was purged with argon for 20 min. Pd(OAc) (99.1 mg, 0.44 mmol, 0.025 equiv.) was added and the solution was purged with argon for another 15 min. The reaction was refluxed for 15 h until TLC monitoring (EtOAc/hexane 1:10, UV light) showed nearly full conversion. The reaction mixture was diluted with DCM (30 mL) and washed with water (3 x 50 mL) and brine (1 x 50 mL). The organic layer was dried over Na_2SO_4, filtered and the solvent was evaporated to give a brown-red oil as crude material. The material was purified by several column chromatographies. First column chromatography (100 g silica column, 0%-10% EtOAc in hexane), second column chromatography (100 g silica column, 0-100% DCM in hexane), third column chromatography (100 g silica column, 0-100% DCM in hexane). Product **26** was obtained as colorless crystals in the end, pure according to NMR analysis. A further fraction of impure material was also collected for later purification.

Yield: 1.440 g (40%)

Physical properties:

Sum formula, m.w.: $C_{12}H_9F_2N$, 205.21

R_f: 0.49 in EtOAc/hexane 1:9

m.p.: 54.6-55.7°C (DCM/hexane)

^{1}H NMR (400 MHz, $CDCl_3$) δ 8.54 (s, 1H, CH), 7.98 (td, J = 8.9, 6.7 Hz, 1H, CH), 7.64 (ddd, J = 8.0, 2.4, 0.9 Hz, 1H, CH), 7.56 (ddd, J = 8.1, 2.3, 0.8 Hz, 1H, CH), 6.99 (dddd, J = 8.8, 7.8, 2.5, 1.0 Hz, 1H, CH), 6.90 (ddd, J = 11.3, 8.9, 2.6 Hz, 1H, CH), 2.38 (d, J = 0.8 Hz, 3H, CH_3) ppm.

^{13}C NMR (126 MHz, $CDCl_3$) δ 163.1 (dd, $^1J_{C\text{-}F}$ = 250.3, 11.9 Hz(CF)), 160.6 (dd, $^1J_{C\text{-}F}$ = 252.0, 12.0 Hz(CF)), 150.4 (CH), 149.9 (d, J = 2.5 Hz(C(q))), 137.1 (CH), 132.2 (C(q)), 132.0 (dd, J = 9.6, 4.6 Hz(CH)), 124.0 (dd, J = 11.9, 3.9 Hz(C(q))), 123.8 (d, J = 9.1 Hz(CH)), 111.9 (dd, J = 20.9, 3.6 Hz(CH)), 104.4 (dd, J = 27.2, 25.1 Hz(CH)), 18.3 (CH_3) ppm.

^{19}F-NMR: (471 MHz, $CDCl_3$) δ -109.04 (p, J = 8.0 Hz(F-Ar)), -112.20 (p, J = 9.1 Hz(F-Ar)) ppm.

Spectral data are in accordance with the literature[33].

3.3.17 [Ir(dF-Me-ppy)$_2$(dtbbpy)PF$_6$] (**27**)

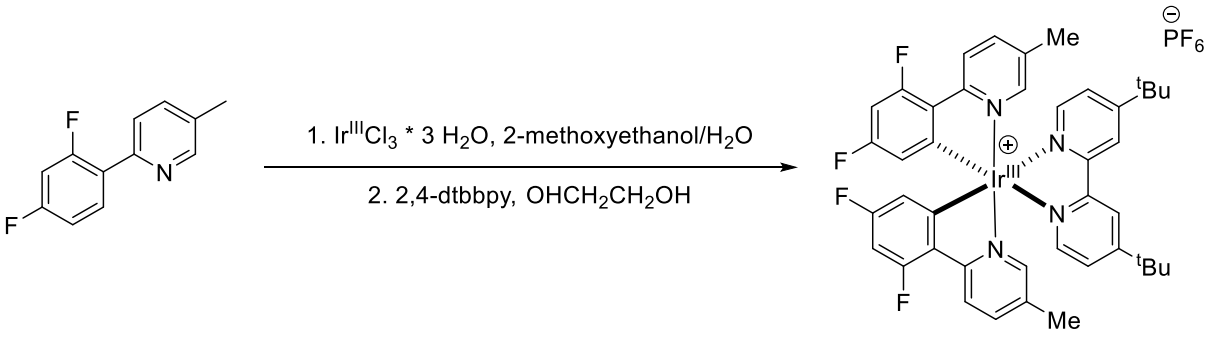

26 **27**

Procedure: Dimerization and ligand exchange at Iridium (similar to[16])

Starting material **26** (1.302 g, 6.34 mmol, 2.25 equiv.) and Ir^{III}Cl$_3$*H$_2$O (961 mg, 2.73 mmol, 1.00 equiv.) were added to a 150 mL sure sealed pressure tube under argon atmosphere. A 2:1 solvent mixture of 2-methoxyethanol (37.3 mL) and water (18.7 mL) was added and the pressure tube was closed. The reaction mixture was refluxed at an oil bath temperature of 120°C overnight. After 26 h the reaction mixture was cooled to rt, filtered and the obtained material was washed with water (3 x 15 mL). After air drying 2.139 g (123%) of the crude chloro-bridged dimer are obtained as yellow powder with assumed 23% of leftover water.

For the setup and calculation of the second step the yield of the first step was assumed to be quantitative with 1.700 g (1.34 mmol, 0.48 equiv.) of dry chloro-bridged dimer. The chloro-bridged dimer and 4,4'-di-tert-butyl-2,2'-dipyridyl (790 mg, 2.94 mmol, 1.05 equiv.) were added to a 150 mL sure sealed pressure tube together with ethylene glycol (46mL) under argon atmosphere. The reaction mixture was refluxed at 150°C oil bath temperature for 18 h. After cooling to rt the reaction mixture was diluted with water (50 mL) and was washed with hexane (3 x 50 mL). The aqueous layer was stirred at 85°C to get rid of leftover hexane. After cooling to rt a solution of ammonium hexafluorophosphate (6.70 g, 41.1 mmol, 15.33 equiv.) in water (65 mL) was added. The solution was stirred for two days during which the product **27** precipitated. The material was filtered, washed with hexane (2 x 50 mL) and water (2 x 50 mL) and dried under vacuum to give a yellow powder with high purity according to ^{1}H-NMR to be used without recrystallization as product **27**. As the only impurity visible in the ^{1}H-NMR is a water peak at 1.55 ppm the purity cannot be quantified due to water in the CDCl$_3$ used for the measurement itself.

Yield: 1.663 g (59%) crude

Physical properties:

Sum formula, m.w.: $C_{48}H_{32}Cl_2F_8Ir_2N_4$, 1272.13

m.p.: >260°C (H_2O)

^{1}H NMR (500 MHz, $CDCl_3$) δ 8.53 (d, J = 2.0 Hz, 2H, 2x CH), 8.17 (dd, J = 8.5, 2.1 Hz, 2H, 2x CH), 7.80 (d, J = 5.9 Hz, 2H, 2x CH), 7.60 (dd, J = 8.4, 2.0 Hz, 2H, 2x CH), 7.45 (dd, J = 5.9, 1.9 Hz, 2H, 2x CH), 7.25 – 7.24 (m, 2H, 2x CH), 6.52 (ddd, J = 12.4, 9.1, 2.4 Hz, 2H, 2x CH), 5.63 (dd, J = 8.4, 2.4 Hz, 2H, 2xCH), 2.19 (s, 6H, 2x CH_3), 1.45 (s, 18H, 2x (3x CH_3)) ppm.

^{13}C NMR (126 MHz, $CDCl_3$) δ 164.9 (2x C), 163.5 (dd, $^{1}J_{C\text{-}F}$ = 256.8, 12.0 Hz(2x CF (dF-Me-ppy))), 161.7 (d, J = 7.0 Hz(2x C)), 161.1 (dd, $^{1}J_{C\text{-}F}$ = 260.5, 12.3 Hz(2x CF (dF-Me-ppy))), 155.8 (2x C), 154.2 (d, J = 6.4 Hz(2x C)), 149.3 (2x C), 148.5 (2x C), 140.0 (2x C), 134.3 (2x C), 128.0 – 127.8 (m(2x C)), 125.7 (2x C), 123.2 (d, J = 19.4 Hz(2x C)), 122.9 (2x C), 113.8 (dd, J = 17.2, 2.5 Hz(2x C)), 98.9 (t, J = 26.6 Hz(2x C)), 36.0 (2x C(q tBu)), 30.3 (2x (3x CH_3)), 18.5 (2x CH_3 (dF-Me-ppy)) ppm.

^{19}F-NMR (471 MHz, $CDCl_3$) δ -71.60 (d, J = 713.2 Hz(PF_6)), -106.02 (q, J = 9.3 Hz(F-Ar)), -108.77 (t, J = 11.4 Hz(F-Ar)) ppm.

3.3.1 General procedure A: δ-functionalization screens

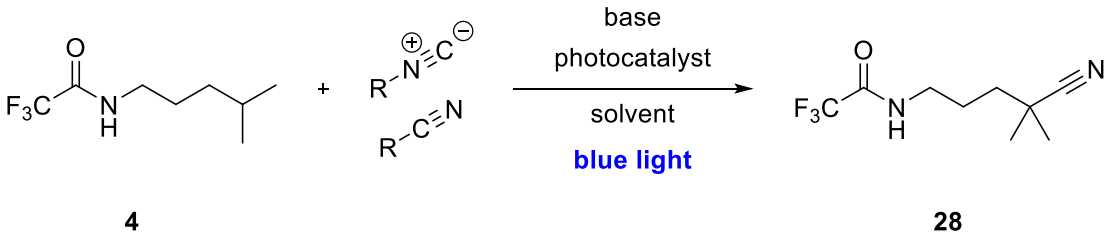

4 **28**

The trifluoroacetamide starting material (0.10 mmol, 1.00 equiv.) was charged into a separate vial. The photocatalyst (0.033 mmol, 0.03 equiv.) was charged into the reaction vial together with base (0.20 mmol, 2.00 equiv.). The vials were transferred into the glove box, where the starting material was transferred into the reaction vial with solvent (0.05 M, 0.1 M, 0.2 M or 0.4 M) and a cyanide-source (0.30 mmol, 3.00 equiv.) was added. The vial was irradiated with blue light (427 nm) for 24 h at rt under argon atmosphere. The reaction mixture was worked up by filtration through a pad of Celite in a pipette, which was afterwards washed with DCM (~5 mL). A freshly prepared internal standard of 0.033 M trimethoxybenzene in MeCN was added to the organic layer, then the solvent was evaporated. Afterwards GC-MS, ^{1}H-NMR and ^{19}F-NMR measurements were run to obtain a reaction yield by NMR and further information about side reactions.

3.3.2 General procedure B: δ-functionalization product isolation

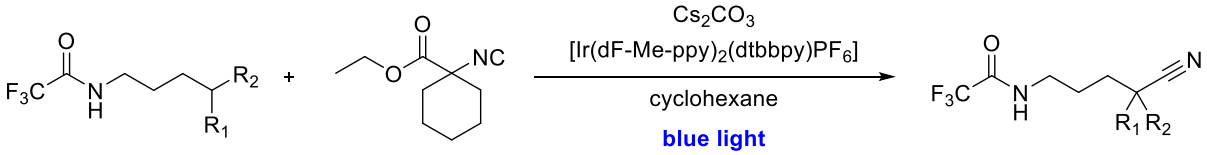

15

The trifluoroacetamide starting material (0.10 mmol, 1.00 equiv.) was charged into a separate vial. The photocatalyst [Ir(dF-Me-ppy)$_2$(dtbppy)PF$_6$] (3.1 mg, 0.033 mmol, 0.03 equiv.) was charged into the reaction vial together with Cs_2CO_3 (66.1 mg, 0.20 mmol, 2.00 equiv.). The vials were transferred into the glove box, where the starting material was transferred into the reaction vial with cyclohexane (2 mL, 0.05 M) and ethyl 1-isocyanocyclohexane-1-carboxylate **15** (54 µL, 0.30 mmol, 3.00 equiv.) was added. The vial was irradiated with blue light (427 nm) for 24 h at rt under argon atmosphere. The reaction mixture was worked up by filtration through a pad of Celite in a pipette, which was afterwards washed with DCM (~5 mL). A freshly prepared internal standard of 0.033 M trimethoxybenzene in MeCN was added to the organic layer, then the solvent was evaporated. After GC-MS, ^{1}H-NMR and ^{19}F-NMR analytics the material was purified by column chromatography (12 g silica column, 0-25% EtOAc in hexane) to give the δ-functionalized trifluoroacetamidecyanide.

3.3.2.1 Tertiary substrate **4**

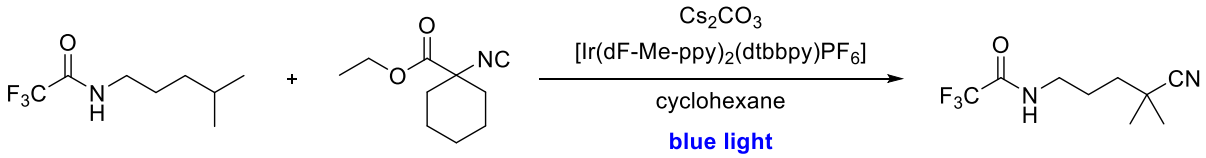

4 **15** **28**

Product **28** was obtained by general procedure B as slightly yellow oil (purity >90% according to NMR analysis) in 63% yield. By starting with 24.2 mg of compound **4**, 17.1 mg of product **28** were obtained.

Physical properties:

Sum formula, m.w.: $C_9H_{13}F_3N_2O$, 222.21

R_f: 0.30 in EtOAc/hexane 1:9

^{1}H NMR: (400 MHz, $CDCl_3$) δ 6.54 (s, 1H, NH), 3.49 – 3.33 (m, 2H, CH_2(NH)), 1.85 – 1.72 (m, 2H, CH_2), 1.59 – 1.53 (m, 2H, CH_2), 1.36 (s, 6H, 2x CH_3) ppm.

^{13}C NMR: (101 MHz, $CDCl_3$) δ 157.56 (d, $^2J_{C\text{-}F}$ = 37.0 Hz(CON)), 124.71 (CN), 121.20 – 111.08 (m(CF_3)), 39.69 (CH_2), 38.10 (CH_2), 32.30 (C(q)), 26.71 (2x CH_3), 25.32 (CH_2) ppm.

^{19}F-NMR: (376 MHz, $CDCl_3$) δ -75.90 (CF_3) ppm.

3.3.2.2 Secondary substrate **29**

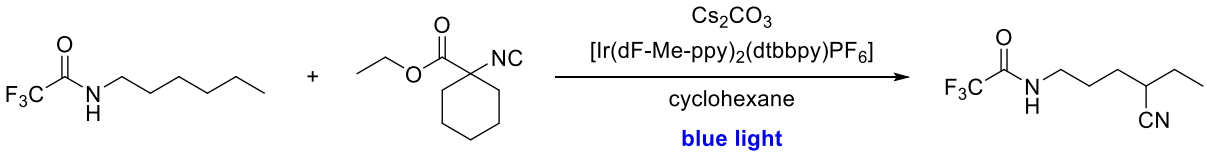

29 **15** **30**

Product **30** was obtained by general procedure B as slightly yellow crude oil (purity >90% according to NMR analysis) in 40% yield. By starting with 20.2 mg of compound **29**, 8.9 mg of product **30** were obtained. Due to time constraints this compound was not purified to homogeneity.

Physical properties:

Sum formula, m.w.: $C_9H_{13}F_3N2O$, 222.21

R_f: 0.26 in EtOAc/hexane 1:3

3.3.2.3 Activated secondary substrate 31

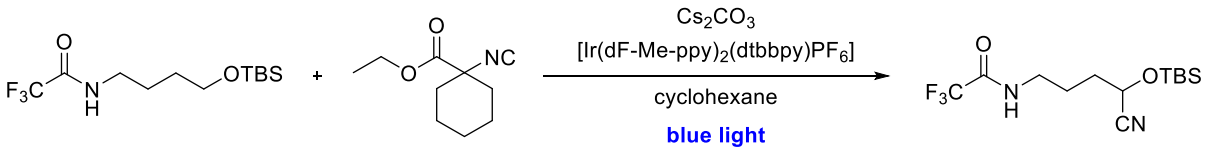

31 **15** **32**

Product **32** was obtained by general procedure B as slightly yellow oil (purity >99% according to NMR analysis) in 27% yield. By starting with 29.9 mg of compound **31**, 8.6 mg of product **32** were obtained.

Physical properties:

Sum formula, m.w.: $C_{13}H_{23}F_3N_2O_2Si$, 324.42

R_f: 0.67 in EtOAc/hexane 1:9

Mass Data: HRMS (ASAP+) m/z: calc. for $C_{13}H_{23}F_3N_2O_2Si$ $[M+H]^+$: 325.1559, found: m/z = 325.1546

^{1}H NMR (500 MHz, $CDCl_3$) δ 6.45 (s, 1H, NH), 4.56 – 4.49 (t, *J* = 5.4 Hz, 1H, CH), 3.45 (p, *J* = 6.2 Hz, 2H, CH_2), 1.89 – 1.78 (m, 4H, 2x CH_2), 0.91 (s, 9H, 3x CH_3), 0.20 (s, 3H, CH_3-Si), 0.15 (s, 3H, CH_3-Si) ppm.

^{13}C NMR (126 MHz, $CDCl_3$) δ 157.5 (q, $^2J_{C-F}$ = 37.0 Hz(CON)), 119.6 (CN), 119.4 – 112.0 (m(CF_3)), 61.5 (CH), 39.2 (CH_2), 33.3 (CH_2), 25.6 (3x CH_3), 24.4 (CH_2), 18.2 (C(q OTBS)), -5.1 (CH_3-Si), -5.3 (CH_3-Si) ppm.

^{19}F-NMR (471 MHz, $CDCl_3$) δ -74.98 (CF_3) ppm.

4. Literature

1. Chu, J. C. K.; Rovis, T., Amide-directed photoredox-catalysed C–C bond formation at unactivated sp3 C–H bonds. *Nature* **2016,** *539*, 272.

2. Chen, D.-F.; Chu, J. C. K.; Rovis, T., Directed γ-C(sp3)–H Alkylation of Carboxylic Acid Derivatives through Visible Light Photoredox Catalysis. *Journal of the American Chemical Society* **2017,** *139* (42), 14897-14900.

3. Vitaku, E.; Smith, D. T.; Njardarson, J. T., Analysis of the Structural Diversity, Substitution Patterns, and Frequency of Nitrogen Heterocycles among U.S. FDA Approved Pharmaceuticals. *Journal of Medicinal Chemistry* **2014,** *57* (24), 10257-10274.

4. Ilardi, E. A.; Vitaku, E.; Njardarson, J. T., Data-Mining for Sulfur and Fluorine: An Evaluation of Pharmaceuticals To Reveal Opportunities for Drug Design and Discovery. *Journal of Medicinal Chemistry* **2014,** *57* (7), 2832-2842.

5. McGrath, N. A.; Brichacek, M.; Njardarson, J. T., A Graphical Journey of Innovative Organic Architectures That Have Improved Our Lives. *Journal of Chemical Education* **2010,** *87* (12), 1348-1349.

6. Li, J. J., Hofmann–Löffler–Freytag reaction. In *Name Reactions: A Collection of Detailed Mechanisms and Synthetic Applications*, Springer Berlin Heidelberg: Berlin, Heidelberg, 2009; pp 292-293.

7. Choi, G. J.; Zhu, Q.; Miller, D. C.; Gu, C. J.; Knowles, R. R., Catalytic alkylation of remote C–H bonds enabled by proton-coupled electron transfer. *Nature* **2016,** *539*, 268.

8. Morcillo, S. P.; Dauncey, E. M.; Kim, J. H.; Douglas, J. J.; Sheikh, N. S.; Leonori, D., Photoinduced Remote Functionalization of Amides and Amines Using Electrophilic Nitrogen Radicals. *Angewandte Chemie International Edition* **2018,** *57* (39), 12945-12949.

9. Xia, Y.; Wang, L.; Studer, A., Site-Selective Remote Radical C-H Functionalization of Unactivated C-H Bonds in Amides Using Sulfone Reagents. *Angew Chem Int Ed Engl* **2018,** *57* (39), 12940-12944.

10. Prier, C. K.; Rankic, D. A.; MacMillan, D. W. C., Visible Light Photoredox Catalysis with Transition Metal Complexes: Applications in Organic Synthesis. *Chemical Reviews* **2013,** *113* (7), 5322-5363.

11. Shaw, M. H.; Twilton, J.; MacMillan, D. W. C., Photoredox Catalysis in Organic Chemistry. *The Journal of Organic Chemistry* **2016,** *81* (16), 6898-6926.

12. March, T. L.; Johnston, M. R.; Duggan, P. J., Diastereoselective Synthesis of Aliphatic α,α-Difluoro-β3-Amino Esters via a Sonocatalyzed Reformatsky Reaction. *Organic Letters* **2012,** *14* (1), 182-185.

13. Frérot, E.; Coste, J.; Pantaloni, A.; Dufour, M.-N.; Jouin, P., PyBOP® and PyBroP: Two reagents for the difficult coupling of the α,α-dialkyl amino acid, Aib. *Tetrahedron* **1991,** *47* (2), 259-270.

14. Odriozola, A.; Oiarbide, M.; Palomo, C., Enantioselective Synthesis of Quaternary Δ4- and Δ5-Dehydroprolines Based on a Two-Step Formal [3+2] Cycloaddition of α-Aryl and α-Alkyl Isocyano(thio)acetates with Vinyl Ketones. *Chemistry – A European Journal* **2017,** *23* (52), 12758-12762.

15. Kalvln, D.; Ramalingam, K.; Woodard, R., A Facile Procedure for the Preparation of Alicyclic α-Amino Acids. *Synthetic Communications* **1985,** *15* (4), 267-272.

16. Singh, A.; Teegardin, K.; Kelly, M.; Prasad, K. S.; Krishnan, S.; Weaver, J. D., Facile synthesis and complete characterization of homoleptic and heteroleptic cyclometalated Iridium(III) complexes for photocatalysis. *Journal of Organometallic Chemistry* **2015,** *776*, 51-59.

17. Xiong, T.; Zhang, Q., New amination strategies based on nitrogen-centered radical chemistry. *Chemical Society Reviews* **2016,** *45* (11), 3069-3087.

18. Ashley, M. A.; Yamauchi, C.; Chu, J. C. K.; Otsuka, S.; Yorimitsu, H.; Rovis, T., Photoredox-Catalyzed Site-Selective α-C(sp3)−H Alkylation of Primary Amine Derivatives. *Angewandte Chemie International Edition* **2019,** *58* (12), 4002-4006.

19. http://chemlabs.princeton.edu/macmillan/wp-content/uploads/sites/6/Merck-Photocatalysis-Chart.pdf.

20. Stache, E. E.; Ertel, A. B.; Rovis, T.; Doyle, A. G., Generation of Phosphoranyl Radicals via Photoredox Catalysis Enables Voltage–Independent Activation of Strong C–O Bonds. *ACS Catalysis* **2018,** *8* (12), 11134-11139.

21. Gottlieb, H. E.; Kotlyar, V.; Nudelman, A., NMR Chemical Shifts of Common Laboratory Solvents as Trace Impurities. *The Journal of Organic Chemistry* **1997,** *62* (21), 7512-7515.

22. Philbrook, G. E., SYNTHESIS OF THE LOWER ALIPHATIC AMIDES. *The Journal of Organic Chemistry* **1954,** *19* (4), 623-625.

23. Chenming, Z. Q. L. Y. L. X. H. 2-substituted parazoleamino-4-substituted amino-5-pyrimidine formamide compound, composition and application thereof 2019.

24. Dai, H.; Yang, M.; Lu, X., Palladium(II)-Catalyzed One-Pot Enantioselective Synthesis of Arylglycine Derivatives from Ethyl Glyoxylate, p-Toluenesulfonyl Isocyanate and Arylboronic Acids. *Advanced Synthesis & Catalysis* **2008,** *350* (2), 249-253.

25. Carta, D.; Brun, P.; Dal Pra, M.; Bernabè, G.; Castagliuolo, I.; Ferlin, M. G., Synthesis and preliminary anti-inflammatory and anti-bacterial evaluation of some diflunisal aza-analogs. *MedChemComm* **2018,** *9* (6), 1017-1032.

26. Balasubramanian, T. M.; Kendrick, N. C. E.; Taylor, M.; Marshall, G. R.; Hall, J. E.; Vodyanoy, I.; Reusser, F., Synthesis and characterization of the major component of alamethicin. *Journal of the American Chemical Society* **1981,** *103* (20), 6127-6132.

27. Angelosante, J. K.; Schopp, L. M.; Lewis, B. J.; Vitalo, A. D.; Titus, D. T.; Swanson, R. A.; Stanley, A. N.; Abolins, B. P.; Frome, M. J.; Cooper, L. E.; Tierney, D. L.; Moore, C.; Rheingold, A. L.; Daley, C. J. A., Synthesis and characterization of an unsymmetrical cobalt(III) active site analogue of nitrile hydratase. *JBIC Journal of Biological Inorganic Chemistry* **2011,** *16* (6), 937-947.

28. Yasuyuki, K. K. N. Antifouling agent for underwater adhering organisms having amino acid isonitrile skeleton 2015.

29. Inoue, Y.; Takashima, S.; Nogata, Y.; Yoshimura, E.; Chiba, K.; Kitano, Y., Isocyanides Derived from α,α-Disubstituted Amino Acids: Synthesis and Antifouling Activity Assessment. *Chemistry & Biodiversity* **2018,** *15* (3), e1700571.

30. Qiu, G.; Sornay, C.; Savary, D.; Zheng, S.-C.; Wang, Q.; Zhu, J., From isonitrile to nitrile via ketenimine intermediate: Palladium-catalyzed 1,1-carbocyanation of allyl carbonate by α-isocyanoacetate. *Tetrahedron* **2018,** *74* (49), 6966-6971.

31. Hoffmann, J.; Kazmaier, U., A Straightforward Approach towards Cyclic Photoactivatable Tubulysin Derivatives. *Angewandte Chemie International Edition* **2014,** *53* (42), 11356-11360.

32. Zhang, Y.; Blackman, M. L.; Leduc, A. B.; Jamison, T. F., Peptide Fragment Coupling Using a Continuous-Flow Photochemical Rearrangement of Nitrones. *Angewandte Chemie International Edition* **2013,** *52* (15), 4251-4255.

33. Porras, J. A.; Mills, I. N.; Transue, W. J.; Bernhard, S., Highly Fluorinated Ir(III)–2,2′:6′,2″-Terpyridine–Phenylpyridine–X Complexes via Selective C–F Activation: Robust Photocatalysts for Solar Fuel Generation and Photoredox Catalysis. *Journal of the American Chemical Society* **2016,** *138* (30), 9460-9472.

5. Appendix

5.1 Complete results for the solvent screens with isocyanide 13

*Table 24: Complete results for the solvent screen conducted with isocyanide **13**, conditions as shown in Scheme 25 were used*

entry	solvent	cat. degr. sp^2 region	yield NMR
1	mesitylene	yes	35%
2	*p*-xylene	yes	34%
3	toluene	yes	29%
4	acetonitrile	no	24%
5	cyclohexane	no	20%
6	dioxane	yes	20%
7	*i*PrOH*	no	18%
8	benzonitrile	no	16%
9	hexane	no	16%
10	THF	yes	13%
11	$PhCF_3$	no	12%
12	DCM	no	8%
13	acetone	yes	7%
14	DCE	no	<5%
15	DMA	n.d.	<5%
16	$CHCl_3$	n.d.	0%
17	DMF	n.d.	0%
18	MeOH	n.d.	0%

* *i*PrOH as solvent led to the formation of several byproducts and severe degradation of the reaction components. Therefore, it was not used in further screens even though the yield of 18% by NMR would have been the seventh highest obtained yield with isocyanide **13**.

5.2 Results for all conducted concentration screens with different solvent-base systems

Table 25: Complete results for all conducted concentration screens with different solvent-base systems, conditions as shown in Scheme 25 were used

entry	conditions	conc.	cat. degr. sp^2 region	yield NMR
1	toluene, K_3PO_4	0.05 M	yes	51%
2	toluene, K_3PO_4	0.1 M	yes	54%
3	toluene, K_3PO_4	0.2 M	yes	52%
4	toluene, K_3PO_4	0.4 M	yes	52%
5	cyclohexane, K_3PO_4	0.05 M	no	49%
6	cyclohexane, K_3PO_4	0.1 M	no	48%
7	cyclohexane, K_3PO_4	0.2 M	no	45%
8	cyclohexane, K_3PO_4	0.4 M	no	45%
9	*p*-xylene, Cs_2CO_3	0.05 M	yes	40%
10	*p*-xylene, Cs_2CO_3	0.1 M	yes	51%
11	*p*-xylene, Cs_2CO_3	0.2 M	yes	46%
12	*p*-xylene, Cs_2CO_3	0.4 M	yes	41%
13	cyclohexane, Cs_2CO_3	0.05 M	no	65%
14	cyclohexane, Cs_2CO_3	0.1 M	no	54%
15	cyclohexane, Cs_2CO_3	0.2 M	no	53%
16	cyclohexane, Cs_2CO_3	0.4 M	no	46%

5.3 Cyclic voltammogram of isocyanide 15

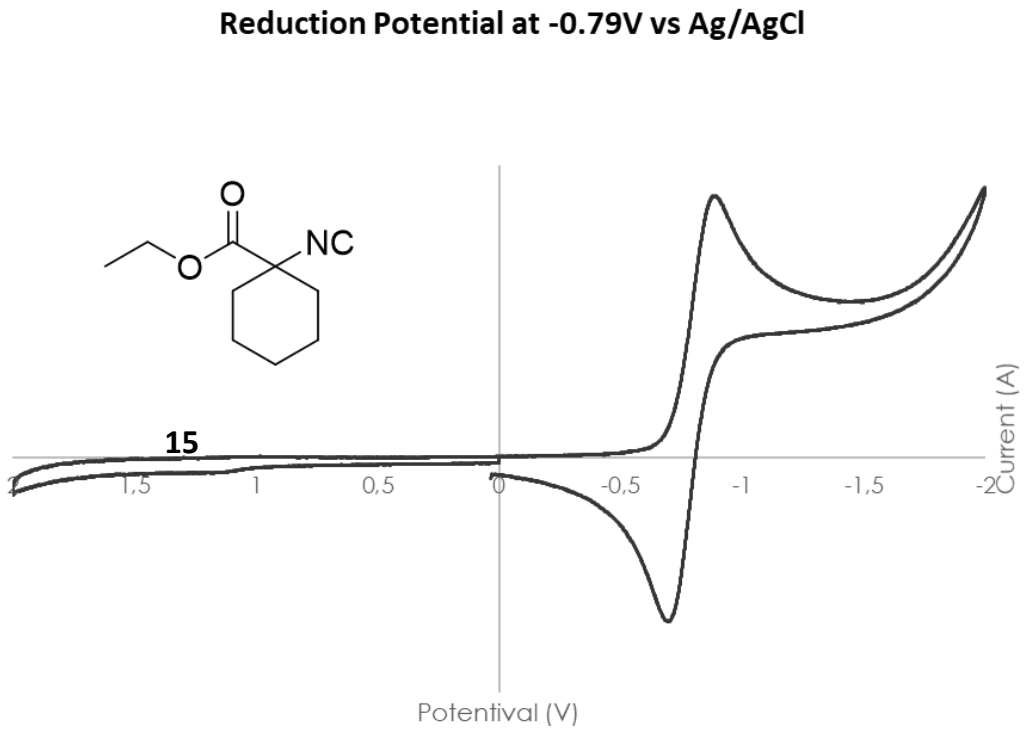

*Figure 4: Cycloc Voltammogram of isocyanide **15***

5.4 Electrochemical series of photocatalysts and common organic compounds

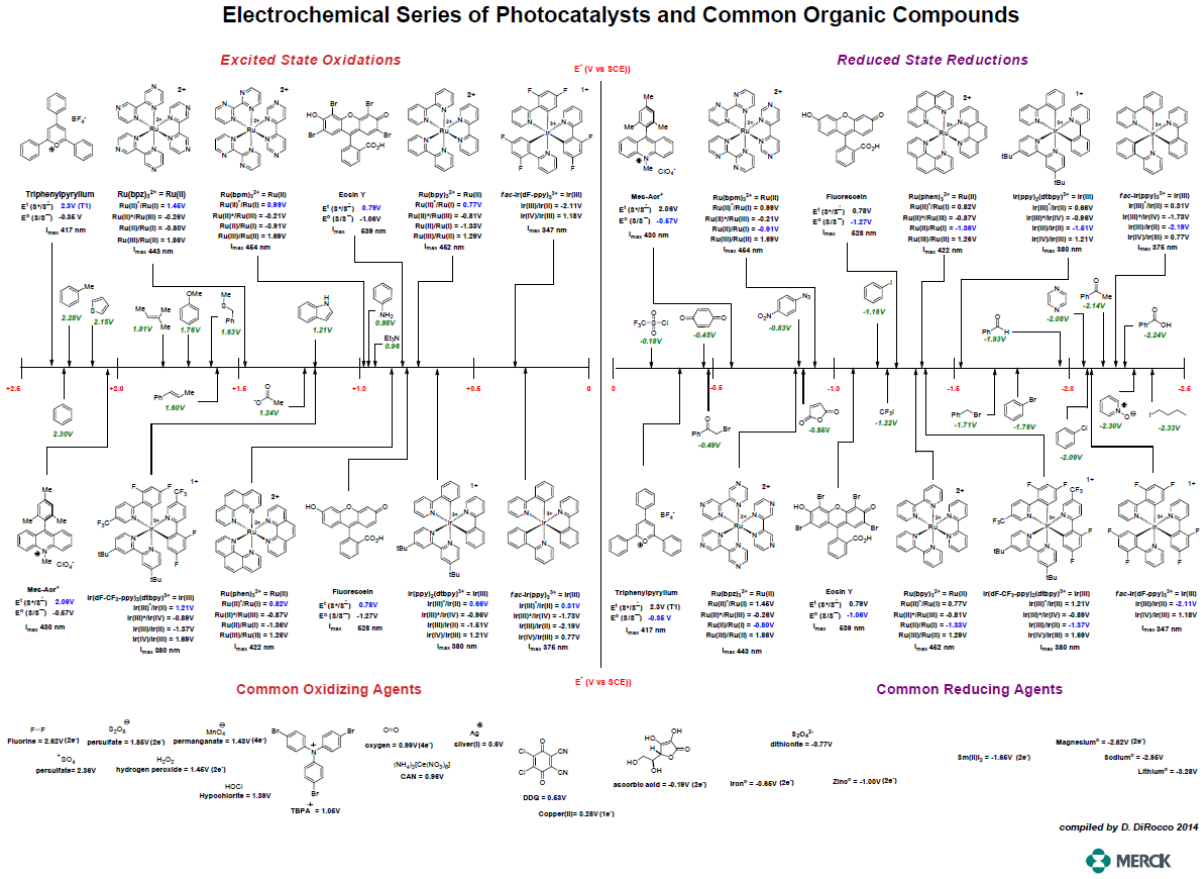

Scheme 44: Chart of compiled electrochemical data of common photocatalysts and organic compounds used to obtain data during this thesis[19]

5.5 Full results of the three NMR time studies

*Table 26: Results for the first NMR time study conducted with isocyanide **15** under optimized reaction conditions*

time [h]	starting material 4 [%]	product 28 [%]	isocyanide 15 [%]	byproduct 15a [%]
0	100	0	100	0
1	87	6	99	15
2	74	6	88	22
3	88	6	111	32
4	63	10	85	35
5	66	11	87	40
6	59	9	87	45
8	59	11	88	54
11	55	12	93	67
24	39	54	77	75

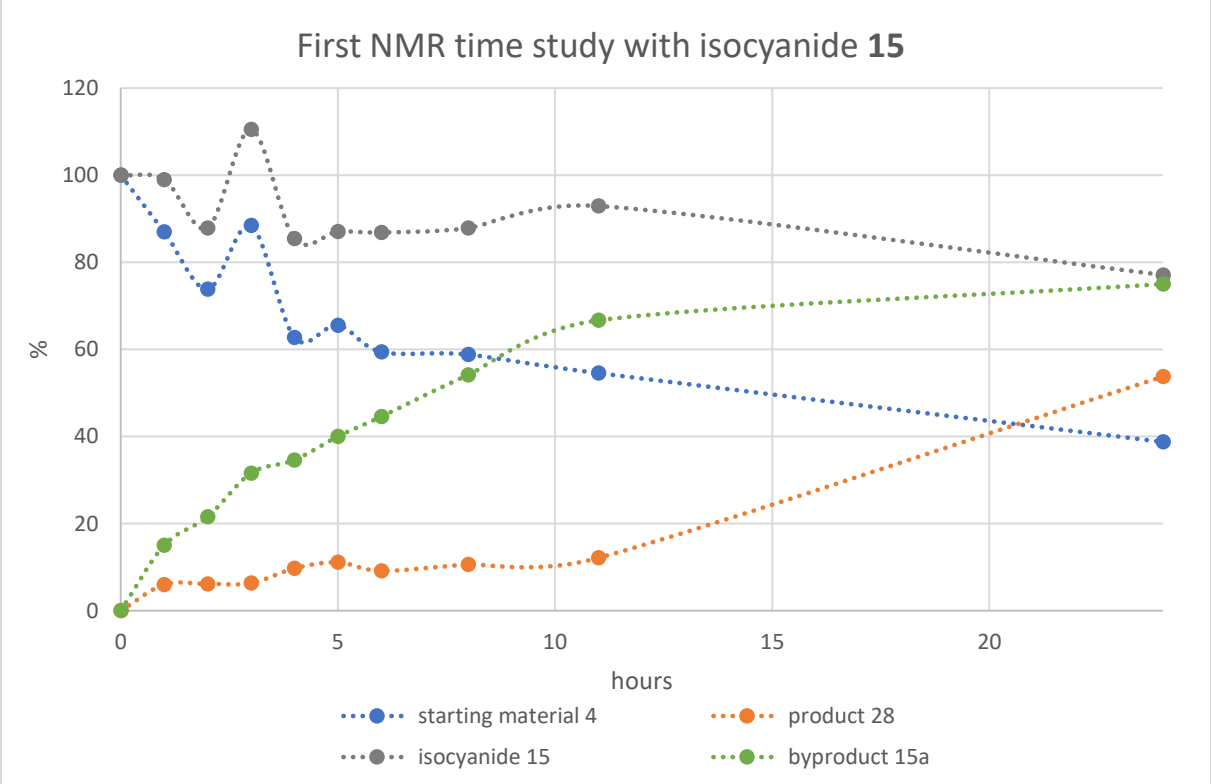

*Figure 5: Results for the first NMR time study conducted with isocyanide **15** under optimized reaction conditions*

*Table 27: Results for the second NMR time study conducted with isocyanide **16** under optimized reaction conditions*

time [h]	starting material 4 [%]	product 28 [%]	isocyanide 16 [%]	byproduct 16a [%]
0	100	0	100	0
1	87	6	99	15
2	74	6	88	22
3	88	6	111	32
4	63	10	85	35
5	66	11	87	40
6	59	9	87	45
8	59	11	88	54
11	55	12	93	67
24	39	54	77	75

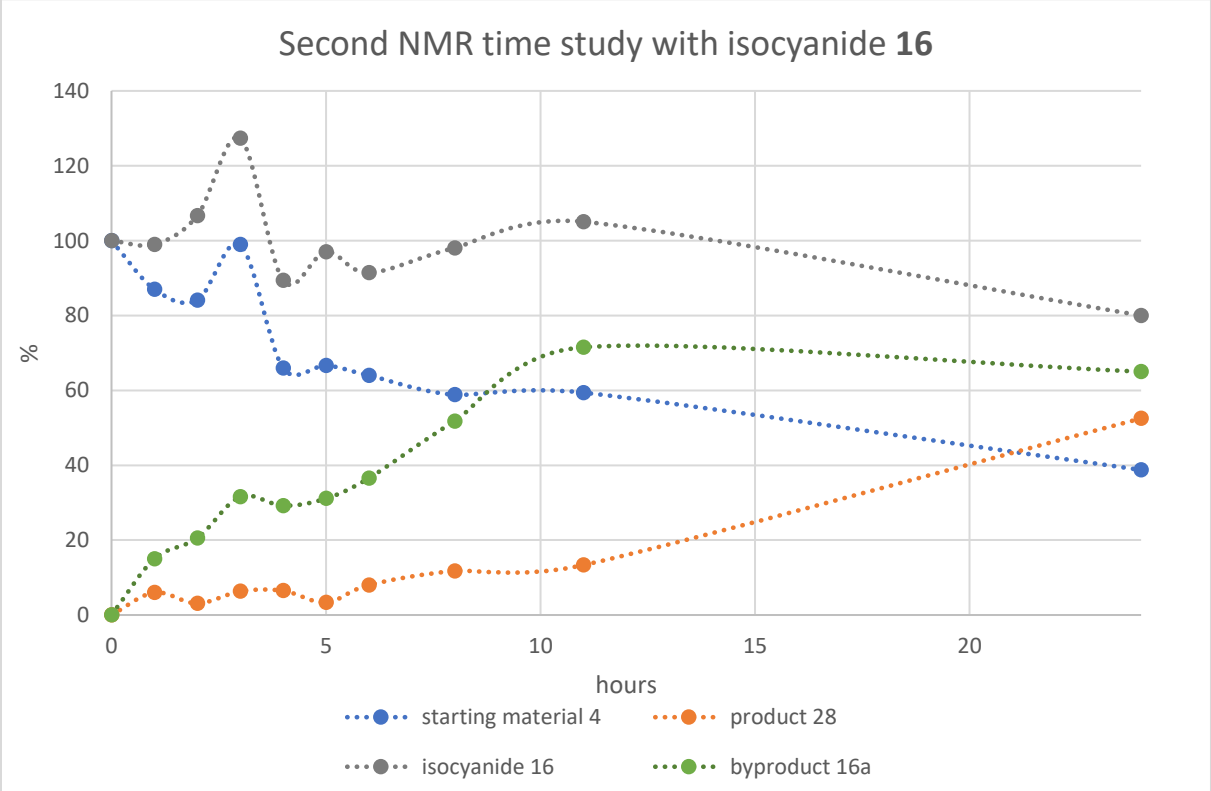

*Figure 6: Results for the second NMR time study conducted with isocyanide **16** under optimized reaction conditions*

*Table 28: Results for the third NMR time study conducted with isocyanide **15** under optimized reaction conditions*

time [h]	**starting material** 4 **[%]**	**product** 28 **[%]**	**isocyanide** 15 **[%]**	**byproduct** 15a **[%]**
0	100	0	100	0
1	96	14	99	13
2	91	16	95	16
3	86	20	90	21
4	80	25	90	26
6	70	39	70	39
9	60	42	60	42
11	53	52	53	60
24	42	56	39	57

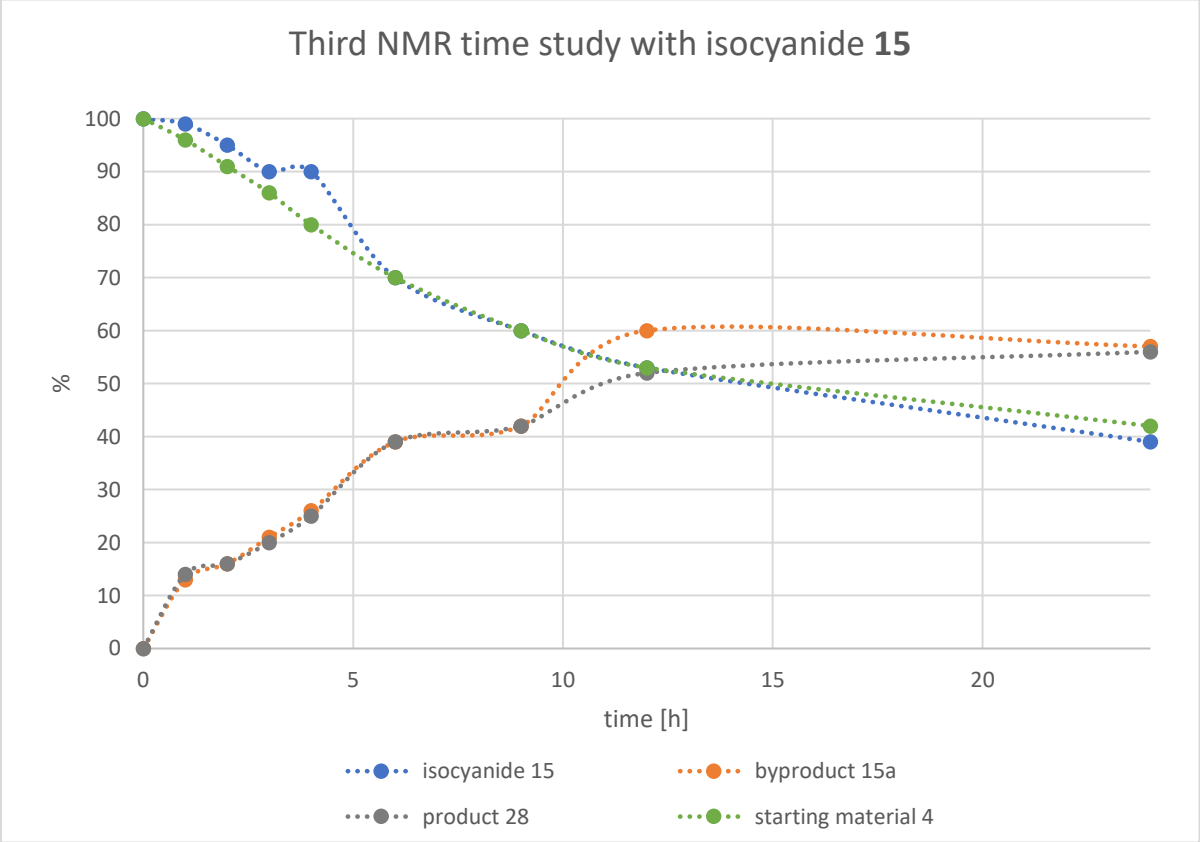

*Figure 7: Results for the third NMR time study conducted with isocyanide **15** under optimized reaction conditions*

Katharina Beate Schlögl

TU Wien, Institute of Applied Synthetic Chemistry, Getreidemarkt 9, 1060 Vienna
e1425254@student.tuwien.ac.at, +43 650 4724 110

Master student of Applied Synthetic Chemistry at TU Wien. Conduct of her master thesis at Columbia University under the supervision of Prof. Tomislav Rovis, home-supervision Prof. Dr. Marko Mihovilovic. Specialization and research interest in bioorganic and medicinal chemistry.

Education

02.2019 – 08.2019	**Visiting Researcher at Columbia University in the City of New York** Research group: Prof. Tomislav Rovis Conduction of master thesis on Photoredox Catalysis
11.2017 – present	**Master Programme at TU Wien** „Technical Chemistry"; Specialization in Applied Synthetic Chemistry
10.2014 – 11.2017	**Bachelor Programme at TU Wien** „Technical Chemistry"; Grade average: 1.7

Research Experience

02.2019 – 08.2019	**Department of Chemistry, Columbia University** Master thesis in the field of Photoredox Catalysis
09.2018 – 10.2018	**Institute of Applied Synthetic Chemistry, TU Wien** Research in the field of Bioorthogonal Chemistry
02.2017 – 03.2017	**Institute of Applied Synthetic Chemistry, TU Wien** Bachelor thesis applying NHC Catalysis in Carbohydrate Chemistry

Additional Experience

07.2017	**Analytec, Department of General Chemistry** Food quality assessment, analytical procedures
08.2016	**OMV, Department of Natural Gas** Plant control and safety checks
07. – 08.2016	**SalzburgMilch, Laboratory for Quality Management** Food quality assessment, plant control, (bio)analytical procedures

Teaching Experience

2017 – present	**Sigmund Freud University Vienna** Lectures on general chemistry for medicine students
2017 – 2018	**TU Wien** Supervision and teaching of students in a bioanalytical lab course

Fellowships

2019	Marshall Plan Fellowship
2018	Merit Scholarship for excellence in studies of the TU Wien
10.2015 – 06.2017	Technical Scholarship of OMV
08.2014 – 10.2015	E-fellows online-Scholarship

Languages & Skills

German (native), English (high proficiency), Latin

Synthetic Chemistry, Organic Chemistry, Analytical Chemistry, Biochemistry and Biochemical Methods (PCR, Gel electrophoresis), Microsoft Office